American Water Works Association
RESEARCH FOUNDATION
®

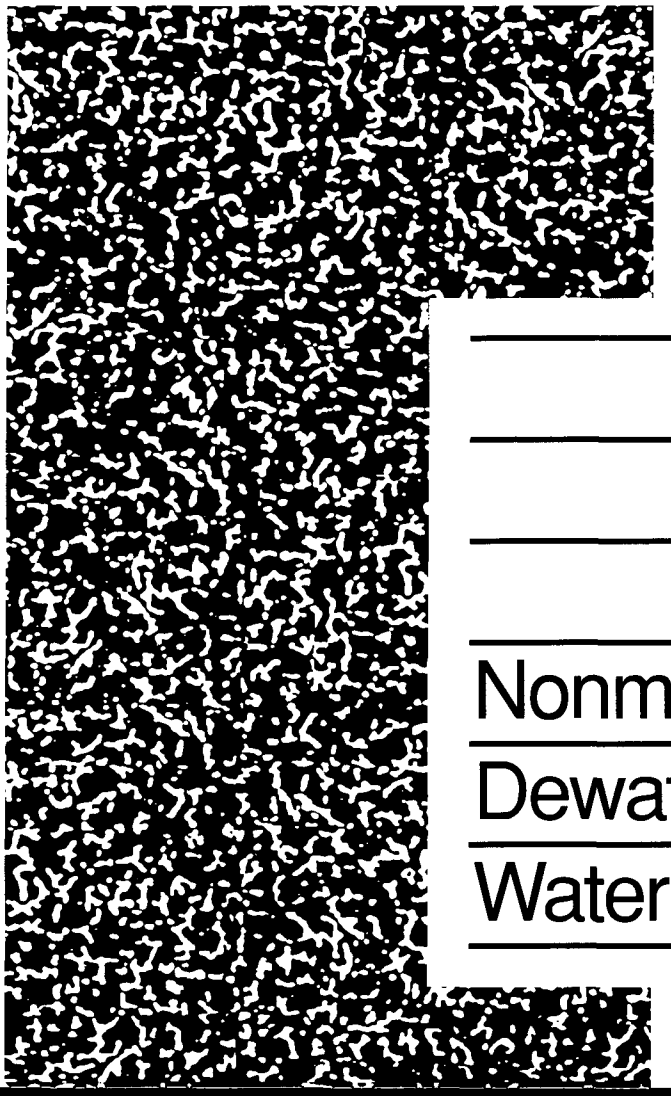

Nonmechanical Dewatering of Water Plant Residuals

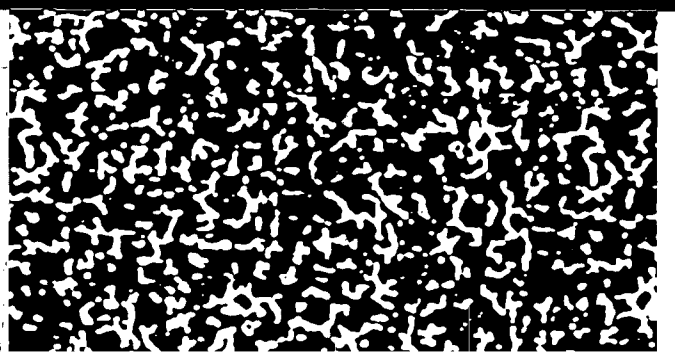

Subject Area:
Water Treatment

Nonmechanical Dewatering of Water Plant Residuals

The mission of the AWWA Research Foundation is to advance the science of water to improve the quality of life. Funded primarily through annual subscription payments from over 900 utilities, consulting firms, and manufacturers in North America and abroad, AWWARF sponsors research on all aspects of drinking water, including supply and resources, treatment, monitoring and analysis, distribution, management, and health effects.

From its headquarters in Denver, Colorado, the AWWARF staff directs and supports the efforts of over 500 volunteers, who are the heart of the research program. These volunteers, serving on various boards and committees, use their expertise to select and monitor research studies to benefit the entire drinking water community.

Research findings are disseminated through a number of technology transfer activities, including research reports, conferences, videotape summaries, and periodicals.

Nonmechanical Dewatering of Water Plant Residuals

Prepared by:

Carel Vandermeyden and
David A. Cornwell
Environmental Engineering & Technology, Inc.
712 Gum Rock Court
Newport News, VA 23606

Sponsored by:
AWWA Research Foundation
6666 West Quincy Avenue
Denver, CO 80235

Published by the
AWWA Research Foundation and
American Water Works Association

Disclaimer

This study was funded by the AWWA Research Foundation (AWWARF). AWWARF assumes no responsibility for the content of the research study reported in this publication or for the opinions or statements of fact expressed in the report. The mention of trade names for commercial products does not represent or imply the approval or endorsement of AWWARF. This report is presented solely for informational purposes.

Library of Congress Cataloging-in-Publication Data
Vandermeyden, Carel.
Nonmechanical dewatering of water plant residuals / prepared by Carel Vandermeyden, David A. Cornwell.
xx, 181 p. 21.5 × 28 cm.
Includes bibliographical references.
ISBN 0-89867-946-X
1. Water treatment plant residuals--Purification 2. Water treatment plant residuals--Drying. I. Cornwell, David A., 1948–. II. Title.
HD899.W3V36 1998
628.1'62--dc21 97-17110
CIP

ISBN 0-89867-946-X

CONTENTS

TABLES

FIGURES

FOREWORD

The AWWA Research Foundation is a nonprofit corporation that is dedicated to the implementation of a research effort to help utilities respond to regulatory requirements and traditional high-priority concerns of the industry. The research agenda is developed through a process of consultation with subscribers and drinking water professionals. Under the umbrella of a Strategic Research Plan, the Research Advisory Council prioritizes the suggested projects based upon current and future needs, applicability, and past work; the recommendations are forwarded to the Board of Trustees for final selection. The foundation also sponsors research projects through the unsolicited proposal process; the Collaborative Research, Research Applications, and Tailored Collaboration programs; and various joint research efforts with organizations such as the U.S. Environmental Protection Agency, the U.S. Bureau of Reclamation, and the Association of California Water Agencies.

This publication is a result of one of those sponsored studies, and it is hoped that its findings will be applied in communities throughout the world. The following report serves not only as a means of communicating the results of the water industry's centralized research program but also as a tool to enlist the further support of the nonmember utilities and individuals.

Projects are managed closely from their inception to the final report by the foundation's staff and large cadre of volunteers who willingly contribute their time and expertise. The foundation serves a planning and management function and awards contracts to other institutions such as water utilities, universities, and engineering firms. The funding for this research effort comes primarily from the Subscription Program, through which water utilities subscribe to the research program and make an annual payment proportionate to the volume of water they deliver and consultants subscribe based on their annual billings. The program offers a cost-effective and fair method of funding research in the public interest.

A broad spectrum of water supply issues is addressed by the foundation's research agenda: resources, treatment and operations, distribution and storage, water quality and analysis, toxicology, economics, and management. The ultimate purpose of the coordinated effort is to assist water suppliers to provide the highest possible quality of water economically and reliably. The true benefits are realized when the results are implemented at the utility level. The foundation's trustees are pleased to offer this publication as a contribution toward that end.

Residuals management is one of the significant challenges that utilities continue to address. As disposal options become more limited and costs increase, new technology and disposal options, including beneficial reuse, will be needed. To accomplish this utilities will need cost-effective methods that produce a high-solids content in dewatered residuals. This in turn will reduce the cost of disposal whether it be in the form of lower transportation costs, reduced landfill tipping fees, or other cost reductions such as reduced power or smaller land requirements for storage/treatment. The results presented in this report offer utilities options that will help accomplish these multiple objectives.

George W. Johnstone
Chair, Board of Trustees
AWWA Research Foundation

James F. Manwaring, P.E.
Executive Director
AWWA Research Foundation

ACKNOWLEDGMENTS

Environmental Engineering & Technology, Inc., wants to thank all of the utilities that participated in this project. Several utilities conducted on-site investigations on the dewatering characteristics and over 60 utilities collected and sent sludge samples for lab characterization. Appreciation is extended to Kraig Schenkelberg for conducting the characterization works on the 80 sludges. We thank Mark La Guardia, EE&T laboratory manager, and Robert Hicks, chemist, for overseeing much of the lab work and summer student Brendon Cornwell for conducting pilot studies. The Project Advisory Committee (PAC) was James R. DeWolfe, Process Engineer, Gannett Flemming, Inc., Harrisburg, PA; C. James Martel, Environmental Engineer, Civil and Geotechnical Engineering Research Branch, Experimental Engineering Division, U.S. Army Cold Regions Research and Engineering Laboratory; and Chuck Beer, retired, Denver Water, Denver, Colo. The assistance of A. Terry Rolan of the City of Durham, N.C., in developing the sand drying bed models is appreciated and marks a lasting contribution to the water industry.

We appreciate the assistance of the AWWARF project manager, Albert Ilges.

EXECUTIVE SUMMARY

Environmental Engineering & Technology, Inc., conducted an evaluation of methods to optimize nonmechanical dewatering of water treatment residuals. A lab characterization study was also conducted on the physical properties of residuals based on sampling residuals at over 60 utilities.

The nonmechanical methods that were evaluated included:

- Sand drying beds
- Solar drying beds
- Dewatering lagoons
- Freeze-thaw beds

Residuals were evaluated from coagulation plants that use alum, ferric chloride, and polyaluminum chloride (PACl) and at lime softening plants.

The laboratory physical characterization tests that were conducted included capillary suction time (CST), time to filter (TTF), specific resistance (SR), particle sizing, specific gravity, and textural classification. The CST and TTF tests correlated very well with each other, and it appears that either test could be used for conducting laboratory drainage comparisons. The CST, TTF, and SR tests all showed that the ease of dewatering of the residuals would be in the following order: lime, ferric, alum, and PACl. No direct correlations between any of the physical characteristics tests and full-scale drainage characteristics could be found. However, probability plots for the physical characteristics were presented which allow a utility to obtain qualitative insights into how a particular residual compares to others.

Pilot and full-scale evaluations were conducted at 13 utilities. Three of the utilities used alum, two used PACl, two used ferric, and six were lime softening plants. At five utilities data were collected on the drainage characteristics as predicted by 2-in. diameter pilot tests and on the drainage

---

Information regarding SI equivalent units for U.S. customary units can be found in Appendix C, page 177.

characteristics in the full-scale sand drying beds. The two correlated almost exactly 1:1 (field drainage = 1.0 (pilot drainage) + 2.6) with a correlation coefficient of 0.94 covering the range of 20 to 70 percent drainage. These results show that good prediction of full-scale performance and development of design parameters can be achieved in pilot tests.

The studies showed that the important factor in minimizing the area required for dewatering was to maximize the drained solids concentration; that is, the solids concentration of the residuals after the free water has been drained and decanted. Drained solids concentration was found to be a function of the initial solids concentration, the loading, and the use of polymer conditioning. For residuals produced by coagulation, polymer significantly increased the drained solids concentration and thereby decreased the required area for dewatering. For lime residuals, polymer had no effect on drainage, even though the CST was decreased. For coagulant residuals acceptable loadings were found to be between 2 and 6 lb/ft^2 depending upon the specific residual, and for lime residuals the loadings were 10 to 15 lb/ft^2.

Field tests were also conducted to compare the evaporative cycle of solids drying in field tests to that predicted by pan evaporation models. In all cases, the field evaporation was higher than that predicted by pan evaporation up to the point when the free water had been evaporated. This higher evaporation is probably due to the higher exposed surface area in field residuals' drying conditions than that which occurs in a pan evaporation method.

Laboratory and pilot freeze-thaw tests were also conducted. For coagulant residuals, sludges exposed to freeze-thaw had much higher drained solids concentrations than did polymer-only conditioned residuals. However, for lime residuals, no improvement in drained solids concentrations was found when subjecting the residuals to a freeze-thaw cycle. The average particle diameter of coagulant residuals increased by about two orders of magnitude after freeze-thaw.

Models were presented to allow for the proper sizing of sand drying beds, solar drying beds, dewatering lagoons, and freeze-thaw beds. These models allow a utility to determine the area required for the various dewatering technologies based on pilot data and local climatological data. The modeling showed that proper sizing should be based on monthly residuals production values.

Overall, this document presents the required test procedures and modeling efforts for utilities to size and design nonmechanical dewatering systems.

CHAPTER 1
INTRODUCTION

PURPOSE AND OBJECTIVES

The primary emphasis and objective of this research was the development of a document on the proper design of nonmechanical dewatering systems, with the results aimed specifically for use by utilities and their design engineers. The specific purpose of the project is set out in the following list of main objectives that address:

- General preplanning techniques that utilize residuals characteristics and local environmental factors to determine whether nonmechanical dewatering is a viable option for a specific application
- Laboratory, pilot, and/or modeling procedures and methodologies to properly size nonmechanical dewatering facilities
- Design details for system installation, including items such as size (total land use and size of individual units); need for underdrains; support media; need for decant; residuals application methods; conditioning and thickening requirements; cleaning methods and required design provisions; pump systems; cover requirements; and meeting regulations.

The research approach taken covers the following types of nonmechanical dewatering methods: sand drying beds, solar drying beds, dewatering lagoons, and freeze-thaw beds. The research included residuals produced from the chemical additions of alum, iron, lime, and polyaluminum chloride; moreover, the project considered different geographic and climatic regions.

Chapter 2 of this report outlines the specific analytical procedures that were utilized in this research, including those associated with the following tests: capillary suction time (CST), specific resistance (SR), time to filter (TTF), grain size analysis, total solids analysis, and particle size distribution.

Information regarding SI equivalent units for U.S. customary units can be found in Appendix C, page 177.

Chapter 3 presents the results of laboratory residuals characterization studies. This phase of the project encompassed 61 different utilities. Residuals from these utilities were tested for CST, TTF, SR, and particle size distribution. These tests were done to provide a general characterization of water treatment plant residuals.

After conducting a detailed telephone survey of existing nonmechanical residuals dewatering facilities, representative sampling sites were selected to develop results that could serve as a general guidance. Chapter 4 introduces the test locations and presents the results of field and pilot tests carried out using residuals collected during the various site visits.

Chapter 5 discusses the application of laboratory, pilot, and modeling techniques in order to size nonmechanical dewatering facilities. Examples of sizing sand drying beds, solar drying beds, dewatering lagoons, and freeze-thaw beds are shown.

Chapter 6 examines the design and operation of nonmechanical dewatering systems, specifically sand drying beds, solar drying beds, dewatering lagoons, and freeze-thaw beds. Details of the specific layouts are presented.

DESCRIPTION OF TECHNOLOGIES

Nonmechanical dewatering, as the name implies, is the dewatering of water treatment plant residuals through means that do not require the use of mechanical appurtenances such as centrifuges or filter presses. Often used in locations where land is available and monetary constraints prohibit the use of mechanical dewatering, nonmechanical dewatering can be both economical and efficient for the dewatering of water treatment plant residuals.

A variety of means are employed to accomplish nonmechanical dewatering. The most basic of these is separation of solids and free water through sedimentation followed by natural air drying of the residuals. A second method allows free water to be percolated through sand and into an underdrain system, while additional solids concentration increases are achieved through evaporation. In northern climates, a third system is utilized whereby water treatment plant residuals are subjected to freezing and thawing, which results in a dramatic reduction in residuals volume and a corresponding increase in solids concentration.

Sand Drying Beds

Sand drying beds were initially developed for dewatering municipal wastewater biosolids, but have since also been used to dewater residuals from water treatment plants. Drainage (percolation), decanting, and evaporation are the primary mechanisms for dewatering residuals in sand drying beds and are utilized in a two step process until the desired cake concentration is achieved. Following residuals application, free water is allowed to drain from the residuals into a sand bottom from which it is transported via an underdrain system consisting of a series of lateral collection pipes. This process continues until the sand is clogged with fine particles or until all the free water has been drained, which may require several days. Secondary free water removal by decanting can take place once a supernatant layer has formed. Decanting can also be utilized to remove rain water that would otherwise hinder the overall drying process. Water remaining after initial drainage and decanting is removed by evaporation over a period of time necessary to achieve the desired final solids concentration.

Several variations of sand drying beds are currently in use, and Rolan (1980) proposed the following classification categories:

1. Conventional rectangular beds with side walls and a layer of sand or gravel with underdrain piping. These are built with or without the provisions for mechanical removal of the dried residuals and with or without either a roof or a greenhouse-type covering.
2. Paved rectangular beds. These have a center sand drainage strip, with or without heating pipes buried in the paved section and with or without covering to prevent rain incursion. In this research the paved bottom beds are referred to as solar drying beds and have been treated as a separate category of nonmechanical dewatering technologies.
3. Drying beds with a wedge-wire septum. These incorporate provisions for an initial flood with a thin layer of water followed by introduction of liquid residuals on top of the water layer, controlled formation of cake, and provisions for mechanical cleaning.

Layout and construction of sand drying beds is very site specific—topography, available land, and operational constraints must all be considered. Topography plays a key role in how beds are laid out on a site, and operational constraints, such as residuals pumping distance, must also be considered when siting a bed location. Materials used in construction are typically cast in place concrete or concrete block when the beds are constructed at grade, or earthen sides with a liner when the beds are constructed below grade.

Underdrain systems for sand drying beds are used to collect water that has percolated down through the sand and gravel and to transmit it to a point of discharge. When the plant has the capability to decant, the flow from the decant mechanism is often tied to the underdrains so that a combined effluent is produced. Underdrains are typically constructed of vitrified clay or plastic piping, and a host of underdrain configurations exist, but the most common is collecting drainage with laterals and conveying the flow to a header pipe.

Several sand drying beds are typically used at a given site, which offers some advantages from an operations point of view. Chief among these is the ability to rotate bed use, so that as one sand drying bed is loaded and the residuals begin to dry, another bed could be cleaned and readied for a new application of residuals.

Cleaning of the sand drying bed can be accomplished with mechanical equipment if concrete support runners are properly installed in the bed. Front-end loaders and vac-haul trucks have been used successfully by utilities operating sand drying beds.

Solar Drying Beds

Solar drying beds are similar to sand drying beds in terms of shape and operation; however, solar drying beds are constructed with sealed bottoms and have sometimes been referred to as paved drying beds. These beds have little or no provisions for water to be removed through drainage; all residuals thickening and drying is accomplished through decant of free water and evaporation. The principal advantages of this type of drying bed are low maintenance costs and ease of cleaning. No sand replacement costs are associated with this type of drying bed, and since the bottoms of these beds are sealed, neither initial underdrain costs nor underdrain repair costs are incurred. Also

because the entire solar bed bottom is often paved or concrete, cleaning with front-end loaders can be done quickly and efficiently. Because solar beds rely primarily on evaporation, they typically have lower solids loading rates than sand drying beds. Most solar beds are located in the southern and southwestern parts of the country where evaporation rates are high.

Dewatering Lagoons

A dewatering lagoon has a sand and underdrain bottom, similar to a drying bed, and it can be designed to achieve a desired dewatered residuals cake. The dewatering lagoons are deeper than sand drying beds and have fewer residuals applications per year. The advantage of a dewatering lagoon over a drying bed is that storage is built into the system to assist in meeting peak solids production or to assist in handling residuals during wet weather. The disadvantage is that the bottom sand layers can clog or blind with multiple loadings, thereby increasing the required surface area compared to conventional drying beds. Polymer treatment can be useful in preventing this sand blinding.

Dewatering lagoons may be equipped with inlet structures designed to dissipate the velocity of the incoming residuals. This minimizes turbulence in the lagoons and helps prevent carryover of solids in the decant. The lagoon outlet structure is designed to remove the settled supernatant and is often built with flash boards to vary the draw-off depths.

The basis for design of dewatering lagoons is essentially the same as that for sand drying beds. The difference is that the applied depth is higher and the number of cleanings per year is greatly reduced. During the pilot study phase, careful consideration should be given to the effect that continual or multiple loadings have on the volume of water removed by decanting and drainage. The surface area required for a dewatering lagoon will be equal to or greater than that required for a sand drying bed for the same solids production but may be smaller overall when peak designs are considered.

Freeze-Thaw Beds

It has long been recognized that when residuals are subjected to freezing, the resulting volume reduction and increased solids concentration is appreciable. Typically, the volume reduction is well over 70 percent, and solids concentrations may reach as high as 80 percent when freeze-thaw is followed by evaporation. Freeze-thaw followed by evaporation dramatically converts the residuals from a fine particle suspension to granular particles. The granular particles often resemble coffee grounds in both size and appearance, and they do not break apart even after vigorous agitation. If the frozen mixture is placed on a porous medium, the water drains away easily upon thawing (Martel and Diener 1991). As one might expect, freeze-thaw beds are operated most effectively in northern climates, with a range of effective operation beginning at approximately 40° north latitude and extending northward. (The 40° north latitude runs horizontally across the United States, roughly through Philadelphia, Indianapolis, and Salt Lake City.)

Some water treatment plants in cold climates already take advantage of this process by modifying the operation of their lagoons or drying beds. One technique is to decant a lagoon down to the residuals interface and allow it to freeze over the winter months. Martel and Diener (1991) report that this technique is not always successful because the residuals do not freeze to the bottom. Core samples taken of one lagoon indicated that very little residuals were frozen by this technique; instead the core consisted mostly of clear ice, and the solids were pushed downward into the lagoon. Another technique is to pump a shallow layer (20 to 45 cm) of residuals from a storage lagoon into drying beds or ponds that are then allowed to freeze in the winter. This technique works well because the residuals usually freeze completely, but it requires a considerable amount of land and storage volume.

Combination sand drying beds and freeze-thaw beds can also be utilized. In this case the design must consider the evaporative condition for the drying bed cycle and the freezing and thawing conditions for the freeze-thaw cycle.

Combining the concepts presented in the literature and observations of residuals freezing operations on drying beds and lagoons, a unit operation called a residuals freezing bed was developed (Martel 1989). To maximize residuals dewatering by natural freeze-thaw, a freezing bed includes the following features:

1. It is designed to apply residuals in several thin layers rather than a single thick layer. Each layer is applied as soon as the previous layer has frozen, thereby maximizing the total depth of residuals that can be applied.
2. The bed is covered to prevent snow and rain from entering it. This feature is critical if the bed is to utilize all of the available freezing time in the winter. An open freezing bed would have less capacity because snow accumulations on the surface would slow down the freezing rate. Also, snow removal would be practically impossible if a large snowfall occurred soon after residuals were applied. In this case, the operator would have to delay snow removal until the frozen residuals were thick enough to support snow removal equipment. A covering would also prevent rainfall from rewetting the thawed residuals.
3. The sides of the bed housing are left open to allow free air circulation. However, a half-wall or louvered wall is recommended to prevent drifting snow from entering the bed. Also, the roof is made to be transparent so that solar radiation can help thaw and dry the residuals in the spring. Incoming solar radiation in the winter is expected to be negligible because of the sun's low azimuth and the likelihood of snow on the roof.

Essentially, a freezing bed consists of an in-ground containment structure that is waterproofed to prevent groundwater infiltration. A ramp is provided at one end to allow vehicle access for residuals removal and to distribute the incoming residuals evenly within the bed. The opposite end of the bed is equipped with an overflow gate or drain valves to draw off supernatant during thaw. The bottom of the bed is underdrained with wedge-wire screen or sand to allow drainage of the filtrate. Both overflow and filtrate are collected in a sump and pumped back to the plant (Martel 1989).

The freezing bed must be complemented with appropriate residuals storage in a separate lagoon or tankage.

Martel (1989) has developed a mathematical model to develop design criteria for residuals freezing beds. The model calculates the depth of residuals that can be frozen and thawed naturally

for a proposed site. Martel indicates that freezing occurs in two phases. During phase 1, liquid residuals will be cooled to the freezing point; during phase 2, liquid residuals at the freezing point will be converted to a frozen solid by loss of the latent heat of fusion. Further cooling of the layer below the freezing point should not be significant because the operational plan should call for immediate application of the next layer as soon as the previous layer has frozen. He concluded that phase 1 cooling time was small relative to the total cooling and freezing time and that for design purposes cooling time could be eliminated from freezing time predictions without serious error.

The model developed by Martel for phase 2 freezing predicts the time needed to freeze a residuals layer of specified thickness. It also provides a comparison model for predicting the time required to thaw residuals of a specified thickness that can be used to determine a rational design for freezing beds.

In a recent freeze-thaw study on residuals, Dempsey et al. (1993) examined eight water treatment plant residuals for their content of trace metals, pH, total organic carbon (TOC), total phosphorus (P), total Kjeldahl nitrogen (TKN) concentrations, dithionite-citrate-bicarbonate (DCB) extractable aluminum (Al) concentration, and sequential fractionation of metals. Five residuals in both the wet and freeze-thaw dewatered forms were selected for combination with two soils. These mixtures were examined in a variety of soils tests. Results were compared with respect to the form of the residual (wet or freeze-thaw) and, where appropriate, to results for the soils or residuals alone. In addition, the soil-residuals mixtures were packed into columns and eluted with a calcium nitrate and sodium nitrate solution.

Several conclusions were drawn by Dempsey et al. (1993) regarding wet versus freeze-thaw dewatered residuals. First, the freeze-thaw dewatering process resulted in a statistically significant decrease in TKN concentration versus the wet residual, but a similar decrease was not observed for P. Second, the freeze-thaw dewatering process did not result in a decrease in extractable Al. Third, a significant decrease in plant available P was observed for soil mixed with residuals compared to the soil alone. Furthermore, the decrease in P was greater for the soil-wet residuals mixture compared to the soil mixed with the freeze-thaw dewatered residual.

Original supernatants and freezates (that is, liquid solution after a freeze-thaw cycle) were tested for organic parameters, including TOC, instantaneous trihalomethanes (THMs), and THM formation potential (THMFP). After freezing and thawing, the values for all parameters were affected. As expected, total THM (TTHM) values were greatly reduced for all the freezates due to the volatile nature of the TTHM constituents. The exposure to air, possibly combined with the effects of the latent heat of solidification, likely caused these reductions. TOC values for all freezates increased, as did the THMFP values for two of the three freezates.

Dempsey (1993) found that the concentrations of the metals in the supernatants of residuals were much less than 1 percent of the total concentrations, except for manganese. This indicated that the metals in the raw residuals were predominantly associated with the solid phases. There was an increase in the concentrations for some of the metals in the freezates (for all three residuals) that may be attributed to the freeze-thaw process, indicating a release from the solid to the liquid phase. However, after three weeks, the metals data revealed that most values returned to near original supernatant levels. Aluminum concentrations in the freezate were not higher than the raw residual supernatant, but the concentrations of lead, copper, and zinc in the freezates were typically greater than in the raw residual supernatants.

TELEPHONE SURVEY

The Water Industry Database (WIDB), which was created in 1992 by the American Water Works Association (AWWA) to provide the drinking water community with detailed information on the water industry as a whole, was utilized to identify those utilities using nonmechanical dewatering systems. There were 96 plants identified in this database as using nonmechanical residuals dewatering practices. Figure 1.1 shows the locations of those plants using sand drying beds, while Figure 1.2 illustrates the locations of those plants using freeze-thaw systems. Figure 1.1 indicates that sand drying beds are found in all areas of the country, although the majority of these are concentrated in the east; Figure 1.2 shows, not surprisingly, that freeze-thaw beds are primarily located in the cooler regions of the country, with the bulk of these being found in the eastern half of the nation.

A telephone survey was conducted of the 96 utilities listed in the WIDB as using nonmechanical systems to dewater their WTP residuals (namely, sand drying beds or freeze-thaw beds). Of those 96 utilities included in the survey, 84 chose to participate. The survey was devised to obtain candid opinions and ideas about nonmechanical dewatering practices from water industry professionals charged with operating them. It was aimed at obtaining a snapshot of the residuals handling practices of each of the utilities, as well as general information on plant flows, chemical usage, and water quality data. Furthermore, comments were solicited from the survey respondents on the performance of their particular dewatering system.

Figure 1.3 shows the treatment plant capacity distribution of the 96 utilities identified by the WIDB as using nonmechanical residuals dewatering techniques. The figure clearly indicates that the majority of these plants have capacities of less than 15 mgd, but that nonmechanical residuals dewatering is practiced at treatment plants encompassing a wide range of design capacities.

Although the Water Industry Database listed the 96 water treatment plants described as dewatering their residuals using either sand drying beds or freeze-thaw beds, this telephone survey revealed that these plants actually use a variety of nonmechanical dewatering systems. Moreover, it became apparent as the survey progressed that the definitions of what constituted a given dewatering process were ambiguous. Careful examination of the responses received in the telephone survey, coupled with clear definitions of the various nonmechanical dewatering systems as presented previously, allowed for categorization of the dewatering strategies used by the responding utilities as shown in Figure 1.4. The figure indicates that the largest percentage of utilities surveyed (35 percent) employ lagoon storage for residuals management; a further 28 percent use sand drying beds. The remaining utilities use dewatering lagoons, solar drying beds, freeze-thaw beds, freeze-thaw lagoons, or some combination of these.

Problems associated with nonmechanical dewatering systems described by utilities were generally categorized as problems relating to: (1) weather/climate, (2) capacity, (3) ultimate disposal, and (4) maintenance and equipment issues. Most utilities reported good performance during the warm months, but much poorer performance in the winter. A number of utilities indicated a need for additional capacity in their nonmechanical dewatering systems, particularly during winter when drying times are prolonged. Others noted that they experienced increases in plant production (and

therefore increased residual loadings) but had inadequate dewatering capacity to effectively handle the residuals. Expression of concerns regarding ultimate disposal of residuals was typical in the telephone survey, both for the shrinking number of disposal options available and for the rising hauling and tipping fees charged by landfills or monofills. Lastly, issues related to general operation and maintenance of nonmechanical dewatering systems, such as cleaning and sand replacement, were found to be significant concerns to utilities. Several utilities, for example, noted the need to protect underdrains from being crushed during cleaning with heavy equipment; others cited the importance of proper operation and maintenance of residuals pumps.

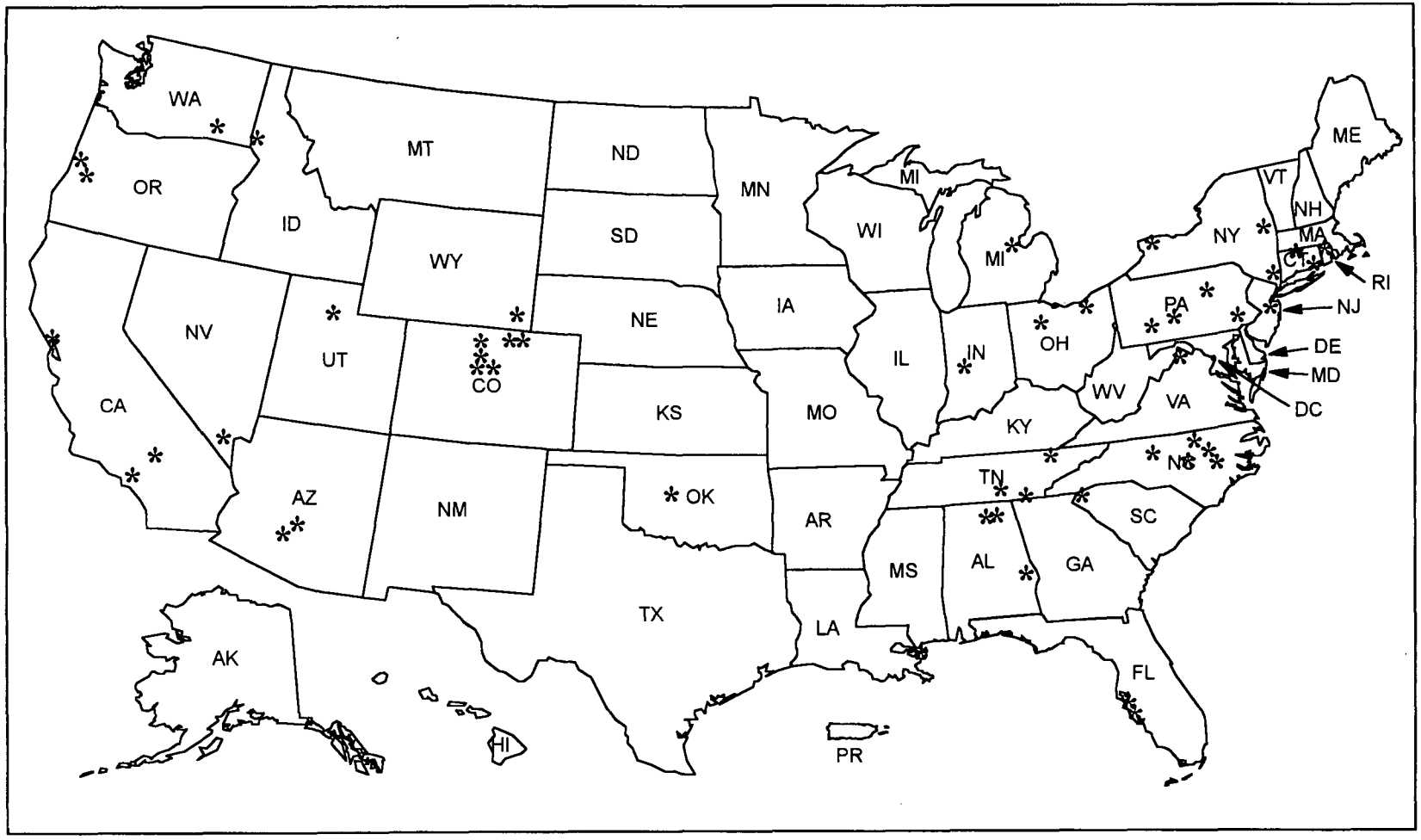

Figure 1.1 Plants identified in the WIDB as using sand drying beds for residuals dewatering

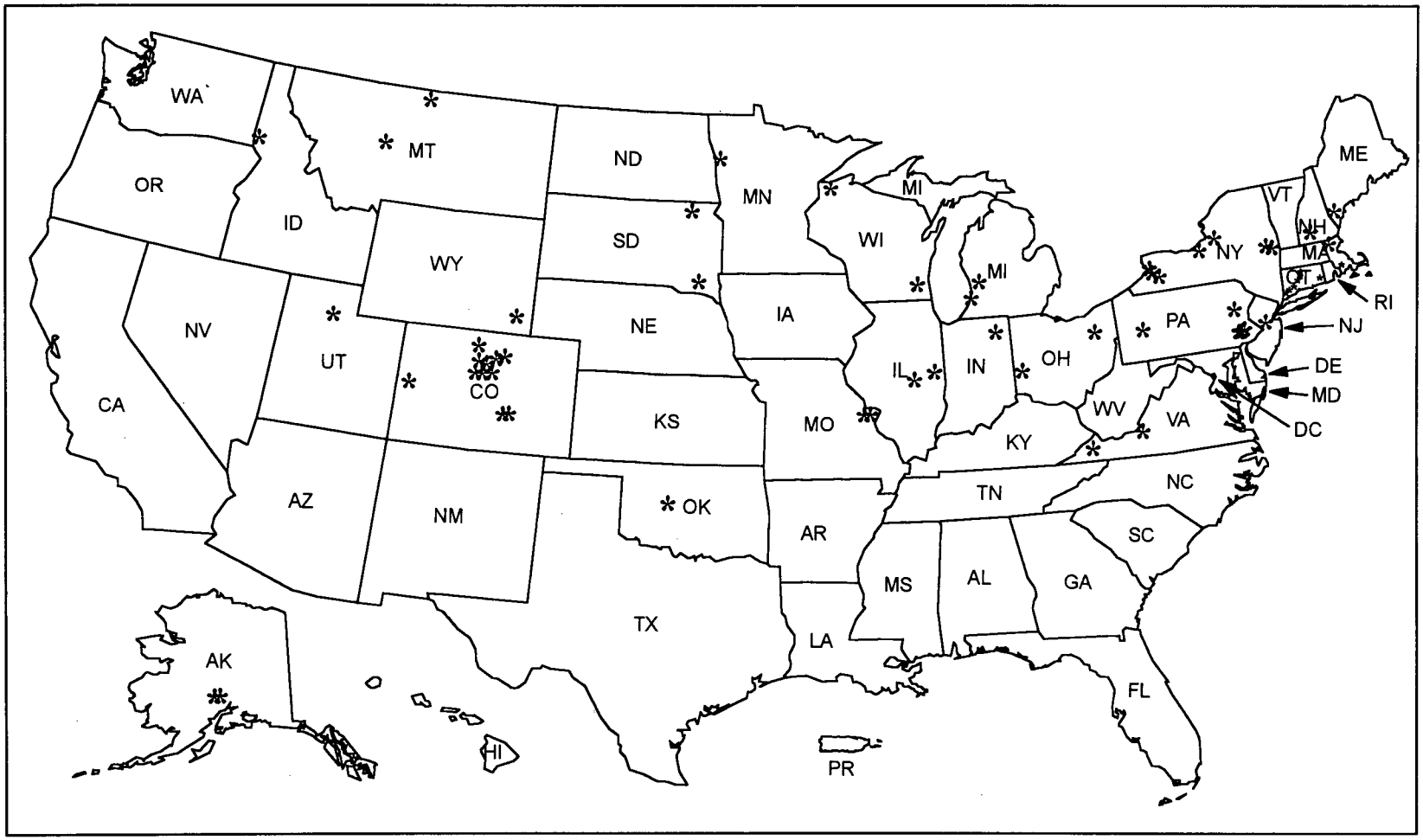

Figure 1.2 Plants identified in the WIDB as using freezing and thawing for residuals dewatering

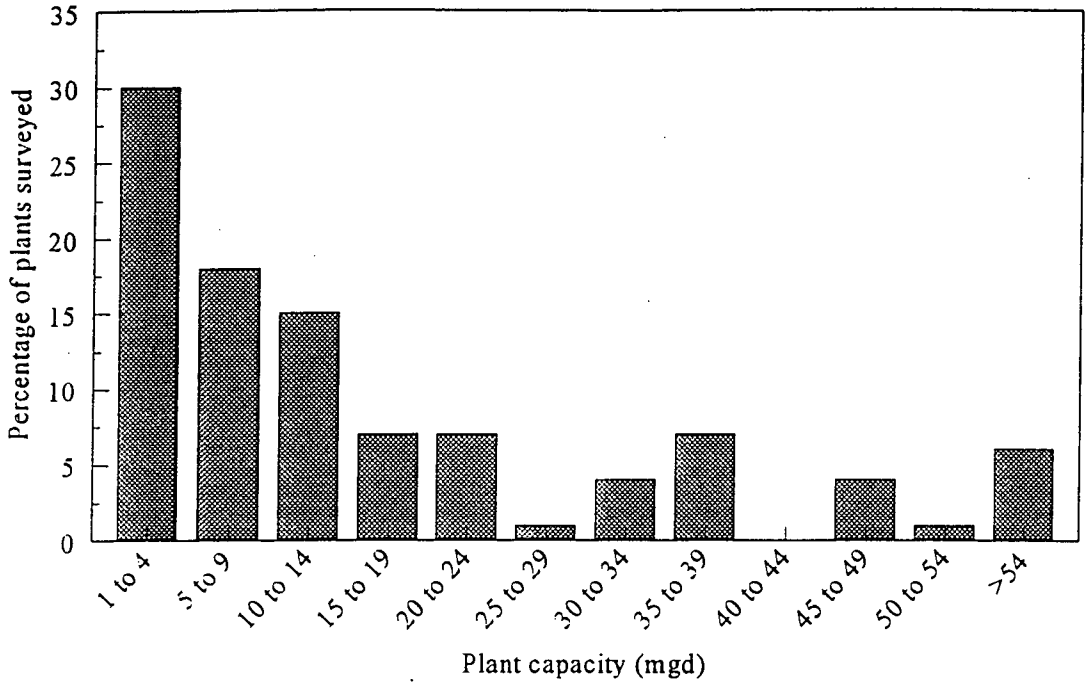

Figure 1.3 Size of plants in nonmechanical dewatering telephone survey

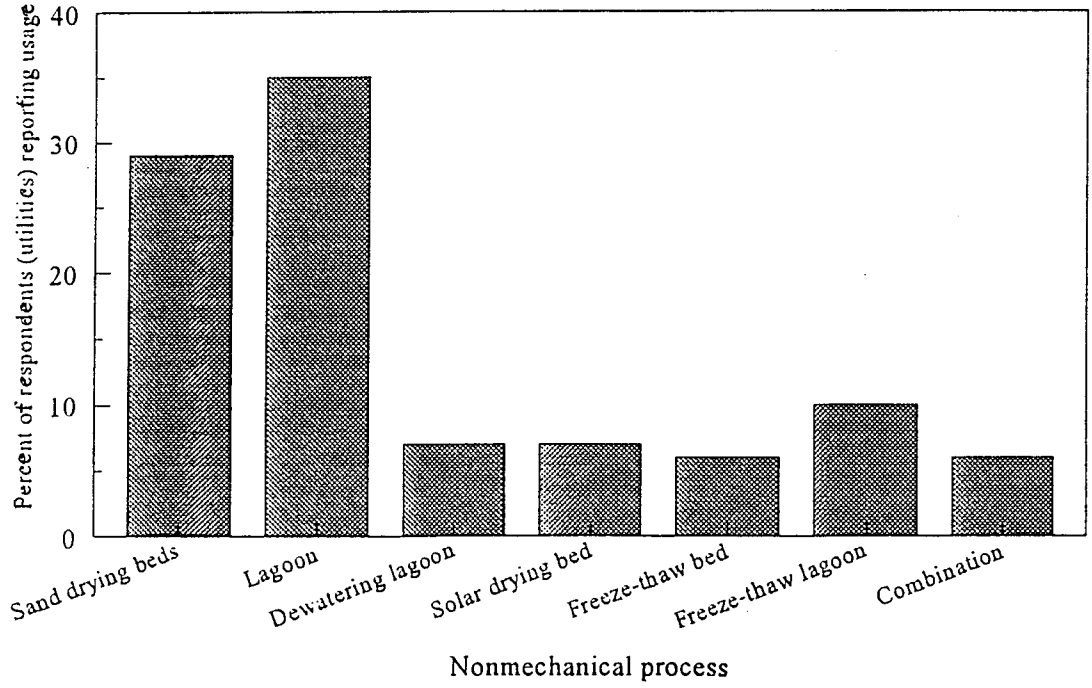

Figure 1.4 Nonmechanical processes employed for dewatering WTP residuals

CHAPTER 2
EXPERIMENTAL METHODS

INTRODUCTION

Nonmechanical dewatering of residuals is a two step process consisting of first, the removal of free water through drainage and decanting, and second, the drying of the remaining residuals through evaporation. One key parameter in optimizing the nonmechanical dewatering process, then, is to maximize the removal of free water from the residuals. The rate of free water release is influenced to a large extent by the residuals' characteristics, chemical conditioning, and freezing.

These residuals drainage characteristics were quantified in this research by laboratory tests including CST, TTF, SR to filtration, and particle size distribution. In laboratory testing, qualitative relationships have been established between the results for some of these tests and residuals characteristics. For example, the SR test is commonly used to evaluate the effect of chemical conditioning on the dewatering performance of a particular residual in the laboratory. To date, however, there has not been a good correlation shown between the results of these tests and the rate of free water release in actual nonmechanical dewatering operation, nor has there been any direct correlation with mechanical dewatering performance.

Part of this research was directed at analyzing a number of samples of residuals from different utilities around the country using the four tests listed above. The purpose of this extensive testing was not only to develop a database of residuals characteristics that could be used by investigators in future research and by utilities in comparing their residuals to others, but also to determine if any correlations could be established between the results of these tests and actual full-scale performance of nonmechanical dewatering systems.

One of the shortcomings of the published results of these tests is that standard procedures are not always followed. For example, a review of the literature indicates that the amount of vacuum applied during the SR test is not standard, although the test is commonly used and its results reported on by researchers. In this chapter, the four tests used are described, and the standard procedures followed in this research project are discussed. The actual methods are included in Appendix A for reference.

Sample Collection

A large volume (5 gal) at a 2 percent total solids concentration (TS) for coagulant residuals and 10 percent total solids concentration for lime residuals was collected from each plant for analysis. If a 2 or 10 percent sample was not available, the concentration was adjusted to 2 percent or 10 percent in the laboratory before the analyses were done.

LABORATORY TEST PROCEDURES

CST Test

The CST test is a fast and relatively simple test that is performed to determine the rate of free water release from a residual sample. The test is especially useful for comparing the CST characteristics of different residuals and for optimizing polymer conditioning of residuals. The test consists of measuring the time in seconds for free water to travel 1 cm when a 5 to 7 mL sample of residuals is placed in a special cylinder which is located on a Whatman number 17 chromatography paper (Whatman International, Ltd., Springfield Mill, Kent, England). As the free water drains from the residuals through the chromatography paper it passes by an electronic sensor that activates a timer. The timer stops when the free water reaches a second electronic sensor, 1 centimeter away. The time, in seconds, recorded by the instrument is the CST. A drawback of this method is that it requires the use of a specialized instrument, the CST meter. Narrow and wide bowls are available for the test. In this research the narrow bowl was used as it had previously been found to be more useful (Cornwell et al. 1987).

SR to Filtration Test

The resistance to fluid flow exerted by a cake of unit weight of dry solids per unit area is defined as specific resistance (SR). In order to evaluate SR, a sample of residuals is subjected to a vacuum using a Buchner funnel apparatus (Corning Incorporated, Corning, N.Y.). Typically,

100-mL portions of residuals are added to the Buchner funnel which is lined with a paper filter, and a vacuum is applied to the filter apparatus. In this research a Whatman number 4 filter paper was used and a vacuum of 0.6 atm was applied. The volume of filtrate generated at various times is recorded. This procedure is continued until enough water has been drawn out to produce cracking in the cake on the filter paper and subsequent loss of vacuum.

SR can be divided into two components—the resistance due to the residual cake and that due to the supporting filter medium. In this application, the resistance due specifically to the residual cake is of interest. An equation based on the Carmen-Kozenky equation for flow through porous media can be developed to describe the flow through a residual cake and supporting media.

TTF Test

A simplification of the SR test is the time to filter (TTF) test. This test is set up with the same Buchner funnel apparatus as the SR test but is much simpler to run. The only data collected is the amount of time it takes for one-half of the sample volume to filter. Vacuum can be applied to the sample; for all work done in this research, a vacuum of 0.5 atm was used. The result is expressed in seconds. For this research, 100-mL volume samples were analyzed.

Particle Size Distribution Analysis

Many methods exist to count and size particles in a sample. Most commonly used in the water industry are analysis by microscope, resistance based particle size analyzers and laser light blockage based particle size analyzers. For residuals analysis, some researchers have used laser light blockage based particle size analyzers, but these instruments have limitations that make them difficult to use in this application. The instruments have an upper concentration limit of around 15,000 particles/mL. Residual samples have more particles than these limits. In order to analyze residuals samples on these instruments, then, the sample must be diluted to an extent that may impact the reliability of the results. In addition, the samples are often pumped through the instruments, which could cause particle shearing.

For this research, particle size distribution was analyzed using a modification of a test commonly used in soils research—the hydrometer test (ASTM D422-63). The test measures particles smaller than 0.075 millimeters, including silt and clay particles (0.05 to 0.001 mm). Since particles of this size are predominant in water plant residuals, the test is applicable for analyzing residual samples.

The test is based on the theory that solid particles dispersed in suspension settle at different rates based on the size and specific gravity of the particles. In the standard hydrometer test for soils, a 50-g sample of soil material is dried and weighed prior to analysis. The dried sample is then mixed with a deflocculating agent to prevent flocculation of small particles through Brownian motion during the test. For this research it was found that the drying portion of this test was impractical for residuals analysis since, when dried, the samples became strongly bonded and could not be separated into a suspension, even after prolonged soaking in the deflocculating agent. Further, a 50-g sample did not allow the hydrometer to sink into the suspension. Therefore, the ASTM method was modified by reducing the sample size to approximately 10 g and by eliminating the drying step. Instead, the sample was added directly to the deflocculating agent, and the amount of solids in the suspension was determined after the experiment. After the experiment was conducted, the sample was dried at 104°C and a determination was made of the amount of solids.

After mixing the sample with the deflocculating agent, the mixture was placed in a graduated cylinder with the hydrometer. The hydrometer gives a measurement of the amount of material that has settled past the zone of measurement during a given period of time. Elapsed time and hydrometer readings are recorded during the test. Settling velocity can then be calculated as the quotient of distance and time. Particle diameter is then determined from the velocity data through an application of Stokes Law.

Results of the hydrometer test are usually plotted on semilogarithmic paper. As in Figure 2.1, percent finer is plotted versus particle diameter, with particle diameter, or grain size, plotted on the logarithmic scale. With the information presented in this format, percentages of fine sand-, silt-, and clay-sized particles as well as median diameter, d_{50}, are easily obtained. The amount of each fraction

is plotted as a cumulative distribution requiring some interpretation to obtain each fraction. The amount of fine sand, silt, clay, and the d_{50} can be determined as follows:

Percent fine sand	=	Percent finer at 0.075 mm
Percent silt	=	Percent of fine sand - percent finer at 0.002 mm
Percent clay	=	Percent finer at 0.002 mm
Median particle size (d_{50})	=	Diameter corresponding to 50 percent finer

Various size classifications are used for soils. In this report, the separation limits used were:

Classification	*Diameter (mm)*
Fine sand	Larger than 0.075 mm
Silt	Between 0.075 mm and 0.002 mm
Clay	Less than 0.002 mm

PILOT DEWATERING TESTS

The primary dewatering mechanisms occurring in nonmechanical dewatering are (1) the drainage of free water, (2) the drying of the residuals due to evaporation, and (3) the separation of chemically and interparticle bound water due to freeze-thaw effects. Regardless of the residuals dewatering process (i.e., sand drying beds, dewatering lagoons, or freeze-thaw beds), the removal of free water by draining or decanting should be maximized to obtain an efficient dewatering process. This would allow the least amount of water to be removed by evaporation, which is the process requiring the longest time frame.

In order to maximize the removal of free water, it is important to characterize the interrelationship between the residuals type, solids concentration, loading rate, and polymer conditioning. For example, applying residuals onto a drying bed at 3 lb/ft^2 can be accomplished at 2 percent solids with a 29-in. depth, or at 4 percent solids and a 14.5-in. depth. Each condition, however, would result in a different drainage rate and volume, which ultimately affects the overall efficiency and performance of the dewatering process.

Pilot dewatering tests were performed to characterize the relationship between the operating parameters. These tests were performed on alum, ferric, polyaluminum chloride, and lime residuals. The test laboratory equipment consisted of 2-in. diameter acrylic cylinders, approximately 6 ft tall. Testing was done to determine the acceptable minimum diameter of the columns. Clearly, the smallest diameter is preferred in order to minimize the quantity of residuals required. To validate the use of 2-in. diameter test cylinders in this research work, several comparisons were performed with 6-in. diameter test cylinders. These data are shown in Figure 2.2 and indicate a good correlation with an R^2 value of 0.91. These data suggested that the 2-in. diameter test cylinder could predict the drainage volume as well as the 6-in. diameter test cylinder. (In Chapter 4 the relationship between pilot column results and full-scale results is presented.) At the range that was tested in this research (40 to 90 percent drainage) the results from the two column diameters matched fairly well with an R^2 of 0.91. The 2-in. diameter columns were used in this study. The cylinders were open at the top and had a ¼-in. drain valve on the bottom to remove water that would drain through the media. Each cylinder had a 6-in. gravel base and an 18-in. sand media. Gradations of the gravel and sand were as follows:

- 1/8-in. diameter gravel (3-in. layer)
- 1/16-in. diameter gravel (3-in. layer)
- 0.55 to 0.65 mm sand (9-in. layer)
- 0.45 to 0.55 mm sand (9-in. layer)

Figure 2.3 shows the typical arrangement of the dewatering test cylinders. A total of seven test cylinders were used simultaneously. This arrangement allowed for one test cylinder to simulate the actual operating parameters (applied depth, loading rate, and polymer conditioning) used by a particular utility, while the six other test cylinders were operated at varying conditions. Specifically, the loading rate was adjusted and polymer was added to the residuals. The initial solids concentration was held constant among all seven columns and was tested as received.

The operating procedures for the pilot dewatering tests consisted of collecting a representative batch sample of residuals from a water treatment plant's dewatering process as the residuals were applied to the on-site dewatering system. A total solids analysis was performed on the sample in order to load the pilot columns with a known solids concentration at various loading

rates. Also, the CST of the residuals was measured, both unconditioned and conditioned with polymer. If the utility used a polymer, then that polymer was used at a dose based on CST testing. If the utility did not use a polymer, then the researchers selected a polymer type and dose based on CST. Polymer was added to the residuals during mixing prior to loading to the column. For each solids loading rate, the volume of residuals was calculated and measured in graduated cylinders. The volume was then poured slowly into the test cylinders to prevent disturbing the sand layer.

During the dewatering test, the volume of water drained through the sand and gravel media was collected and measured to calculate the volume of free water removed as a percentage of the total initial volume. Any supernatant present in the dewatering test cylinders was removed and added to the drainage volume.

Results from the pilot dewatering tests provided information on the following:

- Drainage volume quantification of a utility's current dewatering process,
- Optimization of the drainage volume as a function of solids loading rate,
- Impact of polymer on the drainage volume and drainage rate,
- CST predictions of the dewatering efficiency,
- Performance of different residual types (alum, lime, ferric, PACl)

FIELD TEST PROCEDURES

Field tests were performed to complement the pilot dewatering tests. The field test procedures consisted of observing and documenting the performance of a utility's dewatering process at each site under normal operating conditions (i.e., how the beds performed when loaded per the water plant's "standard" operating practices). Typical data collected for each site visit included the following:

- Drying bed size, design criteria, physical features, sand effective size.
- Volume of solids loaded onto the bed.
- Composite solids concentration of sludge loaded onto the bed and CST.
- Depth of sludge on the bed as a function of time to document the drainage rate over a one week period.

- Weekly analysis of solids concentration on the bed from the time the sludge stopped draining until the bed was cleaned.
- Local net pan evaporation data to correlate solar evaporation, wind effects, and rainfall to the drying pattern of the sludge on the bed.
- Water plant raw water and chemical operating conditions relative to the sludge loaded onto the bed (i.e., raw turbidity, color, TOC, coagulant, lime, powdered activated carbon, polymer, etc.).

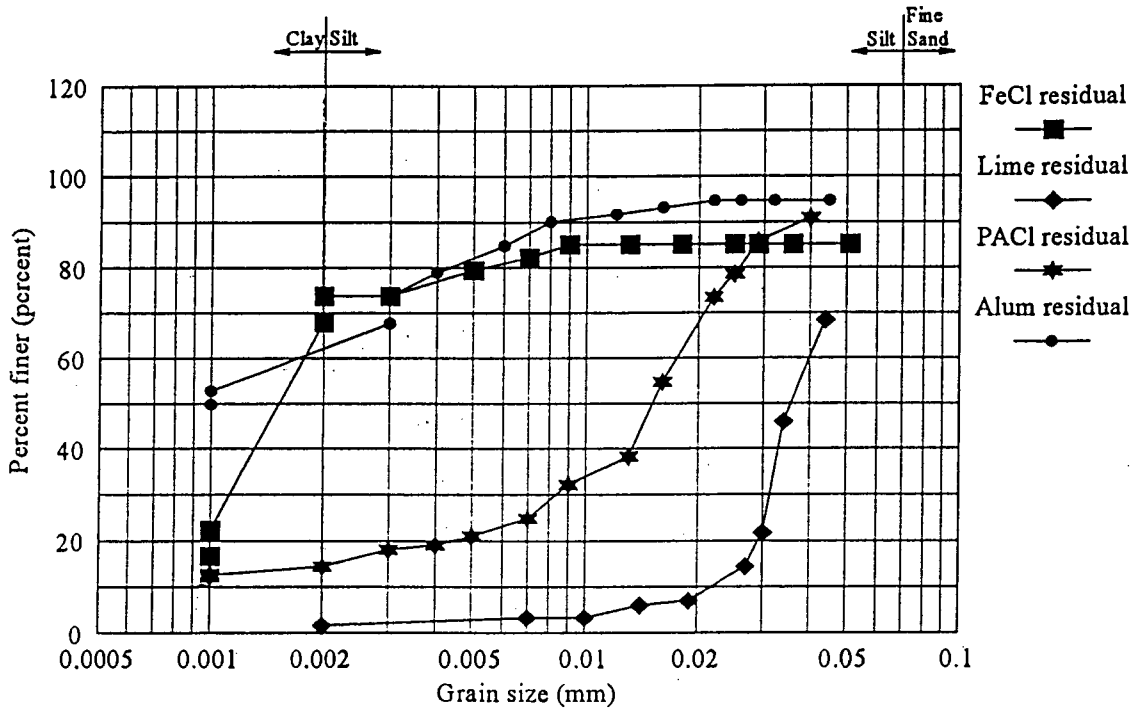

Figure 2.1 Typical grain size analysis: Hydrometer method

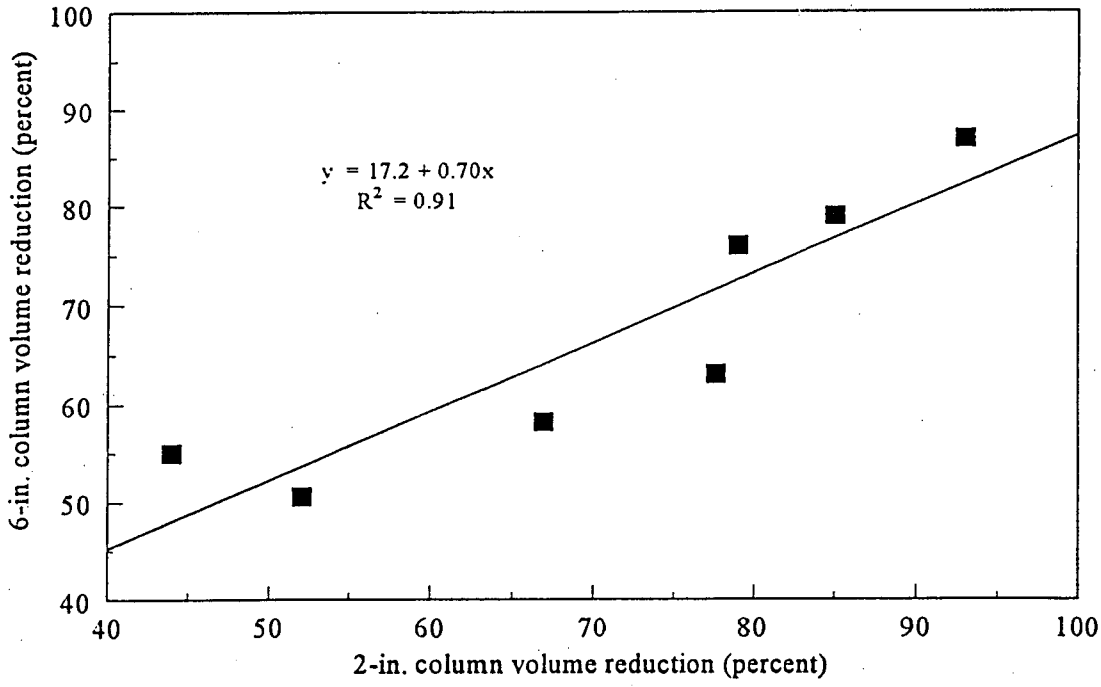

Figure 2.2 Comparison of volume reductions for 2-in. and 6-in. columns

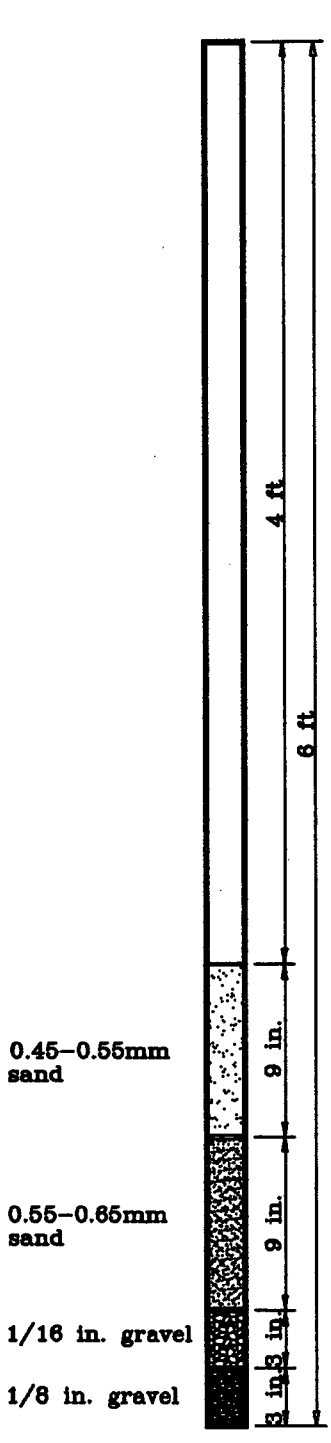

Typical media arrangement

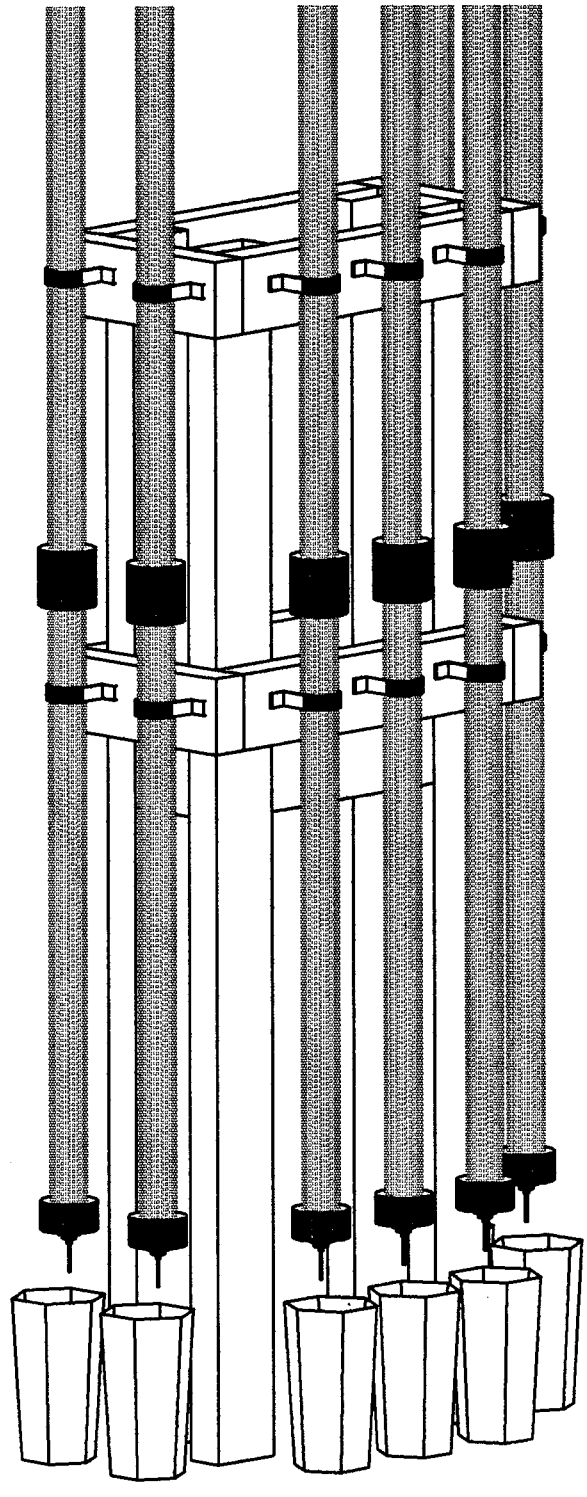

Pilot column arrangement

Figure 2.3 Pilot dewatering system

CHAPTER 3
LABORATORY RESIDUALS CHARACTERIZATION STUDIES

INTRODUCTION

Residuals samples for general characterization were obtained from 61 water treatment utilities across the United States. Collecting this number of samples allowed several samples to be obtained from various source water quality and residual types. Two goals were set in obtaining these samples: first, to ascertain the applicability of small scale laboratory tests to full-scale dewatering performance and secondly to develop a database on dewatering performance of many of these residuals types.

Samples were obtained from various utilities across the United States. Figure 3.1 shows the approximate location and corresponding sludge type for the participating utilities. Diversity in geography and source water quality was a goal in obtaining samples from many locations. As the figure shows, samples were obtained from most regions of the United States.

SUMMARY STATISTICS

Summary statistics were calculated for measured values of CST, TTF, and SR. In addition, frequency distribution plots were created for sample percentages of sand, silt, and clay; specific gravity; and sludge textural classification.

CST, TTF, AND SR

Table 3.1 presents summary statistics for each of the measured drainage parameters. The table presents the data by residual type and gives the number of samples (n), mean value (mean), and sample standard deviation (s^2) for each of the drainage parameters.

Table 3.1

Summary statistics for drainage parameters

	CST (s)			TTF (s)			SR ($10^9 s^2/g$)		
Sludge type	n	mean	s^2	n	mean	s^2	n	mean	s^2
Alum	38	194.1	195.4	38	319.5	412.6	38	16.1	21.7
Ferric	9	103.0	64.5	9	104.7	79.5	9	6.5	8.3
PACl	5	289.8	258.8	5	410.9	562.5	5	14.1	11.2
Lime	9	70.0	34.5	9	34.3	20.4	9	0.55	0.84

n = number of samples
s^2 = standard deviation

Interestingly, the general results from all the tests were similar. For example, lime residuals had the lowest CST, TTF, and SR. The tests would predict the ease of dewatering order to be lime, ferric, alum and PACl.

Probability plots for each of the above parameters were also developed. This type of plot provides a means of comparison between a particular sample and the entire database. The data were divided into either a coagulant residual (alum, ferric, PACl) or a lime residual. Figures 3.2 to 3.7 show the results for CST, TTF, and SR. As an example in using the plots, 90 percent of all the coagulant residuals samples had a CST of less than about 400 s^{-1}. Therefore, if utility personnel ran a CST on their residual and got a value of 700 s^{-1} at a 2 percent TS, they might expect that their residual would be difficult to dewater compared to other utilities.

Percentages of Sand, Silt, and Clay

Hydrometer analyses of each of the characterization samples determined the percentages of sand-, silt-, and clay-sized particles contained in each sample. These particle sizes are defined as follows: sand sized particles are particles with diameters larger than 0.075 mm, silt sized particles have diameters between 0.075 and 0.002 mm, clay sized particles have diameters less than 0.002 mm. It is impractical to measure diameters less than 0.001 mm. Some of the samples had significant distribution of diameters below this lower limit, and therefore d_{20} or even d_{50} could not be calculated.

As a result of analyzing the characterization samples, frequency of occurrence plots of each of these fractions were constructed. Figures 3.8 and 3.9 show distribution of average particle diameters for the coagulant and lime residuals, respectively. The results are presented as percentages of the total number of samples collected.

There also appears to be a great deal of variance associated with the sand, silt, and clay data. Standard deviations are quite large for the measurements. Each of the samples collected represent a variety of both raw water characteristics and treatment processes. Due to large variations in both source water quality and treatment process, it seems only reasonable that this amount of variation would be encountered. (Information on the individual residuals samples analyzed is presented in Tables 3.2 through 3.5.)

Specific Gravity

During hydrometer testing, the specific gravity of the solid material contained in the sludge sample was determined. All specific gravities measured were between 2.0 and 3.0. This range corresponds to the range that one would expect when determining specific gravities for soils. Soils classified as sands typically have specific gravities of about 2.65. Clays and silty soils have specific gravities that can range from 2.6 to 2.9. Samples analyzed for specific gravity indicated that the majority of the specific gravities fell below 2.6. In fact, for the WTP residuals (solid material) that were sampled, the average specific gravity was 2.39. Figure 3.10 shows the distribution of specific gravity for the lime and coagulant residuals. It is important to make the distinction between specific gravity of the solid material and the specific gravity of the residual solution. Specific gravities reported here represent the specific gravity of the dry solid material contained in the sample and vary between 2.0 and 3.0. Specific gravities of residual itself (water and solids) were not measured but are typically close to 1.0.

Table 3.2

Physical properties of alum sludges

Sludge sample location	Geotechnical properties					
	Sand content (percent)	Silt content (percent)	Clay content (percent)	d_{50}* (mm)	Specific gravity	Classification
Harwood's Mill WTP, Newport News, Va.	40.00	45.00	15.00	0.011	2.94	Loam
Main Street WTP, Yuma, Ariz.	23.20	59.90	16.90	0.023	2.51	Silty loam
Chasteen's Grove WTP, Loveland, Colo.	15.10	50.00	34.90	0.004	2.58	Clay
Ten Mile WTP, Helena, Mont.	36.10	45.00	18.90	0.022	2.33	Loam
Phoenix WTP, Phoenix, Ariz.	25.90	60.70	13.40	0.020	2.31	Silty loam
Florence WTP, Omaha, Neb.	15.30	72.00	12.70	0.015	2.45	Silty loam
Butterfield WTP, Pasco, Wash.	30.70	58.50	10.80	0.032	2.36	Silty loam
Elizabeth City WTP, Elizabeth City, N.C.	21.80	63.40	14.80	0.039	2.49	Silty loam
Rivanna South WTP, Charlottesville, Va.	8.00	76.40	15.60	0.005	2.39	Silty loam
Moore's Bridge WTP, Norfolk, Va.	17.50	18.40	64.10	0.000	2.05	Clay
City of Lubbock WTP, Lubbock, Texas	13.60	71.00	15.40	0.022	2.29	Silty loam
Chesapeake WTP, Chesapeake, Va.	18.00	24.00	58.00	0.001	2.30	Clay
Columbus WFP, Columbus, Ga.	24.10	64.80	11.10	0.007	2.71	Silty loam
City of Sacramento WTP, Sacramento, Calif.	17.70	35.00	47.30	0.003	2.87	Clay
Chester Water Authority WTP, Nottingham, Pa.	28.20	36.70	35.10	0.003	2.13	Clay
Crumb Creek WTP, Bryn Mahr, Pa.	0.50	44.20	55.30	0.002	2.32	Clay
Woodacre WTP, Woodacre, Calif.	17.60	70.80	11.60	0.008	2.33	Silty loam
Fairfield WTP, Fairfield, Calif.	24.00	31.20	44.80	0.003	2.30	Clay
Bollman WTP, Contra Costa, Calif.	18.00	56.00	26.00	0.003	2.59	Silty loam
Fremont WTP, Fremont, Calif.	9.70	76.00	14.30	0.015	2.45	Silty loam
Lewiston WTP, Lewiston, Idaho	30.70	60.50	8.80	0.012	2.16	Silty loam
Tennessee-American WTP, Chattanooga, Tenn.	12.30	74.40	13.30	0.006	2.06	Silty loam
Eureaka Springs WTP, Eureaka Springs, Ariz.	25.60	68.20	6.20	0.003	2.07	Silty loam
A.B. Jewel WTP, Tulsa, Okla.	10.20	58.40	31.40	0.008	2.44	Clay
Goldsboro WTP, Goldsboro, N.C.	18.10	66.10	15.80	0.013	2.24	Silty loam
Richmond WTP, Richmond, Va.	25.00	60.00	15.00	0.031	2.48	Silty loam
Betasso WTP, Boulder, Colo.	19.00	53.00	28.00	0.012	2.31	Silty clay loam
Sweeny WTP, Wilmington, N.C.	9.70	42.10	48.20	0.002	2.29	Clay
Manchester WTP, Manchester, N.H.	18.00	26.00	56.00	0.000	2.04	Clay
P.O. Hoffer WTP, Fayetteville, N.C.	16.60	50.50	32.90	0.004	2.44	Clay

(continues)

Table 3.2

Physical Properties of alum sludges (continued)

Sludge sample location	Geotechnical properties: Sand content (percent)	Silt content (percent)	Clay content (percent)	d_{50}* (mm)	Specific gravity	Classification
Lake Chaplin WTP, Everett, Wash.	26.00	48.10	25.90	0.010	2.53	Clay loam
Ipswich WTP, Ipswich, Mass.	33.20	39.00	27.80	0.024	2.16	Clay loam
Tar River WTP, Rocky Mount, N.C.	19.80	8.50	71.70	0.000	2.26	Clay
Port Wentworth WTP, Savannah, Ga.	19.30	56.90	23.80	0.028	2.25	Silty loam
Lake Kilby WTP, Portsmouth, Va.	14.40	35.90	49.70	0.001	2.21	Clay
E.M. Johnson WTP, Raleigh, N.C.	12.50	54.40	33.10	0.008	2.07	Clay
York WTP, York, Maine	18.50	50.60	30.90	0.003	2.18	Clay
Lake Gaillard WTP, North Branford, Conn.	3.00	86.00	11.00	0.005	2.05	Silty loam

*Values of 0.000 indicate that the d_{50} could not be calculated because more than 50 percent of the material had a diameter less than 0.001 mm.

Table 3.3

Physical properties of ferric sludges

Sludge sample location	Geotechnical properties: Sand content (percent)	Silt content (percent)	Clay content (percent)	d_{50} (mm)	Specific gravity	Classification
Sourdough Canyon WTP, Bozeman, Mont.	56.00	31.20	12.80	0.049	2.37	Sandy loam
Plant 1, Louisville, Ky.	34.00	49.10	16.90	0.026	2.80	Silty loam
Plant 2, Louisville, Ky.	36.70	44.90	18.40	0.003	2.84	Silty loam
Sweetwater Authority WTP, Spring Valley, Calif.	15.90	57.40	26.70	0.003	2.35	Silty clay loam
Manatee County WTP, Bradenton, Fla.	37.30	23.10	39.60	0.006	2.44	Clay
Baxter WTP, Philadelphia, Pa.	1.40	60.20	38.40	0.003	2.45	Silty clay
Queen Lane WTP, Philadelphia, Pa.	8.30	58.90	32.80	0.003	2.27	Silty clay
Belmont WTP, Philadelphia, Pa.	12.00	69.20	18.80	0.003	2.30	Silty loam
Winchester WTP, Winchester, Va.	14.00	51.00	35.00	0.005	2.08	Clay

Table 3.4

Physical properties of PACl sludges

Sludge sample location	Geotechnical properties					
	Sand content (percent)	Silt content (percent)	Clay content (percent)	d_{50} (mm)	Specific gravity	Classification
St. Bernard Parish WTP, Chalamette, La.	9.00	76.60	14.40	0.015	2.53	Silty loam
Frostburg WTP, Frostburg, Md.	31.30	55.00	13.70	0.003	2.22	Silty loam
Roxboro WTP, Roxboro, N.C.	0.70	45.50	53.80	0.001	2.26	Clay
Blacksburg-Christiansburg WTP, Blacksburg, Va.	7.00	88.00	5.00	0.004	2.08	Silty loam
Albany WTP, Albany, N.Y.	14.50	61.50	24.00	0.003	2.56	Silty clay loam

Table 3.5

Physical properties of lime sludges

Sludge sample location	Geotechnical properties					
	Sand content (percent)	Silt content (percent)	Clay content (percent)	d_{50} (mm)	Specific gravity	Classification
Bismark WTP, Bismark, N.D.	29.50	66.30	4.20	0.027	2.71	Silty loam
City of Wichita WTP, Wichita, Kan.	6.70	90.10	3.20	0.012	2.52	Silty loam
Platte WTP, Omaha, Neb.	12.80	79.75	7.45	0.016	2.50	Silty loam
Ann Arbor WTP, Ann Arbor, Mich.	8.70	81.40	9.90	0.010	2.54	Silty loam
Austin WTP, Austin, Texas	1.30	88.30	10.40	0.006	2.45	Silty loam
MWD 1 WTP, Kansas City, Kan.	20.00	65.50	14.50	0.022	2.63	Silty loam
Laverne WTP, Laverne, Calif.	11.00	42.80	46.20	0.002	2.26	Clay
Dallas County WTP, Dallas, Texas	4.80	77.30	17.90	0.005	2.50	Silty loam
Grand Forks WTP, Grand Forks, N.D.	21.70	69.10	9.20	0.026	2.40	Silty loam

MWD 1 = Mission Water District number 1

Textural Classification

Using the determined values for the percentages of sand, silt, and clay, the textural classification of each of the samples analyzed was determined. Textural classification refers to a soil's (or in this case sludge's) surface appearance. Textural classification was used as a convenient method for grouping samples that were found to have similar quantities of sand-, silt-, and clay-sized particles. Figures 3.11 and 3.12 show the distribution of the samples collected that were found to be either sandy loam, silty loam, silty clay loam, silty clay, loam, clay loam, or clay. Coagulant residuals tended to be sized similarly to either silty loams (45 percent of the samples) or clay (35 percent of the samples). The lime residuals were almost all classified as silty loam.

Residuals with similar classifications have similar physical characteristics. Silty loams in general have higher silt contents, larger average particle diameters, and small percentages of clay and fine sand. Clays generally have large percentages of clay sized particles, smaller average particle sizes, and small percentages of sand and silt. Results of the classification determination of each of the samples are listed in Tables 3.2 to 3.5.

DRAINAGE CHARACTERISTICS

Drainage of free water from the samples was quantified in three ways: (1) CST of each sample was measured and recorded, (2) TTF for each of the samples was determined, and (3) SR to filtration was measured. One additional parameter was quantified, the filterability constant, which is based on CST and solids concentration.

The following correlations and relationships would be useful to a utility in comparing various test results or in selecting which tests to run. It should be noted that the researchers attempted to make several correlations between the physical parameter tests and the drainage characteristics tests to help explain the data, such as particle size versus CST or SR versus coagulant content in the residual. Unfortunately, no relationships were evident other than the relationships between the drainage tests themselves as indicated in the following sections.

CST Versus TTF

Figures 3.13 and 3.14 present the relationships between CST and TTF for coagulant and lime residuals. A fairly good agreement is found between CST and TTF. The observed relationship between CST and TTF is CST = 56 + 0.52 TTF with R^2 = 0.89 for coagulant residuals and CST = 32.1 + 1.1 TTF with R^2 = 0.43 for lime residuals. Since the TTF test is easy to perform with minimum equipment, the correlation would suggest that a utility could use the TTF test in place of a CST test and obtain similar drainage predictions.

CST Versus SR

Figure 3.15 shows the relationship between CST and SR. The plot appears to be fairly linear for coagulant residuals. No correlation was attempted for lime residuals due to the data scatter in the few points. The relationship between CST and SR for coagulant residuals is CST = 70.4 + 8.3 SR with a corresponding R^2 value of 0.69. Since SR is a much more involved test than TTF, TTF would be preferred for routine utility characterization work.

Fairly good agreement between CST, TTF, and SR was found. Therefore, a utility could use any of these tests interchangeably and use the test which is most convenient to run.

Filterability Constant

Vesilind (1988) presented a model for what occurs during the performance of a CST test. He proposed that the rate at which water is released from the sludge material into the chromatography paper is a function of two distinct and separate processes. The first is absorption associated with the test instrument and the second is water release associated with the sludge material.

The absorption associated with the test instrument can be quantified as a function of the test apparatus and the chromatography paper. In terms of the test apparatus the flow of free water from the solids is a function of the bottom diameter area of the stainless steel reservoir, the permeability

of the chromatography paper used, and viscosity. The values and effects of each of these parameters can be evaluated and determined through simple measurements conducted on the test instrument. Viscosity is a function of temperature, so its value must be determined for each test conducted. Since in all likelihood these tests will all be conducted on the same piece of test equipment, an instrument constant can be evaluated.

This instrument constant accounts for the change in diameter between the first and second sets of electrodes used to measure the CST. It also quantifies the permeability of the chromatography paper and the effects on dewatering associated with the reservoir. This instrument constant is labeled Φ, and for all tests conducted in this study the Φ used was 0.012.

Vesilind further proposed that the water released from the sludge material is a function of solids concentration and viscosity. It has long been recognized that solids concentration has an effect on CST. The sludge concentration is directly proportional to the filterability constant. The filterability constant can be determined as follows:

$$\chi = \Phi\left[\frac{\mu SS}{CST}\right] \tag{3.1}$$

where

χ	=	filterability constant (kg^2/s^2m^4)
Φ	=	dimensionless instrument constant
μ	=	viscosity (centipoise)
SS	=	solids concentration (mg/L)

Tables 3.6 to 3.9 present the drainage results for each of the residuals tested and their filterability constant.

Table 3.6

Drainage properties of alum sludges

Sludge sample location	CST (s)	TTF (s)	SR ($10^9 s^2/g$)	χ ($10^{-6} kg^2/s^2m^4$)
Harwood's Mill WTP, Newport News, Va.	11.30	307.10	2.30	19.100
Main Street WTP, Yuma, Ariz.	27.10	16.70	1.30	8.000
Chasteen's Grove WTP, Loveland, Colo.	40.90	130.30	3.29	5.300
Ten Mile WTP, Helena, Mont.	50.60	42.30	4.20	4.300
Phoenix WTP, Phoenix, Ariz.	50.90	48.60	2.90	4.200
Florence WTP, Omaha, Neb.	51.90	48.91	0.73	4.200
Butterfield WTP, Pasco, Wash.	54.80	50.40	2.70	3.900
Elizabeth City WTP, Elizabeth City, N.C.	60.30	41.10	3.70	3.600
Rivanna South WTP, Charlottesville, Va.	69.40	117.00	1.10	3.100
Moore's Bridge WTP, Norfolk, Va.	82.50	283.30	18.20	2.600
City of Lubbock WTP, Lubbock, Texas	84.00	65.20	5.40	2.600
Chesapeake WTP, Chesapeake, Va.	84.50	660.00	3.70	2.600
Columbus WFP, Columbus, Ga.	92.10	169.20	15.80	2.400
City of Sacramento WTP, Sacramento, Calif.	104.60	45.60	4.60	2.100
Chester Water Authority WTP, Nottingham, Pa.	116.33	146.16	1.28	1.900
Crumb Creek WTP, Bryn Mahr, Pa.	116.60	133.70	12.80	1.900
Woodacre WTP, Woodacre, Calif.	134.80	165.20	13.70	1.600
Fairfield WTP, Fairfield, Calif.	152.70	70.20	9.20	1.400
Bollman WTP, Contra Costa, Calif.	155.90	121.30	1.20	1.400
Fremont WTP, Fremont, Calif.	163.50	166.30	8.00	1.300
Lewiston WTP, Lewiston, Idaho	167.30	228.30	0.33	1.300
Tennessee-American WTP, Chattanooga, Tenn.	176.10	168.10	1.53	1.200
Eureaka Springs WTP, Eureaka Springs, Ariz.	177.50	240.60	2.40	1.200
A.B. Jewel WTP, Tulsa, Okla.	177.80	231.40	15.20	1.200
Goldsboro WTP, Goldsboro, N.C.	181.80	314.10	25.40	1.200
Richmond WTP, Richmond, Va.	185.30	203.00	2.10	1.200
Betasso WTP, Boulder, Colo.	185.70	194.60	19.30	1.200
Sweeny WTP, Wilmington, N.C.	207.90	204.10	17.70	1.000
Manchester WTP, Manchester, N.H.	236.30	1,610.60	9.30	0.900
P.O. Hoffer WTP, Fayetteville, N.C.	246.20	327.40	32.80	0.900
Lake Chaplin WTP, Everett, Wash.	260.70	429.80	37.50	0.800
Ipswich WTP, Ipswich, Mass.	275.80	340.10	14.30	0.800

(continues)

Table 3.6 (continued)

Sludge sample location	CST (s)	TTF (s)	SR ($10^9 s^2/g$)	χ ($10^{-6} kg^2/s^2m^4$)
Tar River WTP, Rocky Mount, N.C.	394.00	479.60	38.90	0.600
Port Wentworth WTP, Savannah, Ga.	416.40	455.99	41.70	0.500
Lake Kilby WTP, Portsmouth, Va.	504.40	613.20	48.60	0.400
E.M. Johnson WTP, Raleigh, N.C.	844.80	1,210.00	70.50	0.300
York WTP, York, Maine	930.80	1,961.40	106.70	0.200
Lake Gaillard WTP, North Branford, Conn.	102.30	98.30	10.60	2.100

Table 3.7

Drainage properties of ferric sludges

Sludge sample location	CST (s)	TTF (s)	SR ($10^9 s^2/g$)	χ ($10\text{-}^6 kg^2/s^2m^4$)
Sourdough Canyon WTP, Bozeman, Mont.	24.20	18.40	1.40	8.900
Plant 1, Louisville, Ky.	44.80	43.60	2.70	4.800
Plant 2, Louisville, Ky.	45.20	43.90	3.10	4.800
Sweetwater Authority WTP, Spring Valley, Calif.	173.70	221.90	29.30	1.200
Manatee County WTP, Bradenton, Fla.	237.30	231.60	2.50	0.900
Baxter WTP, Philadelphia, Pa.	94.90	69.60	8.50	2.300
Queen Lane WTP, Philadelphia, Pa.	75.70	77.90	5.00	2.900
Belmont WTP, Philadelphia, Pa.	159.70	187.10	2.20	1.400
Winchester WTP, Winchester, Va.	71.80	47.60	4.20	3.000

Table 3.8

Drainage properties of PACl sludges

Sludge sample location	CST (s)	TTF (s)	SR ($10^9 s^2/g$)	χ ($10^{-6} kg^2/s^2m^4$)
St. Bernard Parish WTP, Chalamette, La.	120.70	78.70	0.15	1.800
Frostburg WTP, Frostburg, Md.	164.70	196.20	10.20	1.310
Roxboro WTP, Roxboro, N.C.	792.40	1,385.10	16.40	0.270
Blacksburg-Christiansburg WTP, Blacksburg, Va.	95.40	90.90	9.00	2.300
Albany WTP, Albany, N.Y.	276.00	889.10	30.70	0.780

Table 3.9

Drainage properties of lime sludges

Sludge sample location	CST (s)	TTF (s)	SR ($10^9 s^2/g$)	χ ($10^{-6} kg^2/s^2m^4$)
Bismark WTP, Bismark, N.D.	37.80	11.21	0.01	28.600
City of Wichita WTP, Wichita, Kan.	39.40	13.80	0.10	27.400
Platte WTP, Omaha, Neb.	44.00	33.20	0.56	24.600
Ann Arbor WTP, Ann Arbor, Mich.	52.40	14.80	0.20	20.600
Austin WTP, Austin, Texas	53.50	18.80	0.00	20.200
MWD 1 WTP, Kansas City, Kan.	71.10	52.80	2.80	15.200
Laverne WTP, Laverne, Calif.	84.20	72.90	0.90	12.800
Dallas County WTP, Dallas, Texas	96.30	38.33	0.37	11.200
Grand Forks WTP, Grand Forks, N.D.	151.33	52.60	0.03	7.100

MWD 1 = Mission Water District number 1

The purpose in utilizing such a model is to make the filterability constant a fundamental measure of sludge dewaterability. Due to the cumbersome nature of the SR test it is often preferable to use an easily determined value such as CST that allows calculation of a measure of dewaterability that is independent of solids concentration.

If the filterability index and specific resistance are both measures of dewaterability, then they should plot linearly. Figure 3.16 shows plot of the inverse of the filterability constant and SR. The

inverse of the filterability constant was plotted so that increasing values of the ratio denote higher difficulty in dewatering.

SR to filtration is a measure of a sludge's ability to dewater under the presence of a vacuum. As values of SR increase, the ease in dewaterability decreases. Filterability index is a measure of a sludge's ability to release water through drainage.

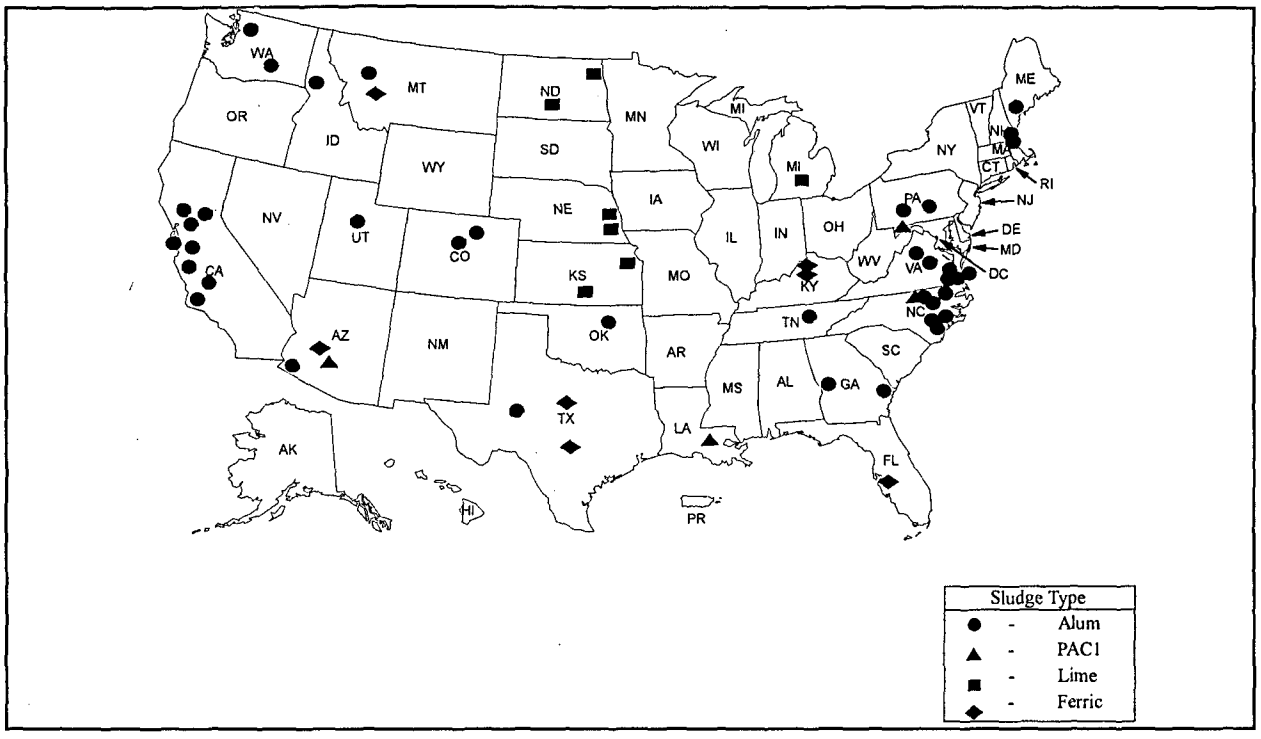

Figure 3.1 Characterization sample locations

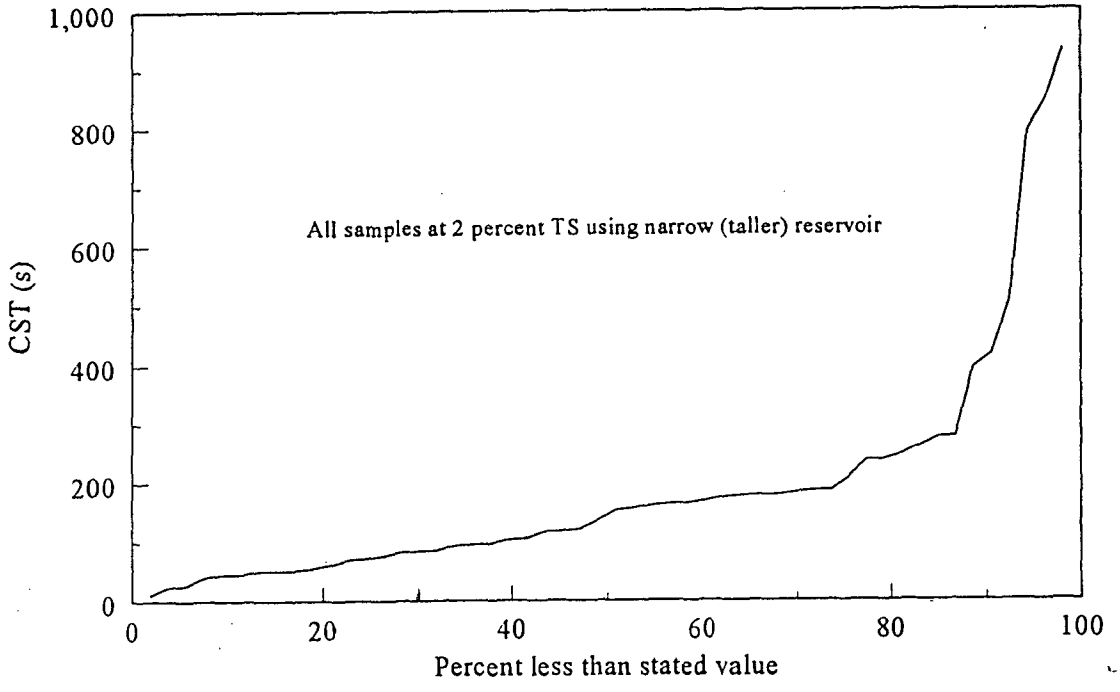

Figure 3.2 CST distribution for coagulant residuals

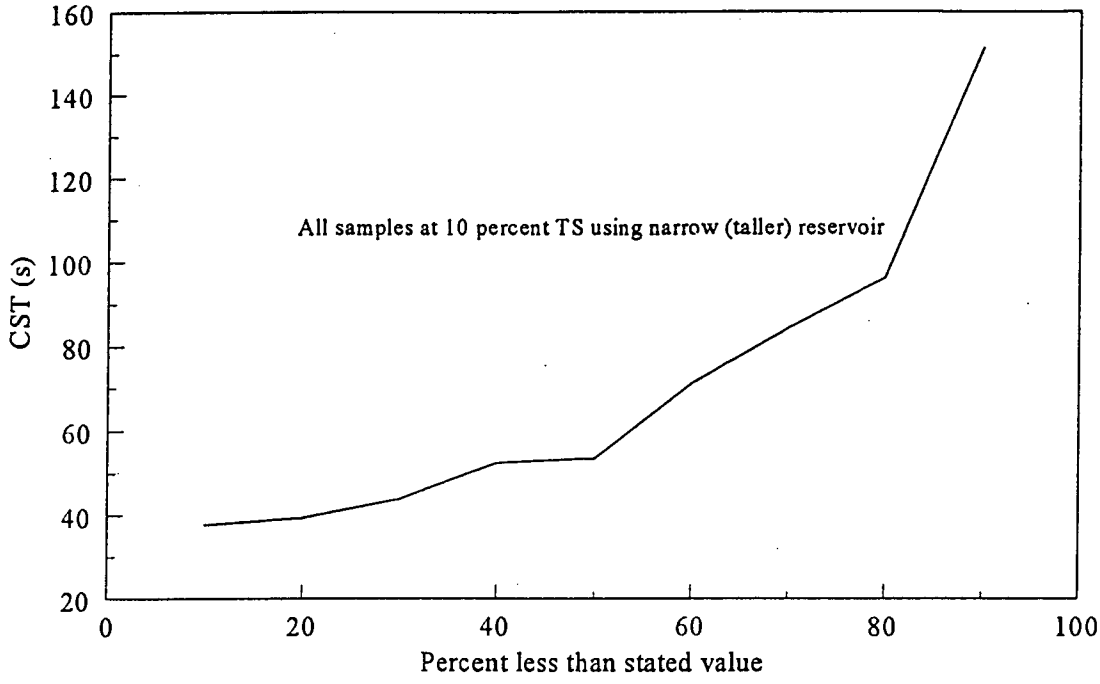

Figure 3.3 CST distribution for lime residuals

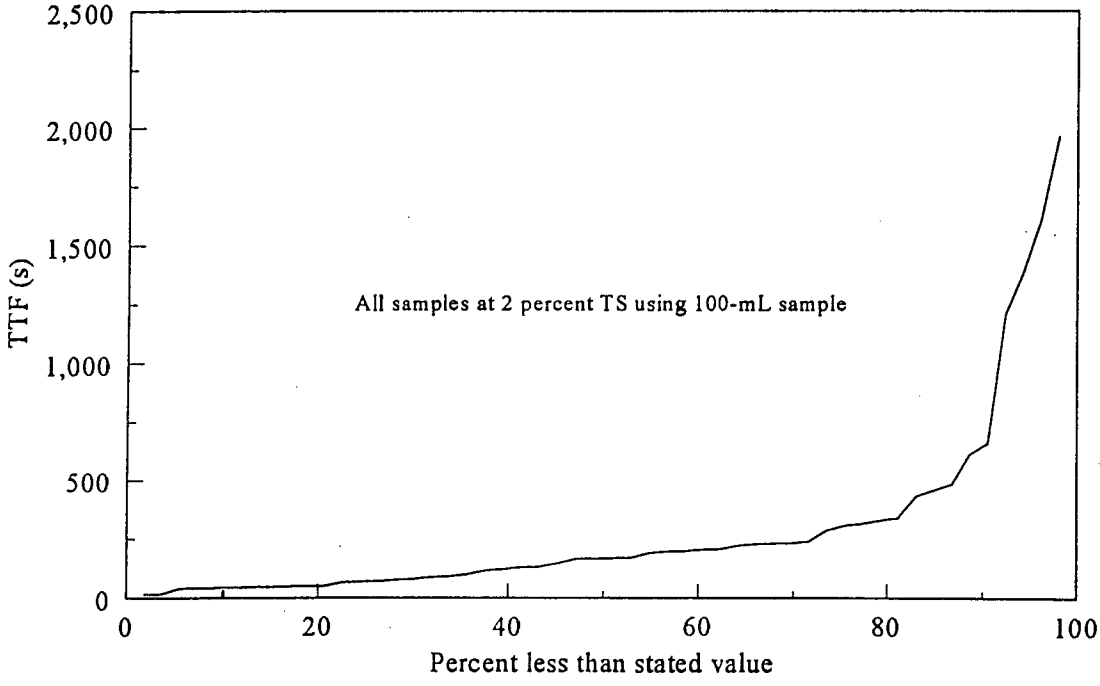

Figure 3.4 TTF distribution for coagulant residuals

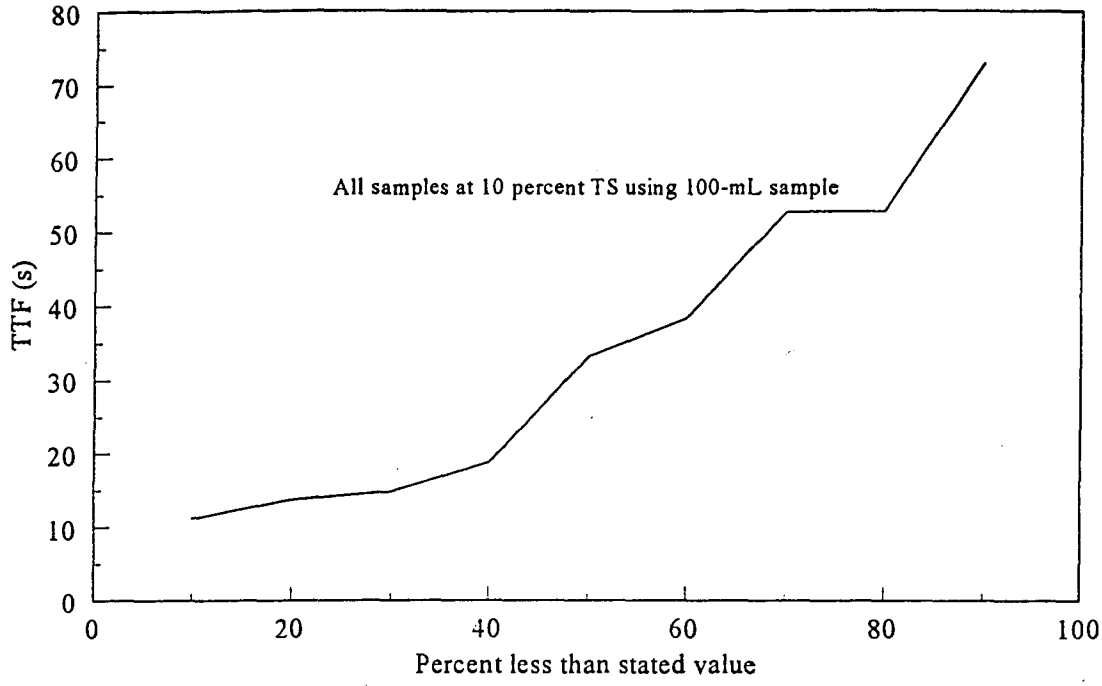

Figure 3.5 TTF distribution for lime residuals

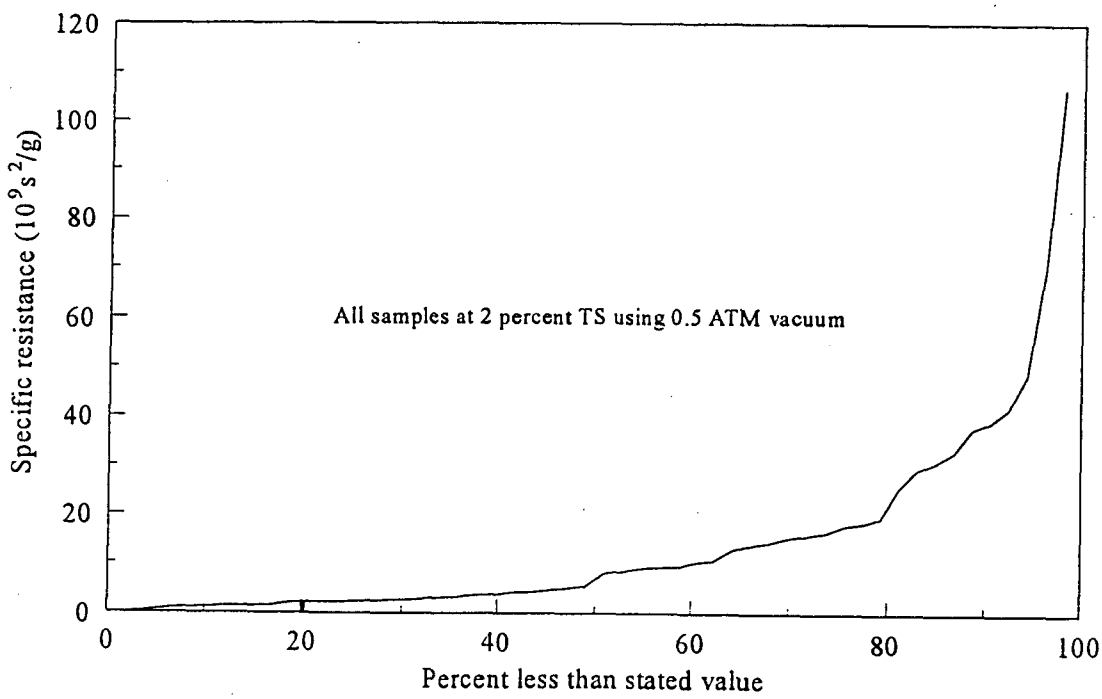

Figure 3.6 SR distribution for coagulant residuals

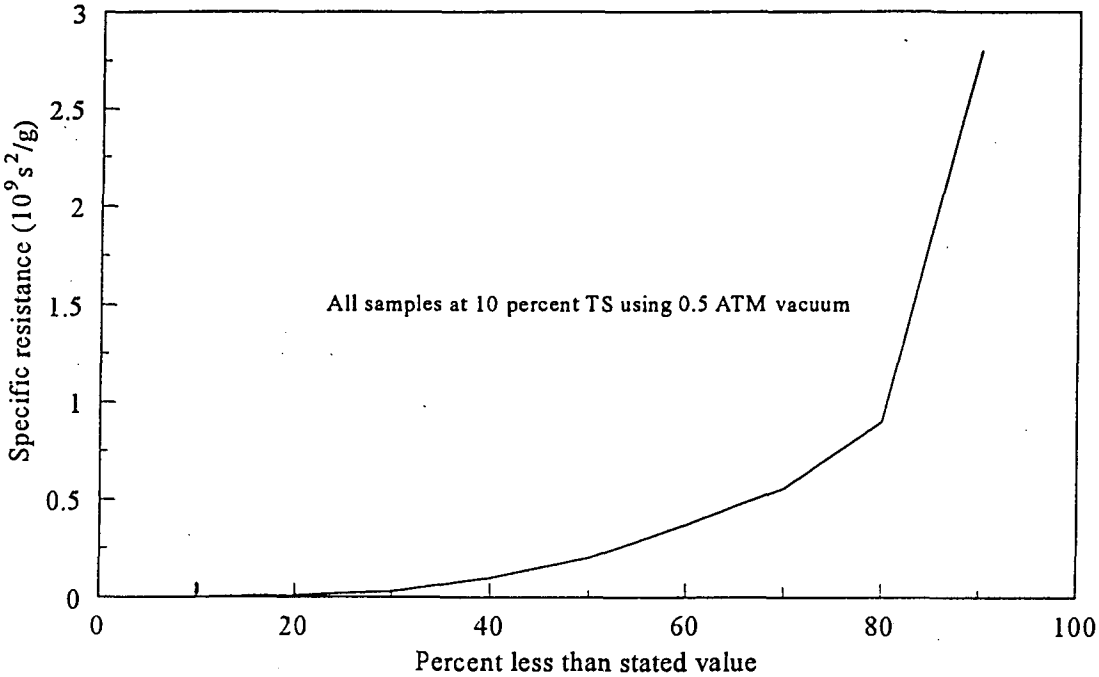

Figure 3.7 SR distribution for lime residuals

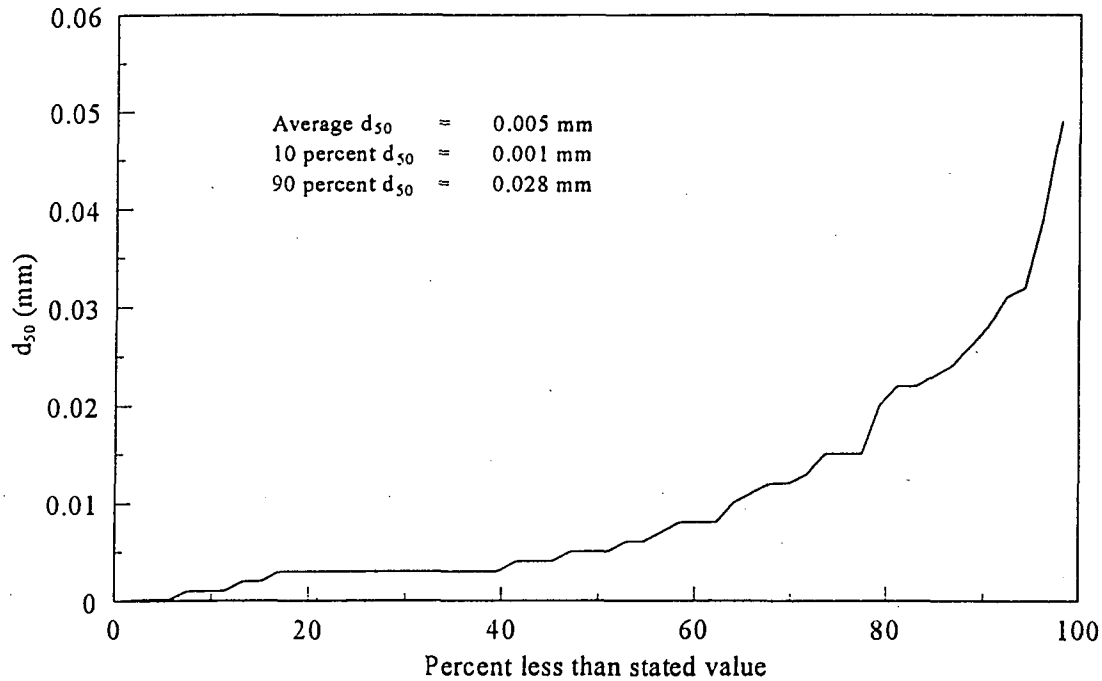

Figure 3.8 Average particle diameter for coagulant residuals

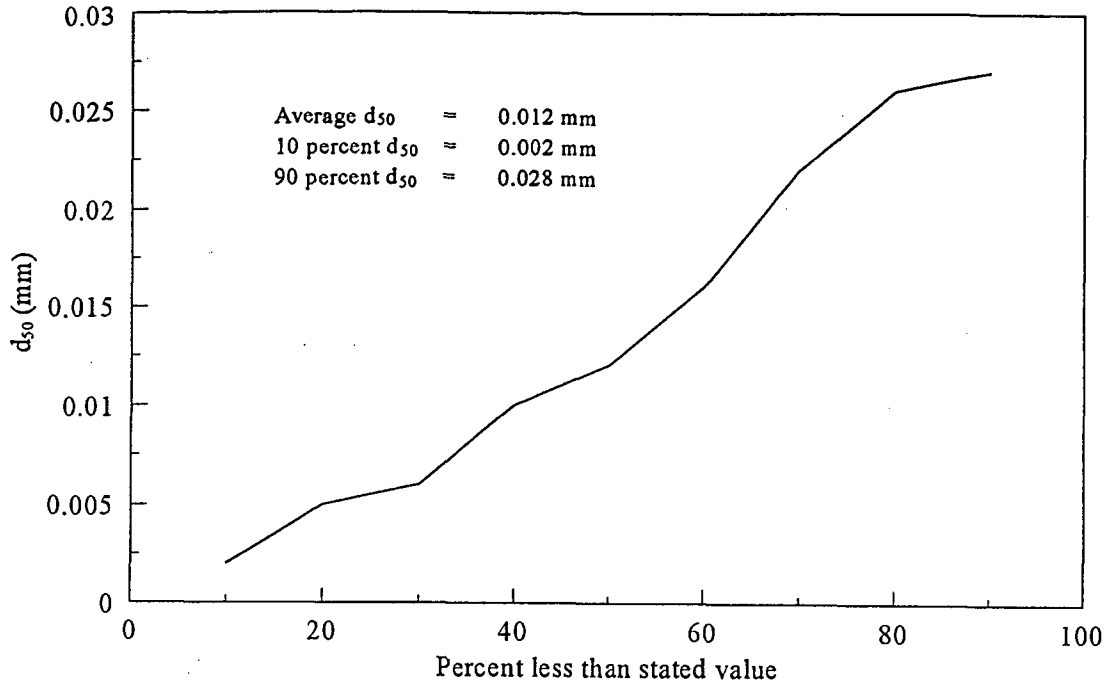

Figure 3.9 Average particle diameter for lime residuals

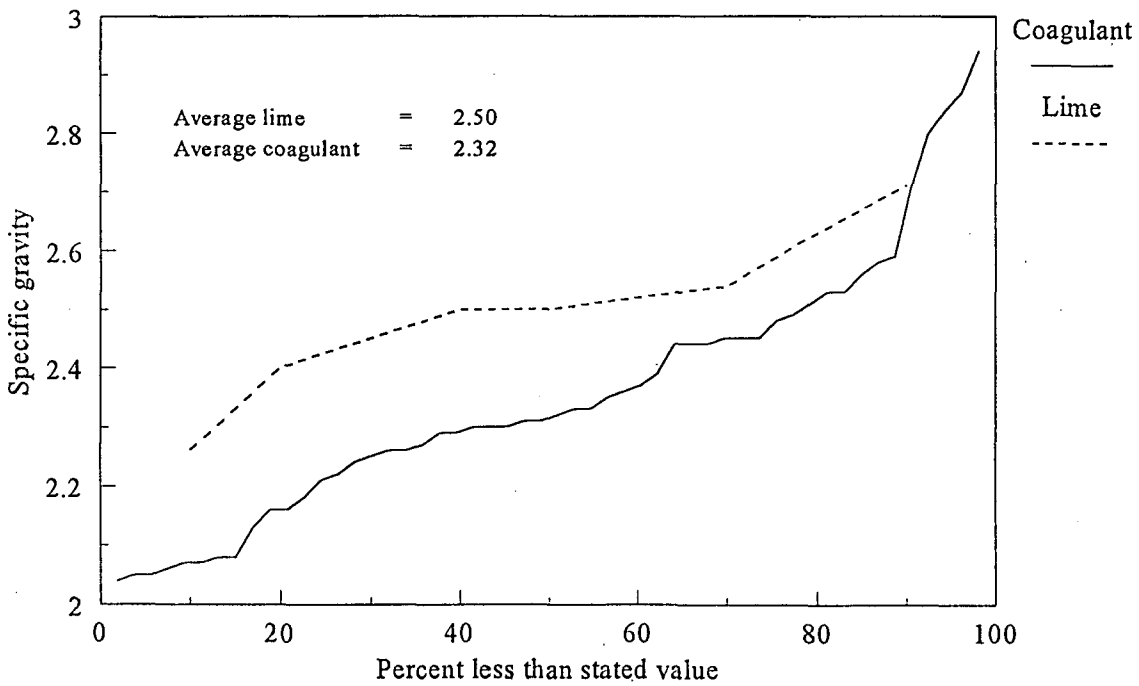

Figure 3.10 Specific gravity distribution for coagulant and lime residuals

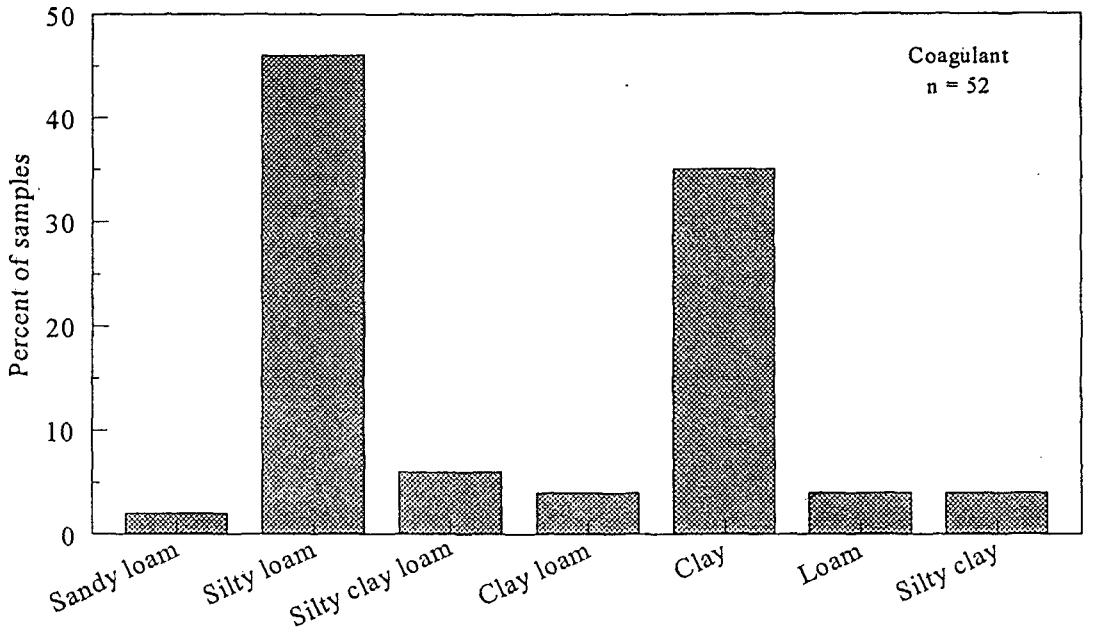

Figure 3.11 Frequency distribution for coagulant residuals texture classifications

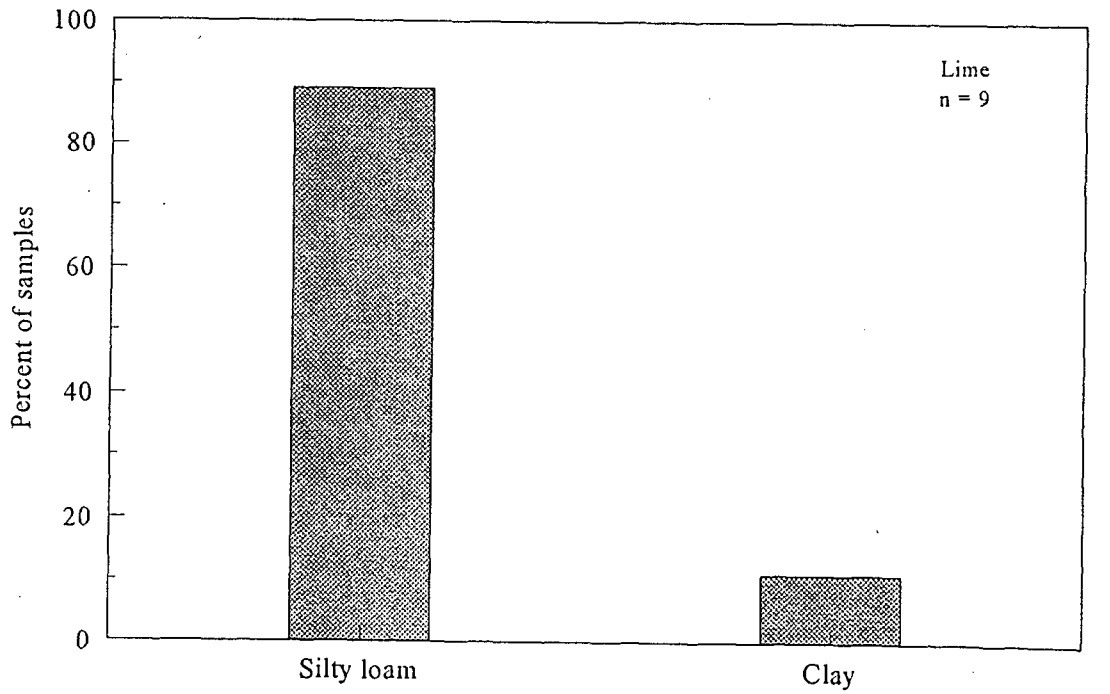

Figure 3.12 Frequency distribution for lime residuals texture classifications

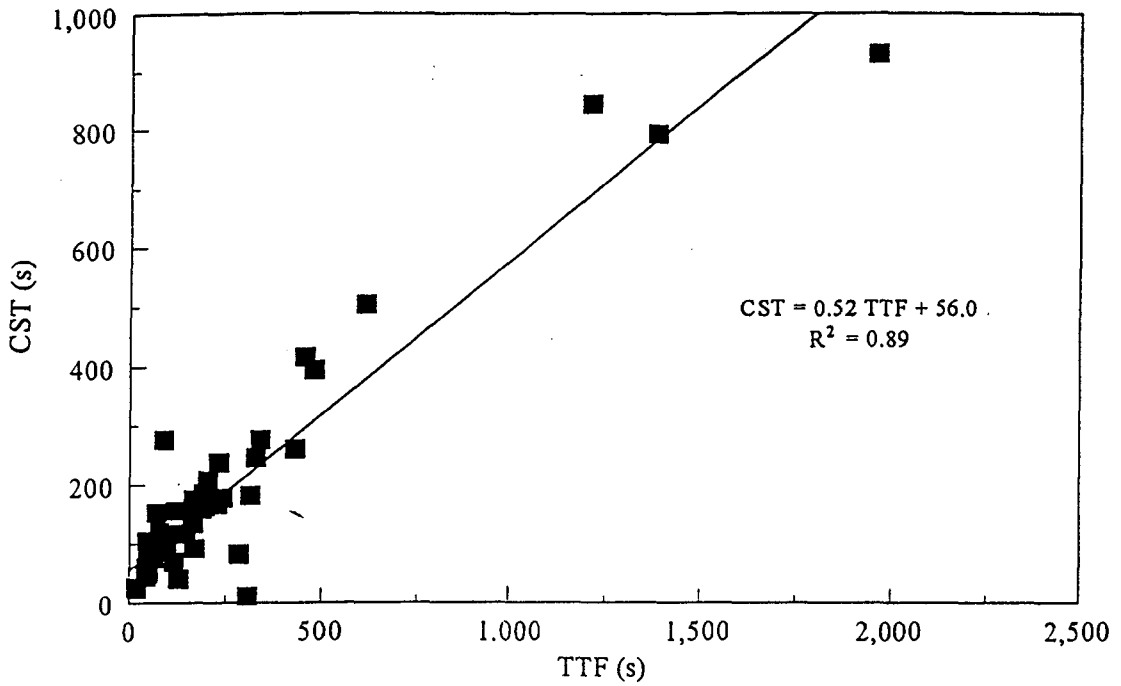

Figure 3.13 CST versus TTF for coagulant residuals

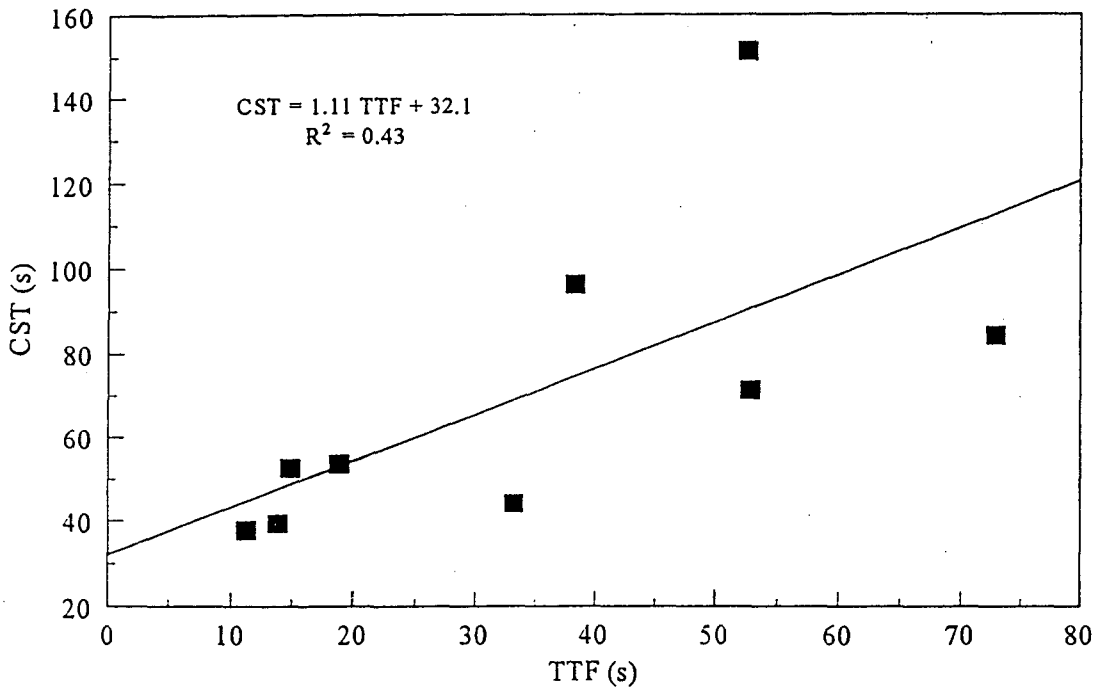

Figure 3.14 CST versus TTF for lime residuals

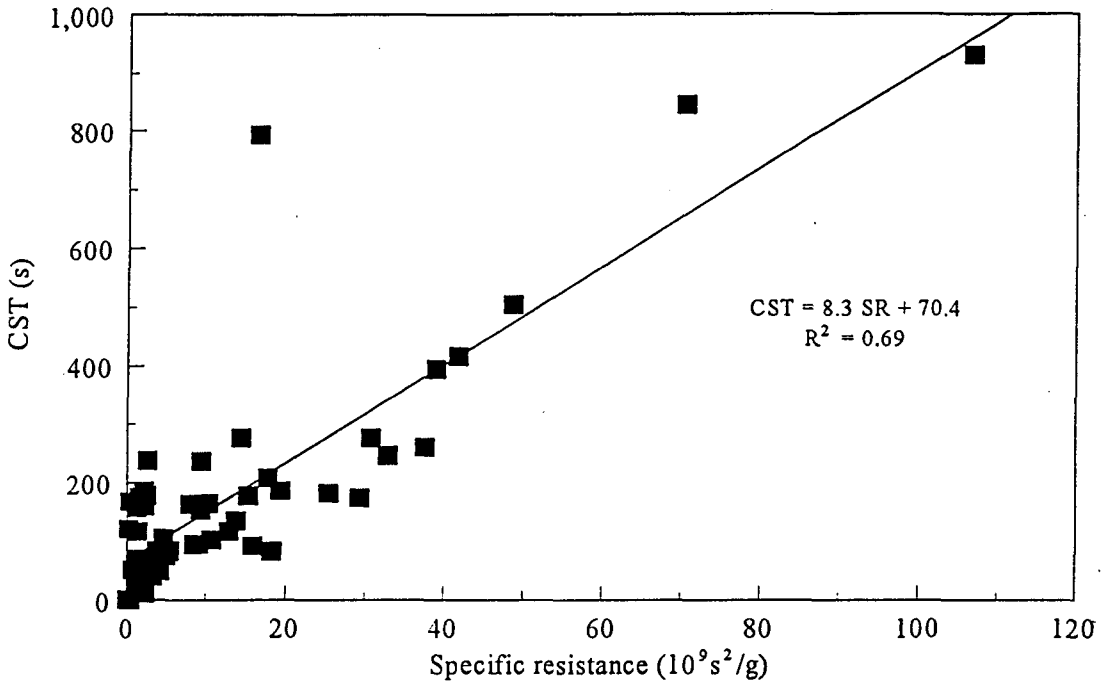

Figure 3.15 CST versus SR for coagulant residuals

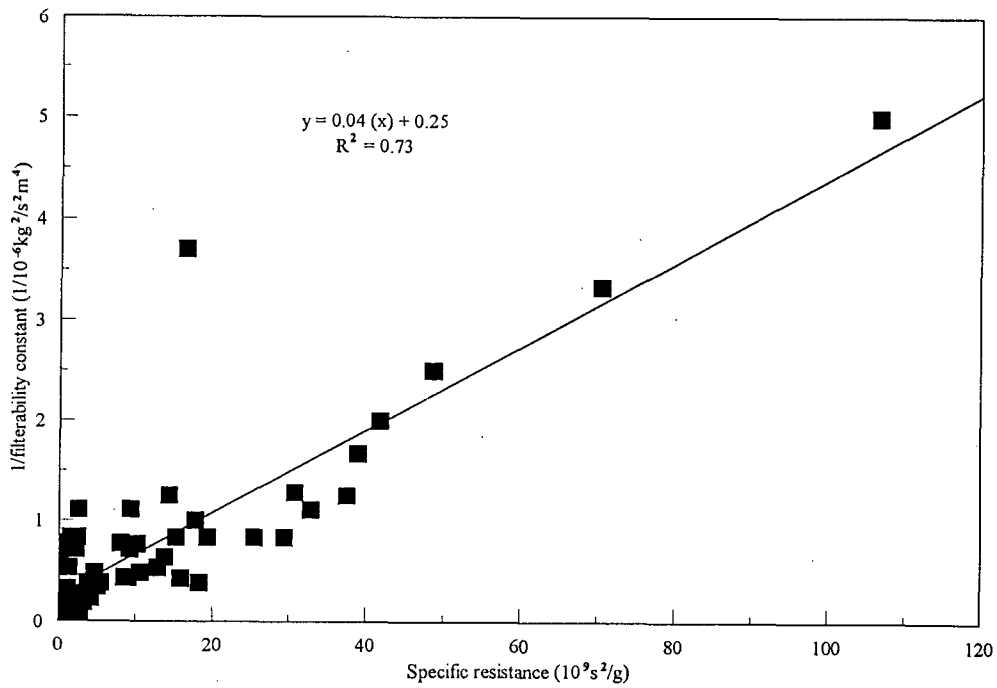

Figure 3.16 Inverse filterability constant versus specific resistance

CHAPTER 4
PILOT AND FIELD STUDIES

INTRODUCTION

Dewatering characterization and optimization studies were conducted in pilot columns and on-site in full-scale at several water treatment plants across the country. The objectives of these studies were as follows:

- Determine if pilot results could predict full-scale
- Characterize the performance of operating facilities where possible
- Optimize the performance of these facilities where possible
- Compare dewatering data from the field and pilot studies to see if any common trends result

In order to meet these objectives, 13 different water treatment plants that employ nonmechanical dewatering were selected for detailed evaluation in this project. For ten of the facilities pilot drainage tests were conducted. Both Durham, N.C., and Buffalo, N.Y., have two plants which have similar residuals characteristics, so only one plant at each location was used for pilot studies. At one facility (Edmonton, Alta.) only field freeze-thaw tests were completed. Additional utilities were selected for laboratory freezing tests only.

SELECTION OF UTILITIES

Information collected during the utility phone survey was the basis for selecting the 13 water treatment plants for detailed evaluations of their residuals handling operations. Selections were based on several criteria, including the following:

- The residuals dewatering method had to be a well managed operation and truly represent a dewatering system. Utilities which operated lagoons with no form of underdrainage, decanting, or regular cleaning were not included when possible.

- Four residuals types were selected—alum, ferric, PACl, lime.
- For each residuals type, both sand drying beds and freeze thaw beds were to be included, if possible.
- For each residuals type and dewatering technology, geographical and/or raw water quality variability had to be present.

Table 4.1 summarizes the name and location of the water treatment plants selected along with general information on capacity, raw water characteristics, and chemical usage. The geographic distribution of these utilities is shown in Figure 4.1.

For the alum residuals, sand drying bed locations in Durham, N.C., and in Huntsville, Ala., were selected because the telephone survey suggested that these are well operated residuals handling facilities. Also, these two locations had significantly different raw water turbidity (Huntsville 5 ntu and Durham 30 ntu) and alum dose (Huntsville 18 mg/L and Durham 30 mg/L). One solar bed location was selected which was also operated by the City of Durham, N.C., but at a different plant than the sand drying beds. The Durham plants provided the opportunity to compare sand drying versus solar drying beds.

For the PACl residuals, two plants at the Erie County Water Authority in Buffalo, N.Y., were selected. Both utilities have similar raw water turbidity (8 ntu) and PACl dose (4 mg/L). The utilities use dewatering lagoons and freeze-thaw lagoons.

For the lime residuals, there were only a limited number of utilities utilizing nonmechanical dewatering systems. Many of these utilities operated a large lagoon storage/dewatering system. The City of Midland, Michigan, was the only utility located which operated sand drying beds for their lime residuals. Lime residuals were collected from five utilities for evaluating drainage characteristics on a pilot scale. In addition, field freeze-thaw tests were conducted at Edmonton, Canada.

Table 4.1

Utilities selected for detailed studies

Sludge type	Owner	Location	Plant capacity (mgd)	Raw water turbidity (ntu)	Raw water color (cu)	Coagulant dose (mg/L)	Lime dose (mg/L)	Sludge dewatering technology
Alum	City of Durham	Durham, N.C.	22	30	18-24	30-40		sand drying beds
	Huntsville Utilities	Huntsville, Ala.	36	5	10	18		sand drying beds
	City of Durham	Durham, N.C.	30	30	18-24	30-40		solar beds
PACl	Erie County Water Authority	Buffalo, N.Y.	90	8	2	3.8		drying lagoons
	Erie County Water Authority	Buffalo, N.Y.	90	8	2	3.8		freeze-thaw beds
Lime	St. Louis County Water Company	St. Louis, Mo.	56	400	16	137	113.5	freeze-thaw lagoon
	City of Taylorville	Taylorville, Ill.	4	40	69	115	169.3	drying lagoons
	City of Fort Wayne	Fort Wayne, Ind.	75	50	52.9	202	305.1	drying lagoons
	City of Midland	Midland, Mich.	36	2.1	NA	2.0	7.7	sand drying beds
	City of Findlay Water Department	Findlay, Ohio	16	3	—	11	85.4	freeze-thaw beds
	Edmonton, Canada	Alberta	84	38	20	58	72	freeze-thaw bed
Ferric Chloride	Southern Nevada Water System	Boulder City, Nev.	400	0.15	<2.5	0.5		solar drying beds
	Pennsylvania-American Water Company	Indiana, Pa.	6	10	—	5		sand drying beds; freeze-thaw beds

— indicates no data
NA = not applicable

Plants producing ferric chloride residuals included a plant using solar beds in Boulder City, Nev., and a facility using a combination of freeze-thaw and sand drying beds in Indiana, Pa., operated by the Pennsylvania-American Water Company.

TECHNICAL APPROACH FOR FIELD AND PILOT STUDIES

Proper operation of nonmechanical dewatering systems is influenced by a number of variables including the residual's physical characteristics, initial solids concentration, loading rate, and polymer conditioning. During the pilot- and full-scale testing phases of the project, the relationship between these variables and their effect on the overall dewatering performance was investigated.

Field test procedures consisted of observing and documenting the performance of the dewatering process at each site under normal operating conditions. Typical data collected for each site included the following:

- Drying bed size, sand effective size, and design information
- Physical features such as influent structures, decant systems, underdrains, and cleaning methods
- Composite solids concentration of residuals loaded onto the bed
- Volume and depth of residuals applied to the bed
- Time required for the residuals to complete the draining cycle on the bed and estimates of the residuals volume reduction through drainage
- Periodic analysis of solids concentration on the bed during the drying phase, to characterize the evaporative drying rate
- Any applicable plant information such as chemical feed data and raw water quality data

A description of the facilities is contained in Appendix B. Data from field testing provided detailed insight into the working mechanisms of the two primary phases of nonmechanical dewatering, namely (1) drainage of free water and (2) drying of the remaining residuals through evaporation.

During the field visits, a 5-gal (18.9-L) sample of the residuals that were placed onto the bed was further analyzed in subsequent pilot studies with a focus on characterizing and optimizing the dewatering process encountered in the field. The pilot test program was previously described in Chapter 2 and consisted generally of the following:

- Simulating the field test conditions with similar application depths, solids concentrations, and sand media
- Optimizing the drainage of free water by conditioning the residuals with polymer and varying loading rates
- Comparing the laboratory results with field results to identify potential methods of obtaining better performance of the drying bed

TESTING RESULTS OF COAGULANT RESIDUALS

At five locations that use sand drying beds or solar beds, field visits were made to observe the operation and collect data on the drainage characteristics of the residuals. Table 4.2 shows the solids concentrations of the residuals applied to the bed at the visit and the calculated loading rate. Drainage and decant data were collected by recording the depth change until it leveled out. The results for the volume percentage of water that was drained as decanted is shown in Table 4.3. A sample was also collected and pilot tested at the same loading rate, with the results also shown. Figure 4.2 shows a plot for the five locations of field drainage results versus predicted pilot results using the 2-in. diameter columns. A remarkably good correlation was obtained, with an R^2 value of 0.94. This is a significant finding in that it confirms that pilot drainage studies can be used to predict full-scale performance. This allows a variety of loading rates, solids concentrations, etc., to be pilot investigated in order to develop design criteria.

Table 4.2

Summary of coagulant residuals field and pilot test drainage results*

Location	Initial solids (percent)	Loading rate (lb/ft^2)	Field drainage without polymer (percent)	Pilot control drainage without polymer (percent)
Durham, N.C.	1.1	0.9	73	73
Huntsville, Ala.	6.5	3.4	37	47
Buffalo, N.Y.	1.7	5.0	64	63
Indiana, Pa.	1.9	3.4	48	44
Boulder City, Nev.†	6.5	3.1	20	21

*Drainage includes decant volume

†Field and pilot tests performed on solar beds without underdrains

Each of these five utilities' residuals were then subjected to a series of pilot tests such as a utility might do in conjunction with development of design criteria.

Table 4.3 shows the pilot test conditions and results of the testing. The initial solids concentrations were not varied, but were tested as received. In an actual design basis test plan, the utility may wish to vary the solids concentrations to evaluate the impact of thickeners or solids removal systems. The main factors that varied in this research were loading and polymer conditioning. Since the initial solids concentration was held constant, the applied depth was varied in order to vary the solids loading. Polymer dose and type was determined by a series of lab tests to minimize the CST. The appropriate polymer dose was then mixed into the sludge prior to pilot sand bed application with a laboratory mixer for a short duration to simulate polymer feeding to a transfer pump. The results in Table 4.3 show the volume reduction and the drained solids concentration. The volume reduction was found by the change in sludge depth in the pilot column. The drained solids concentration was calculated based on this volume reduction. One of the important comparisons to note in the results is that drained solids concentration is more meaningful than volume reduction. The objective through drainage is to maximize the drained solids concentration, which will in turn maximize the bed yield. For example, the Huntsville, Ala., unconditioned sludge had a 51 percent drainage and Durham, N.C., had a 74 percent drainage, but

Table 4.3

Coagulant residuals pilot drainage test results

Location	Residuals type	Initial solids conc. (percent)	Loading (lb/ft^2)	Initial depth (in.)	Unconditioned			Polymer conditioned				
					CST (s)	Volume reduction (percent)	Drained solids conc.* (percent)	CST (s)	Volume reduction (percent)	Drained solids conc.* (percent)	Polymer dose (lb/ton)	Polymer type
Durham, N.C.	Alum	1.1	1.0	17.5	168	—	—	17	87	8.5	2.0	N
			1.5	26.2	168	73	4.0	17	—	—		
			2.0	35.0	168	74	4.0	17	85	7.3		
			3.0	52.5	168	60	2.8	17	84	6.9		
			4.0	70.0	168	—	—	17	81	5.8		
Buffalo, N.Y.	PACl	1.7	2.0	22.6	92	80	8.5	17	86	12.2	2.4	C
			4.0	45.2	92	77	7.4	17	83	10.0		
			6.0	67.8	92	73	6.3	17	86	12.1		
Indiana, Pa.	$FeCl_3$	1.9	1.0	10.1	128	67	5.7	21	70	6.3	8.4	C
			2.0	20.2	128	58	4.5	21	70	6.3		
			4.0	40.4	128	40	3.2	21	40	3.2		
Huntsville, Ala.	Alum	6.5	2.0	5.9	217	51	13.3	22	60	16.2	3.1	A
			4.0	11.8	217	46	12.0	22	66	19.1		
			6.0	17.7	217	33	9.8	22	45	11.8		
Boulder City, Nev.	$FeCl_3$	6.5	2.0	5.9	829	52	13.5	26	72	23.2	2.5	A
			3.0	8.8	829	45	11.8	26	70	21.7		
			4.0	17.7	829	28	9.0	26	68	20.3		

*Calculated values
A = High anionic, high molecular weight
C = Medium cationic, low molecular weight
conc. = concentration
N = Nonionic, very high molecular weight
— indicates no data

the drained solids concentrations were 13 percent for Huntsville versus 4 percent for Durham. The yield will be much higher for Huntsville than for Durham. Similarly, Buffalo, N.Y., at a 2 lb/ft^2 loading had 80 percent volume reduction without polymer compared to 86 percent with polymer. The difference appears minor and one could conclude that polymer had little impact. However, the drained solids concentrations are 8.5 percent versus 12.2 percent, almost a 50 percent improvement through the use of polymer.

The drained solids concentrations versus loading rate for each of the studies is shown in Figures 4.3 through 4.7. Several general trends can be observed. First, the drained solids concentrations were essentially always higher when polymer was used. Except for the Indiana, Pa. sludge, the results were much better with polymer than without; Durham improved by about 80 percent, Buffalo by 50 to 60 percent, Huntsville by about 30 percent, and Boulder City by 70 to 80 percent. The Indiana improvement was only about 10 percent. The second general trend is that as loading rates increased, polymer conditioning tended to maintain the achievable drained solids concentration whereas without conditioning the drained solids concentration more rapidly decreased as the loading rate increased. This means that higher loading rates could be used for polymer conditioned coagulant sludges.

One additional interesting observation was made when comparing the drained solids concentrations to laboratory testing results. Recall that the filterability index, which combines initial suspended solids and CST, is theoretically a measure of how well a sludge will drain. A plot of a pseudo-filterability index (SS/CST) versus drained solids concentrations is shown in Figure 4.8. The graph is for unconditioned sludges, and the drained solids concentrations are based on the loading rates where sand blinding is not taking place, as happens at some of the high loading rates. A very good correlation of $R^2 = 0.94$ was obtained, although the Boulder City data did not match and was eliminated. The researchers do not feel that results based on four sludges is sufficient to conclude that the laboratory filterability index can be used to predict drained solids concentrations, and in fact the relationship only "worked" for non-polymer conditioned residuals and one utility's data didn't fit. However, it seems likely that an individual utility could develop such a relationship for its specific sludge and thereby predict performance through a combination of laboratory and pilot studies, minimizing the number of pilot studies needed.

TESTING RESULTS OF LIME RESIDUALS

Testing conducted for the lime residuals was limited to conducting the laboratory pilot column tests. Of the five utilities selected for detailed studies, only the utility in Midland, Mich., operated an actual nonmechanical sand drying bed. The other utilities managed the lime residuals dewatering through large storage lagoons. These lagoons did not provide the opportunity to conduct field dewatering tests similar to those conducted for the coagulant residuals. The results from the pilot column tests are presented in Table 4.4. As was done for the coagulant residuals, the lime sludges were tested at the suspended solids concentrations as received. The loading rates were varied by changing the applied depth, and polymer conditioning was evaluated. Figures 4.9 through 4.13 show the results for each plant of plotting drained solids concentrations versus loading rate for conditioned and unconditioned residuals. The initial suspended solids concentration and hence the loading rates are much higher for lime residuals than for coagulant residuals; however, lime residuals require a higher dewatered solids concentration for acceptable disposal.

The loading rate versus drained solids concentration data (Figures 4.9 through 4.13) show that for lime residuals, polymer had little impact on improving the drainage. This was the case even though polymer conditioning improved the CST values—in the case of Midland, Mich., substantially so (Table 4.4). Except for Midland, Mich., within the range of loading rates tested there was not a decrease in performance as the loading rate increased. Also unlike coagulant residuals, a relationship between the filterability index and drained solids concentration was not found.

SAND DRYING BED FILTRATE CHARACTERISTICS

To characterize the general quality of the underdrainage, four plants were chosen at random. The underdrainage from the pilot test columns was collected and analyzed for pH, turbidity, iron, manganese, aluminum, and particle counts. Table 4.5 summarizes the laboratory results.

Table 4.4

Lime residuals pilot drainage test results

Location	Initial solids conc. (percent)	Loading (lb/ft^2)	Initial depth (in.)	Unconditioned			Polymer conditioned				
				CST (s)	Volume reduction (percent)	Drained solids conc. (percent)	CST (s)	Volume reduction (percent)	Drained solids conc. (percent)	Polymer dose (lb/ton)	Polymer type
Ft. Wayne, Ind.	4.0	4.0	19.2	47	85	26.7	24	87	30.8	1.0	C
		6.0	28.8	47	80	20.0	24	85	26.7		
		8.0	38.4	47	82	22.2	24	84	25.0		
St. Louis, Mo.	8.1	10	23.7	57	79	38.6	17	82	45.0	4.0	C
		15	35.5	57	75	32.4	17	80	40.5		
		20	47.5	57	74	31.1	17	80	40.5		
Findlay, Ohio	9.5	10	20.2	61	62	25.0	24	60	23.8	1.0	A
		15	30.3	61	58	22.6	24	58	22.6		
		20	40.5	61	57	22.1	24	53	20.2		
Taylorville, Ill.	12.0	10	16.0	25	82	66.7	22	83	70.6	0.2	N
		15	24.0	25	79	57.1	22	80	60.0		
		20	32.0	25	80	60.0	22	80	60.0		
Midland, Mich.	24.0	10	8.0	246	54	52.2	45	57	55.8	0.8	C
		12	9.6	246	42	41.4	45	41	40.7		
		13	10.4	246	33	35.8	45	35	36.9		

A = High anionic, high molecular weight
C = Medium cationic, low molecular weight
conc. = concentration
N = Nonionic, very high molecular weight

Table 4.5

Sand drying bed drainage characteristics

	Utility			
Parameter	1	2	3	4
Residuals type	Alum	Lime/ferric	$FeCl_3$	$FeCl_3$
pH	6.86	7.05	7.32	7.43
Turbidity (ntu)	32	30	1.6	28
Iron (mg/L)	0.4	0.2	0.3	0.4
Manganese (mg/L)	1.81	5.7	0.14	1.34
Aluminum (mg/L)	<0.5	<0.05	<0.5	<0.5
Total particles/mL	19,687	60,726	19,695	307,249
Total particles/mL (1-15 μm)	18,712	57,690	19,098	304,207

Management options for the filtrate would normally be sewer disposal, direct discharge, or recycle. None of the characteristics evaluated here would prohibit sewer discharge. Suspended solids measurements were not taken, but often suspended solids are higher than turbidity, therefore direct discharge would probably not be possible for utilities 1, 2, and 4 with a typical NPDES permit of 30 mg/L suspended solids. However, the filtrate could be combined with the spent filter backwash water and discharged after appropriate settling. For direct recycle, the manganese and particle counts would be of concern. Other research (Cornwell and Lee 1993) has shown that these filtrates have high TOC and THM and that the manganese can be quite high. In that research, direct recycle of these streams was not recommended. It may be possible to produce a reasonable recycle stream through dilution with the spent filter backwash water; however, sewer disposal or treatment and discharge appear more reasonable.

SAND DRYING BED AND SOLAR DRYING BED COMPARISON

For purposes of comparing the performance of sand drying beds and solar drying beds, a full-scale side by side comparison was conducted in Durham, N.C. While the sand drying beds and solar drying beds are located at different water plants, both plants use the same raw water source. The sand drying beds had underdrains and decant mechanisms, while the solar beds had concrete bottoms, a 12-in. wide sand strip along the sides to allow for some drainage, and decant mechanisms. Care was taken in an attempt to maintain consistent solids concentrations for each loading; however, variability was experienced due to the different operating practices of the two plants. The initial solids concentrations were 2.4 and 3.2 percent for the unconditioned and polymer conditioned sand drying beds, while the unconditioned and conditioned solar beds had solids concentrations of 2.2 and 1.5 percent, respectively. The solids loading for the sand drying bed were 1.8 to 2.0 lb/ft^2. The solids loading for the solar bed were 1.0 to 1.5 lb/ft^2.

Figures 4.14 and 4.15 show the volume reduction as a function of time for both the sand drying bed and the solar bed. Clearly the sand drying bed drainage was much more rapid than the solar bed because the solar bed only had a narrow 12-in. sand strip for drainage. For the sand drying beds, drainage was complete in about four days allowing evaporation of the pore water to begin. Drainage was not completed in the solar beds even at 15 days.

Figures 4.16 and 4.17 show solids concentrations on the beds as a function of time. As was pointed out earlier, the drained solids concentration is directly related to bed yield. The sand drying beds exhibited a rapid increase in solids concentration over time while the solar drying beds exhibited very little change in solids concentration over time. Solids concentrations remained at or below 5 percent for the solar drying beds well beyond 45 days. The corresponding solids concentrations for the sand drying beds are approximately 18 to 20 percent. The noticeable decrease in solids concentrations after 45 days was the result of several days of poor weather conditions. While the solids on the sand drying beds rewetted from 19 to 14 percent solids concentration, the solids also dried fairly quickly again.

These tests illustrate that the sand drying beds performed notably better than the solar drying beds. It should be noted, however, that these tests were performed in October through December when the average evaporation in Durham, N.C., is typically about 2.0 in./month or less. The solar beds were loaded at initial solids concentrations of 1.5 and 2.2 percent solids, and after drainage the

solids concentration was less than 5 percent. This would still contain high amounts of moisture that cannot be evaporated efficiently when the evaporation rate is less than 2.0 in./month.

This comparison also illustrates the ability of the sand drying bed to continue to operate during low evaporation and wet weather seasons. While the dried residuals did show rewetting and a lowering in solids concentration from 19 to 14 percent, the solids concentration returned to 20 percent in about two weeks during the month of December.

SOLAR DRYING BED PERFORMANCE

While the previous evaluation of sand drying beds and solar drying beds showed that in the case of Durham, N.C., the sand drying beds performed better, the use of solar beds are popular in the arid southwest. A field test was performed at the Alfred Merritt Smith WTP operated by the Southern Nevada Water System in Boulder City, Nev. This utility has 120,000 ft^2 of solar drying beds for an estimated residuals production of 1,100 tons/yr, corresponding to a yield of 18.3 $lb/ft^2/yr$.

Figure 4.18 shows the performance of the solar drying bed in terms of volume reduction through decanting of the supernatant. At a solids loading rate of 3.1 lb/ft^2 without polymer addition, approximately 20 percent volume reduction was achieved in about 48 hours. This performance was matched with 1,000-mL graduated cylinders. However, as shown in Figure 4.18, the addition of polymer to the residuals achieved a 29 percent volume reduction through decanting in about 24 hours.

The advantage of using solar drying beds in the arid southwest is illustrated in Figure 4.19, which shows the drying pattern of residuals after the supernatant has been decanted. From an initial 8.5 percent solids concentration, a 60 percent solids concentration was achieved in about 15 days. During the period, the evaporation rate was about 12.8 in./month. By observing the data in Table 4.3, polymer conditioned sand drying beds would result in a drained solids concentration of about 25 percent. This polymer conditioned sand bed design would approximately double the yield (theoretically triple) of the solar bed. However, the solar beds are easier to clean than sand beds, and the solar beds would have maintenance advantages compared to the sand beds.

RESIDUALS DRYING CHARACTERISTICS

At several locations where on-site dewatering tests were conducted, the rate of residuals drying through evaporation was characterized. The previous sections in this chapter characterized the drainage cycle of the residuals. This section characterizes how the residuals subsequently dry to a final solids concentration.

Drying of residuals is a phenomenon that is quite difficult to mathematically quantify as a function of evaporation. Rolan (1980) presented a series of equations that assumed that the increase in solids concentration through evaporation is proportional to a decrease in residuals depth on the bed. This model, however, does not consider the effects of residuals cracking during drying, which causes greater exposed surface areas and enhanced drying rates. In this work, field tests were performed to measure the actual rate of drying on the drying beds and to compare the results to the predicted solids drying based on pan evaporation data.

Field Test Procedures

The field test procedures consisted of loading a sand or solar drying bed at a specific solids loading rate. After the residuals were loaded onto the bed, depth measurements were taken until the free water had been drained. The free water on the surface of the residuals was also decanted off. Next, over a 30- to 40-day period, residuals samples were collected several times a week from the drying bed and analyzed for total solids concentration. Simultaneously, the net pan evaporation was monitored. At least three different locations were sampled and analyzed separately. Care was taken not to obtain sand in the sample, which could produce erroneous results. After the samples were analyzed, the average of the samples was reported.

Estimated Cake Solids Calculations

The estimated cake solids concentrations based on evaporation at various time intervals while the residuals remain on the sand drying bed after drainage are calculated as follows:

$$D(t) = D(d) - E \bullet t \tag{4.1}$$

where

D(d)	=	drained residuals depth after the free water has been removed
E	=	total depth of net pan evaporation per time
D(t)	=	dewatered residuals depth at time, t
t	=	drying time

The solids concentration at time, t, can be found as follows:

$$D(t) = D(d) \times \left(\frac{SS(d)}{SS(t)} \right) \tag{4.2}$$

or

$$SS(t) = \frac{D(d) \times SS(d)}{D(d) - E \bullet t} \tag{4.3}$$

where

SS(t)	=	solids concentration at time, t
SS(d)	=	drained solids concentration

Thus, with these equations, one could calculate the cake solids on the bed at any time provided the initial drained depth solids concentration and the evaporation rate are known. Evaporation rates can be obtained from the National Oceanic and Atmospheric Administration (NOAA).

Field Test Results

Tests were conducted at three different locations. The test locations were Durham, North Carolina; Huntsville, Alabama; and Boulder City, Nevada. Both Durham, North Carolina, and Huntsville, Alabama, use sand drying beds for alum residuals dewatering. Boulder City, Nevada, applies ferric chloride residuals to solar drying beds. The results for Durham, North Carolina, are shown in Figure 4.20. The sand drying beds were loaded at 1.0 lb/ft^2 with 7 lb/dry ton of polymer conditioning. The initial solids concentration was 1.0 percent. As shown in Figure 4.20, the drained residuals on the sand drying bed were measured at 3.75 and 9.50 in.; the significant difference in depths was due to variable distribution of the residuals when applied to the bed. Under both residuals depths, the field measured residuals solids concentrations were higher than the concentrations estimated by a simple pan evaporation model. For example, at the 9.50-in. depth a 25 percent solids concentration (suitable for landfill disposal) was achieved in approximately 27 days, while the model estimated a drying time of 40 days.

The results from the Huntsville, Alabama, tests are shown in Figure 4.21. At this location, the beds were loaded at 3.4 lb/ft^2 at a 5.6 percent solids concentration. The city typically does not add any polymer to the residuals when loading the sand drying beds. As in the Durham test results, the field measured solids concentrations were higher than the model predicted solids concentrations. A 25 percent solids concentration was achieved in 18 days in the field, compared to 27 days predicted by the model.

Results obtained from the tests conducted on the solar drying bed in Boulder City, Nevada, are shown in Figure 4.22. At this location, ferric chloride residuals were loaded at 3.1 lb/ft^2. Residuals drying patterns were monitored for the period of August 31 through October 1, 1994. Due to the extremely arid climate in southern Nevada, rapid drying was observed. Residuals were applied to the bed at 6.2 percent solids concentration. Within 2 days the solids concentration had approximately doubled. Within 14 days solids concentrations were quickly approaching 50 percent. Utilizing Rolan's model, a 25 percent solids concentration was predicted after 8 days of drying. Field drying conditions indicated that 25 percent solids concentration was achieved in about 6 days.

The results from these tests suggest that the model, that is, using pan evaporation, underestimates the evaporation through the initial drying cycle. In these three tests, a 25 percent solids concentration was reached in about two-thirds of the time predicted by the model. Thus under

these test conditions, using the model would result in a slightly conservative sizing of the sand drying beds or solar drying beds. At higher solids concentrations, the model predicts evaporation at much higher rates than actually take place. This point of crossover is probably when the free water and pan water have been evaporated and the chemically bound water remains. The bound water would be more difficult to evaporate. The slower drying at the higher solids concentrations could also reflect a crusting of the surface wherein tillage could be used to increase the field evaporation.

LABORATORY FREEZE-THAW TESTING

Laboratory freeze-thaw tests were conducted on several residuals samples. The objectives of these tests were to quantify the volume and solids reduction levels achievable through the freeze-thaw processes and to investigate if any similarities existed between different sludge types. It was not the intent to simulate the actual freezing process encountered in the field with respect to soil and snow insulation, temperatures, and wind chill. All samples were completely frozen in the laboratory, such as could easily be done by a utility to test the impact of freezing on its residuals.

All tests were conducted on 200-mL samples. The 200-mL residuals samples were placed in disposable 500-mL plastic beakers and frozen for 48 hours at -15°C in a laboratory type freezer. When the samples were completely frozen, they were removed from the freezer and allowed to thaw at room temperature. During the thawing process, the supernatant above these solids was decanted and measured. The remaining solids were gravity filtered through a Whatman filter paper to simulate drainage with underdrains. The supernatant and drainage volumes were added to determine the overall volume reduction achieved. Drained solids concentrations on the remaining solids were then analyzed to determine the increase in solids concentration. Therefore, the drained solids concentrations achieved would approximate freeze-thaw periods prior to evaporative drying and are analogous to the drainage cycle of a sand drying bed.

Table 4.6 shows the results of the laboratory freeze-thaw tests. The volume reduction due to the freeze-thaw process, followed by draining and decanting, was typically 80 to 90 percent by volume. These residuals are representative of the solids remaining immediately after the thawing process is completed and water has been removed by decanting and draining. Subsequent air drying of the remaining solids would be required in order to achieve the desired final solids concentration.

Table 4.6

Laboratory freeze-thaw results

Sludge type	Location	Initial solids volume (mL)	Final solids volume (mL)	Volume reduction (percent)	Initial solids concentration (percent)	Thawed and drained concentration (percent)
Alum	Durham, N.C.	200	24.0	88.0	3.0	24.8
	Hunstville, Ala.	200	29.0	85.5	3.2	31.8
	Bridgeport, Conn.	200	36.0	82.0	2.6	22.2
PACl	Buffalo, N.Y.	200	13.0	93.5	1.5	29.3
	Blacksburg, Va.	200	27.0	86.5	4.0	28.3
	Albany, N.Y.	200	29.0	85.5	1.4	14.3
Lime	St. Louis, Mo.	200	18.0	91.0	3.0	47.5
	Taylorville, Ill.	200	71.0	64.5	15.0	36.5
	Midland, Mich.	200	22.0	89.0	6.0	46.4
	Findlay, Ohio	200	52.0	74.0	10.0	38.6
Ferric	Winchester, Va.	200	28.0	86.0	3.9	57.3
	Boulder City, Nev.	200	38.0	81.0	2.7	24.5
	Indiana, Pa.	200	8.0	96.0	0.9	35.1

Figures 4.23 and 4.24 compare the results from a sand drying bed drainage system using polymer conditioning and a freeze-thaw bed using freeze-thaw as the conditioning method. The types and doses of polymers are shown in Tables 4.3 and 4.4. For the coagulant residuals, in all cases except Boulder City, freeze-thaw drainage resulted in substantially higher drained solids concentrations than did polymer conditioning. The comparison clearly shows the benefit of complete freeze-thaw in achieving a high drained solids concentration and thus reducing the evaporative drying time. For lime residuals, freeze-thaw achieved significantly higher drained solids concentrations for only one residual and was actually lower for two of the residuals. Therefore, freeze-thaw does not appear to be as beneficial for lime residuals as it is for coagulant residuals.

Freeze-Thaw Evaporation Characteristics

Frozen and thawed residuals obtained as previously described were spread on a 216 $in.^2$ drying area at a depth of approximately ½ in. and allowed to naturally air dry. The drained solids concentration was 29 percent. Simultaneous to this drying, an evaporation pan was also subjected to identical conditions. Solids concentration as well as the amount of water evaporated were measured at regular intervals. Figure 4.25 shows the solids concentration increase as a function of time for the freeze-thawed residuals. This test was conducted on polyaluminum chloride residuals from the Erie County Water Authority in Buffalo, N.Y. During this test, the net pan evaporation rate was 0.36 in./month. The residuals solids concentration increased from 29 percent solids to 81 percent solids in 13 days. Also shown is the predicted solids increase based on Rolan's model. As was the case for polymer conditioned residuals, actual drying was faster than that predicted by the model.

The remaining solids were then subjected to a sieve analysis. Residual material was weighed prior to passing it through a series of sieves. Once the sample was fractioned by size, each sieve was weighed and the corresponding amount of material on each sieve was determined and a particle size distribution calculated.

Figure 4.26 is a plot showing both pre and post freeze-thawed residuals particle size distribution of the ECWA residuals. The pre-freeze plot is fairly typical for a water treatment plant residual in that it has a fairly broad size range of particles. In fact, the size range spans over 2-log cycles on the graph. The original average particle size was 0.0023 mm. After the samples were frozen and allowed to dry the particle diameters become much more uniform. However, the most interesting result is that the average particle size increased 2 orders of magnitude above its original size. After thawing the average particle size was 0.28 mm. The curve for the post-freeze solids indicates a relatively uniform size distribution of particles.

FIELD FREEZE-THAW TESTS

Two field freeze-thaw tests were conducted. One was performed in Edmonton, Canada, and the other at the Sturgeon Point WTP located near Buffalo, N.Y. In Buffalo, PACl residuals were tested, and in Edmonton, Canada, lime residuals were used.

Edmonton, Canada

The City of Edmonton, Alberta, Canada, evaluated the use of freeze-thaw lagoons as an alternative to mechanical dewatering. Two 100-ft^2 freeze-thaw lagoons were excavated for this pilot test, which lasted from the beginning of winter in November through the spring thaw in April. The lagoons were approximately 5 ft deep and had 1:1 side slopes. The side slopes were covered with 10-mil thick plastic during the pilot test to prevent interference of wall effects. The bottom of the lagoon was natural soil consisting of fairly sandy material which could drain free water as necessary.

Prior to the start of the pilot plant test, the theoretical freezing depth was calculated with the use of a model developed by Martel (1989), as described in the next chapter. The model predicted a maximum freezing depth of 80 in. if the residuals were applied in 6-in. layers, while a one time bulk application would freeze to approximately 43 in. The city staff felt that a onetime bulk loading would be the preferred method of operation in a full-scale operation since it would eliminate the need for residuals storage. Based on the theoretical freezing depth of 43 in., the two pilot freeze-thaw beds were loaded, one at 36-in. depth and one at 48-in. depth.

The residuals applied to the lagoons were obtained from the plant's gravity thickener and had a total solids concentration of 25 percent. The total solids volume applied to each lagoon was 3,700 and 5,700 gal for the 36 and 48 in. solids depths, respectively. At the end of the five month period, there remained approximately 27 in. of residuals in the lagoon loaded at 36 in. and 36 in. of residuals in the lagoon loaded at 48 in. This resulted in a total volume reduction of 33 to 34 percent for both lagoons. There was no free water present in the lagoons, and no decanting was performed at any time. Consequently, all the water from the residuals had drained through the lagoon bottom. Samples collected in the shallower lagoon at 2-, 15-, and 27-in. depths had total solids concentrations of 58, 55, and 55 percent, respectively. Samples collected in the deeper lagoon at 2-, 18-, and 36-in. depths had total solids concentrations of 57, 54, and 54 percent, respectively. It appeared that both lagoons had frozen over the entire depth, as the 55 to 60 percent solids concentration achieved was comparable to the solids concentration expected for freeze-thawed lime solids as previously shown with the laboratory tests in Table 4.6. Thus, the model appeared to be quite good in predicting the freeze depth.

Erie County Water Authority, N.Y.

Six freeze-thaw beds were loaded at the Sturgeon Point Water Filtration Plant owned and operated by the Erie County Water Authority. Three beds were loaded without polymer at solids loading rates of 10 to 21.3 lb/ft^2. This corresponded to residuals depths of 18 to 36 in. Based on Martel's model, the calculated freezing depth in Buffalo for a onetime loading is 9 in. It was thought that the applied depths used would be in the 9-in. range after drainage occurred. Three other beds were loaded at comparable depths but with the addition of polymer. Table 4.7 summarizes the initial loading conditions for the six freeze-thaw beds.

Table 4.7

Erie County Water Authority

Pilot freeze-thaw testing conditions

Bed number	Loading (lb/ft^2)	Polymer dose (lb/ton)	Initial applied depth (in.)	Drained depth after 21 d (in.)	Initial solids concentration (percent)	Initial volume applied (gal)
1	19.2	0.6	36	12	5.3	6,239
2	20.5	0.0	36	15	5.6	6,239
3	10.0	0.0	18	7	6.3	2,323
4	9.4	0.6	18	7	6.3	2,559
5	21.3	0.0	30	13	7.5	4,875
6	26.3	0.3	30	14	9.3	4,875

The lagoons were equipped with underdrains which allowed the removal of drainage from the residuals shortly after the application was completed. Figure 4.27 shows the volume reduction for each freeze-thaw lagoon over a 21-day period. Typically, a volume reduction of 60 to 75 percent was achieved. As shown in Table 4.7, the residuals depth remaining after 21 days was between 7 and 15 in., compared to a predicted freezing depth of 9 in. No freezing conditions occurred during these initial 21 days, and therefore the volume reduction was mostly attributable to the drainage of the residuals.

When the freeze period is modeled using Martel's freeze-thaw model (Martel 1989, see Chapter 5), an estimated freezing depth of at least 8 in. should be achieved. Composite samples of the residuals on the bed had a solids concentration of 35.5 to 45.1 percent as shown in Table 4.8. Table 4.6 previously showed that laboratory freeze-thaw and drainage for this facility had about a 30 percent solids concentration.

Table 4.8

Erie County Water Authority

pilot freeze-thaw data

Bed number	Drained depth (in.)	Predicted freezing depth (in.)	Depth remaining* (in.)	Composite solids remaining (percent)
1	12	9	7	43.7
2	15	9	4	45.1
3	7	9	4	42.6
4	7	9	4	48.4
5	13	9	4	35.5
6	14	9	4	37.8

*Remaining depth after 118 days

It can thus be concluded that the residuals probably froze completely and that the model did a fairly good job in predicting the freeze depth, and may have underestimated the freeze depth. The field solids concentrations were slightly higher than the lab values, probably because evaporation was also taking place in the field.

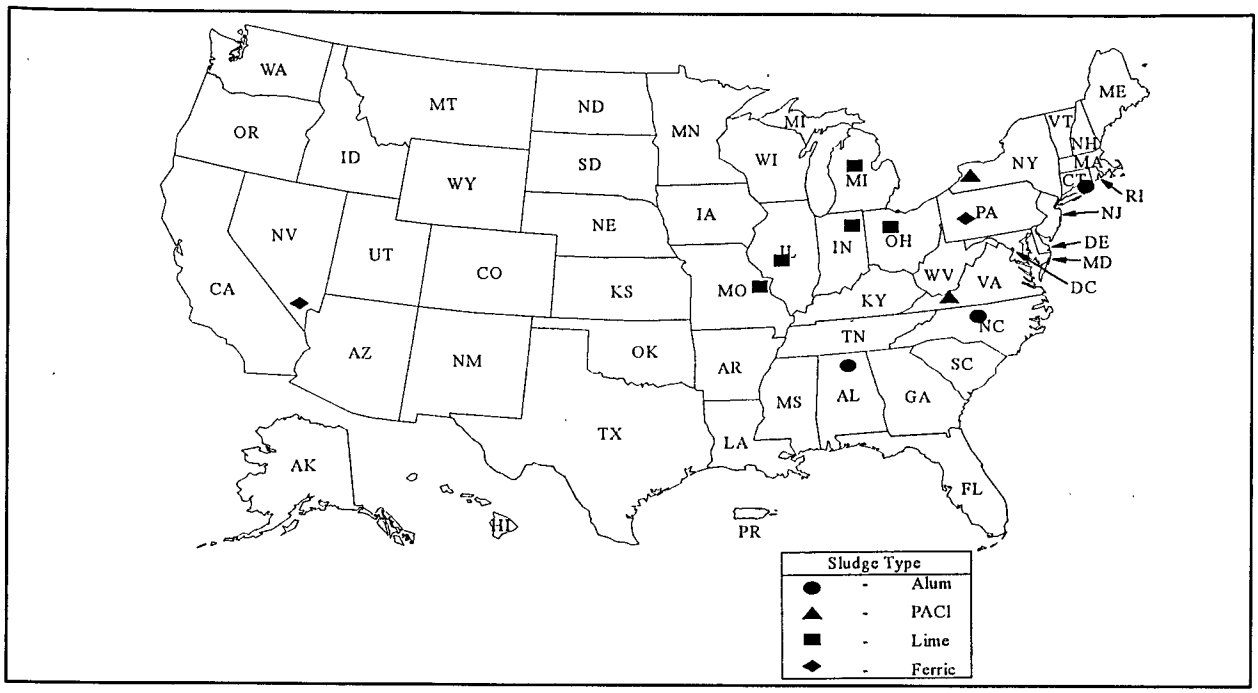

Note: Edmonton, Alta (not pictured here), with lime sludge, was also evaluated.

Figure 4.1 Selected utilities for detailed evaluation

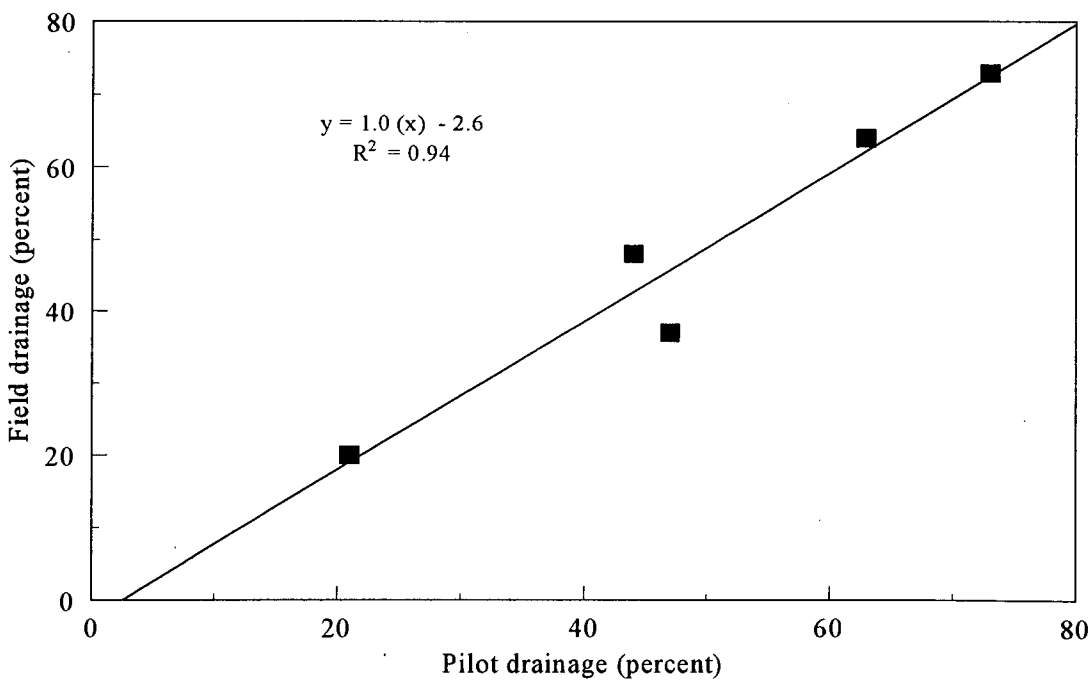

Figure 4.2 Summary of field and pilot test drainage results

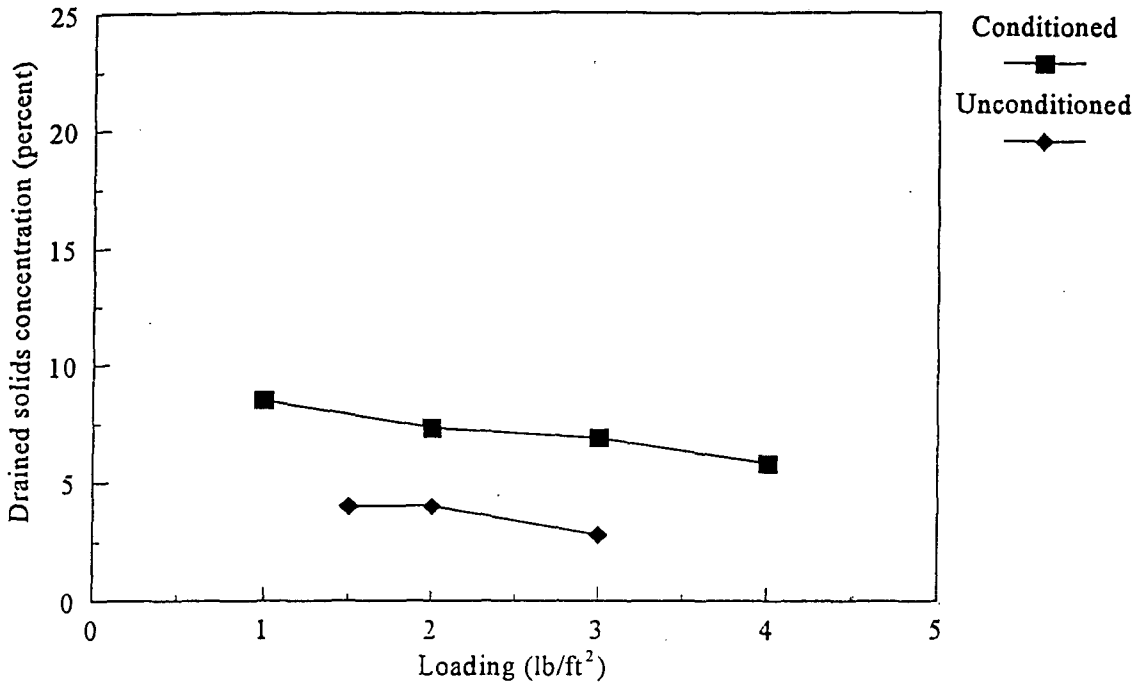

Figure 4.3 Pilot drainage tests for Durham, N.C.

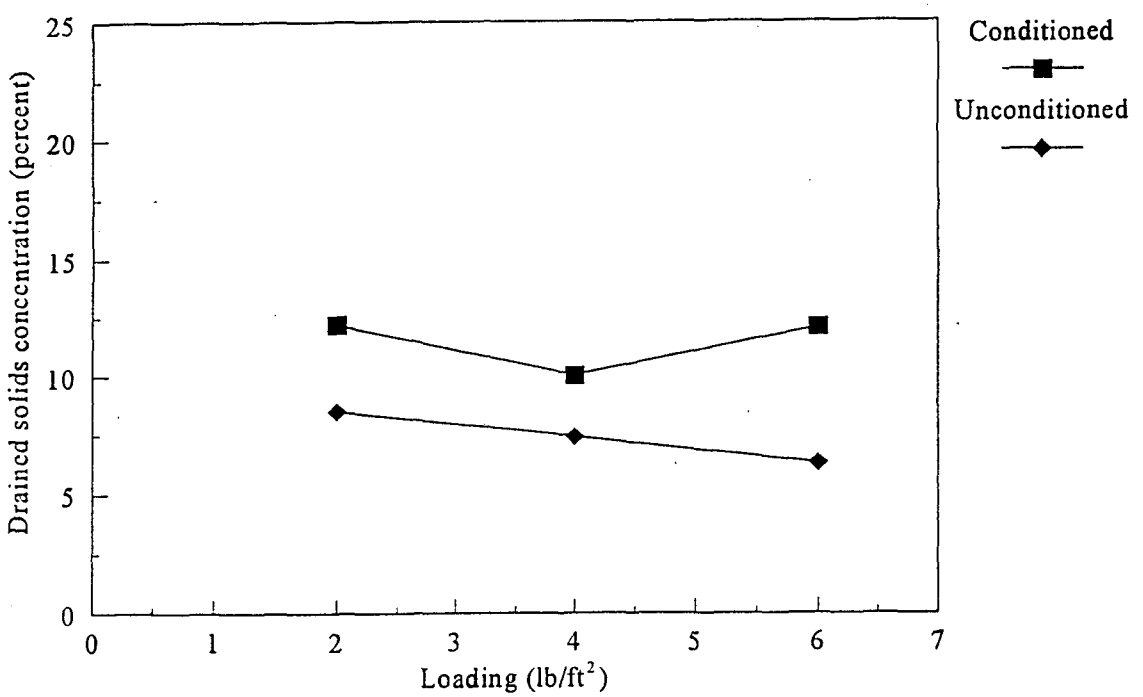

Figure 4.4 Pilot drainage tests for Buffalo, N.Y.

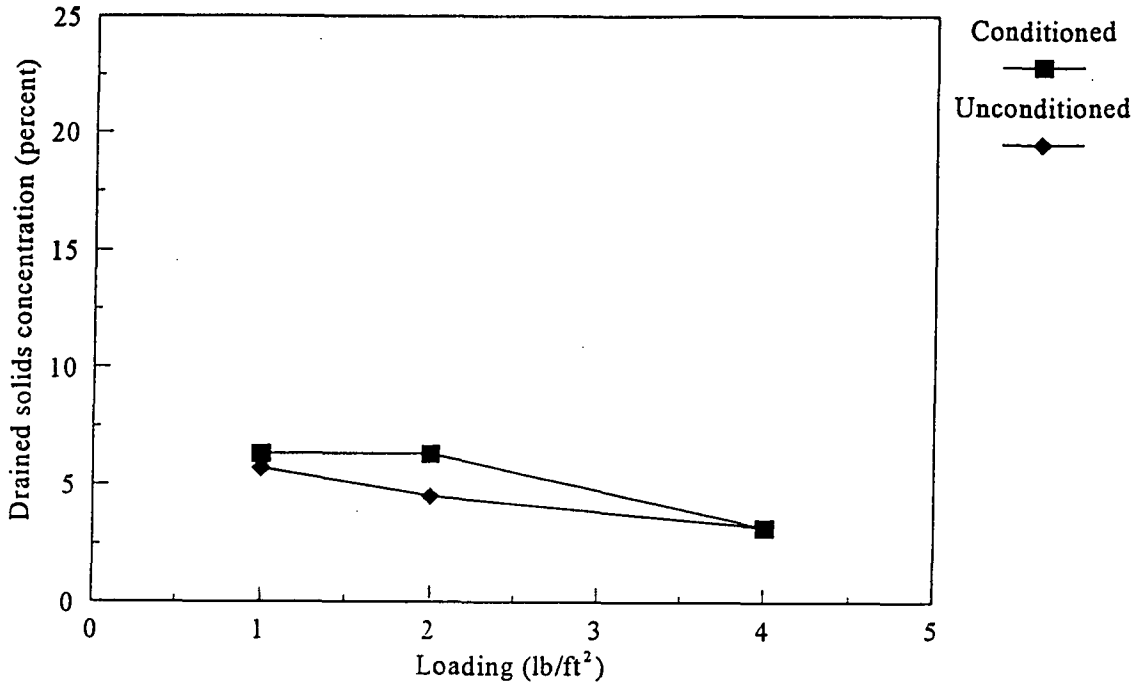

Figure 4.5 Pilot drainage tests for Indiana, Pa.

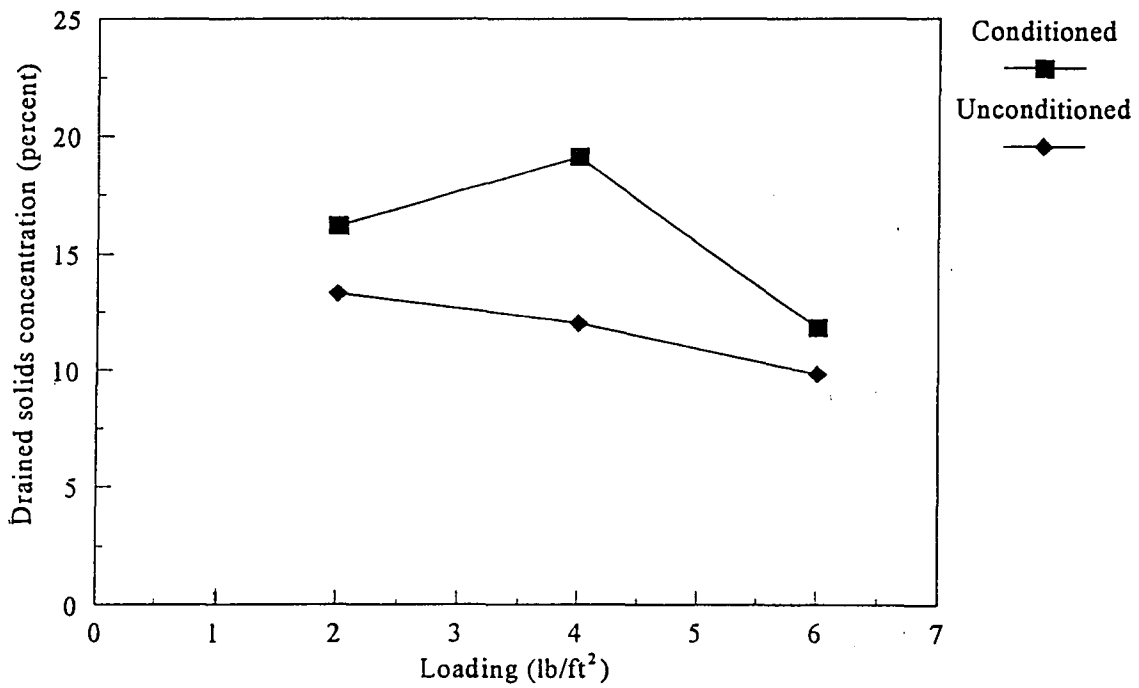

Figure 4.6 Pilot drainage tests for Huntsville, Ala.

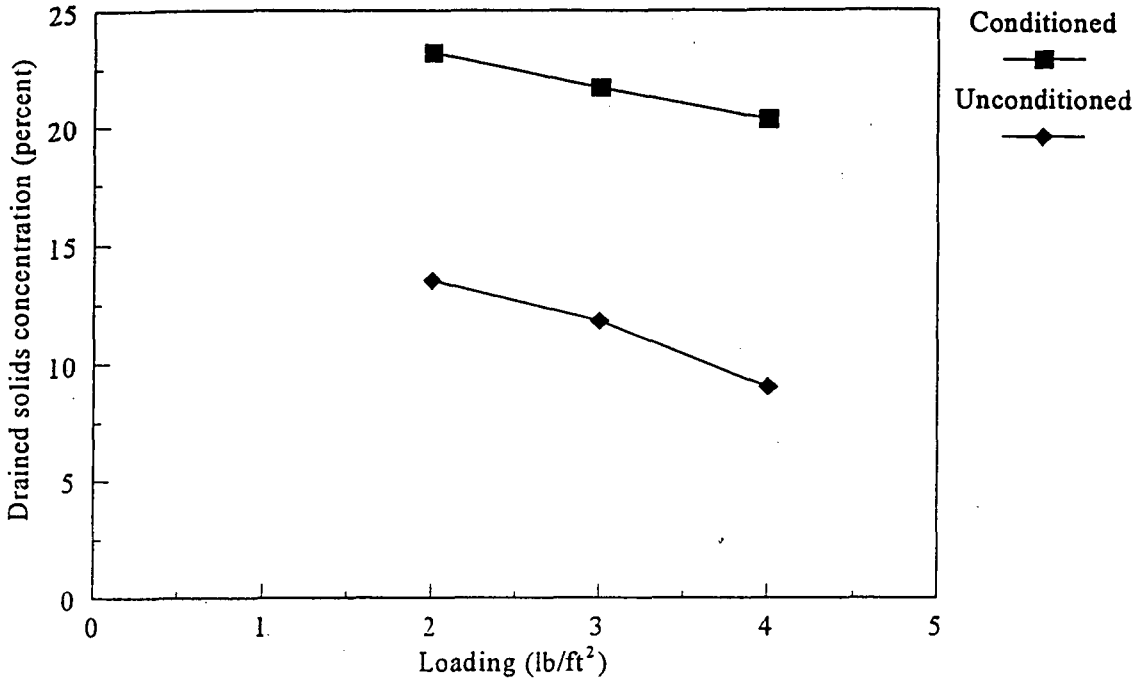

Figure 4.7 Pilot drainage tests for Boulder City, Nev.

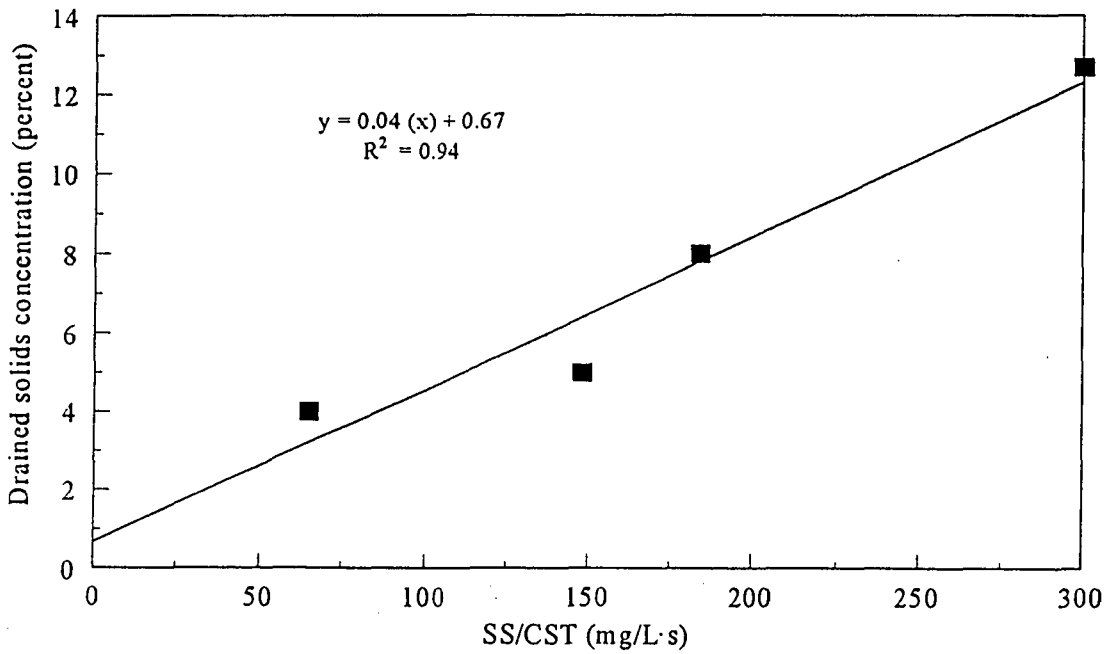

Figure 4.8 Relationship between drained solids concentration and filterability index for coagulant residuals

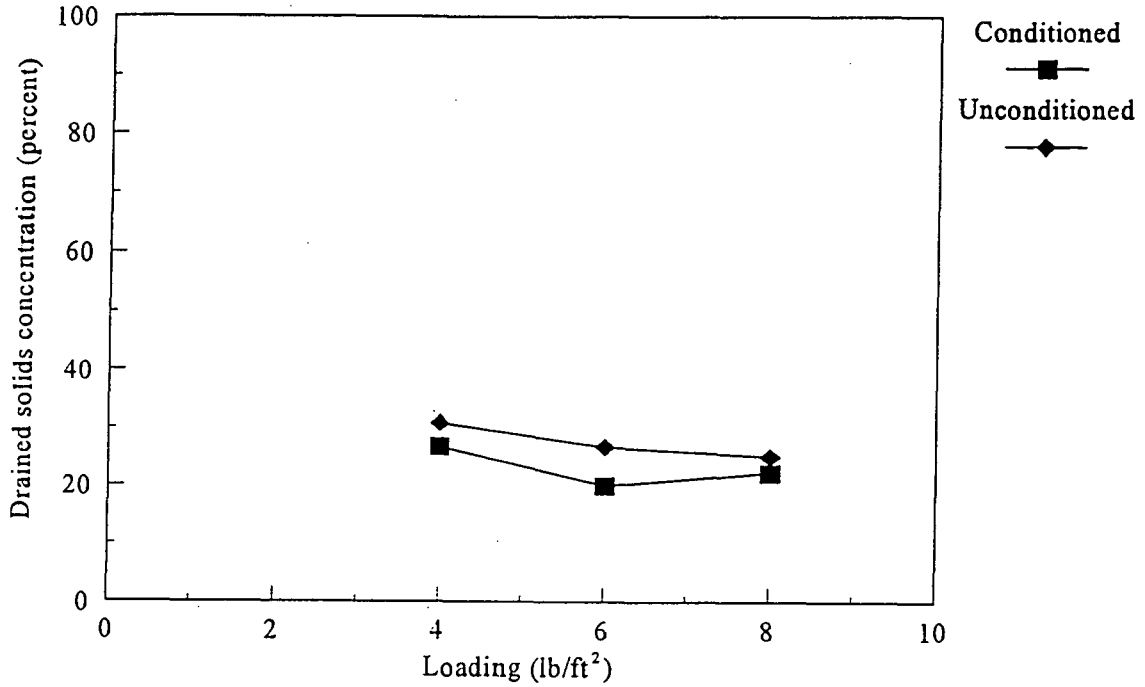

Figure 4.9 Pilot drainage tests for Ft. Wayne, Ind.

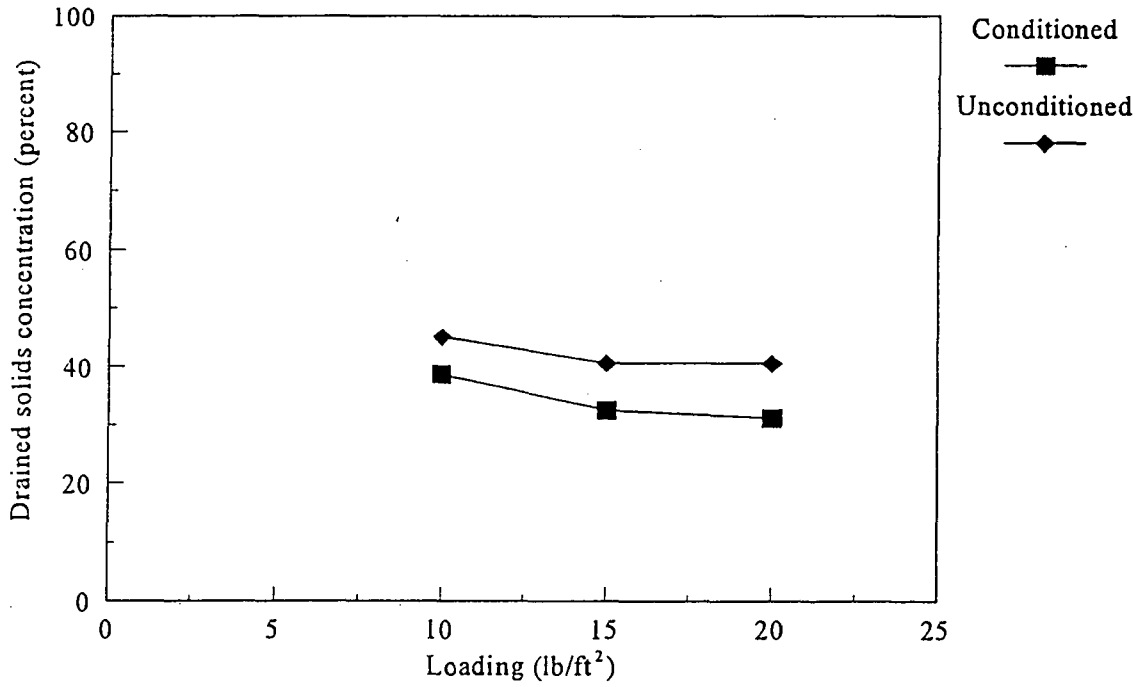

Figure 4.10 Pilot drainage tests for St. Louis, Mo.

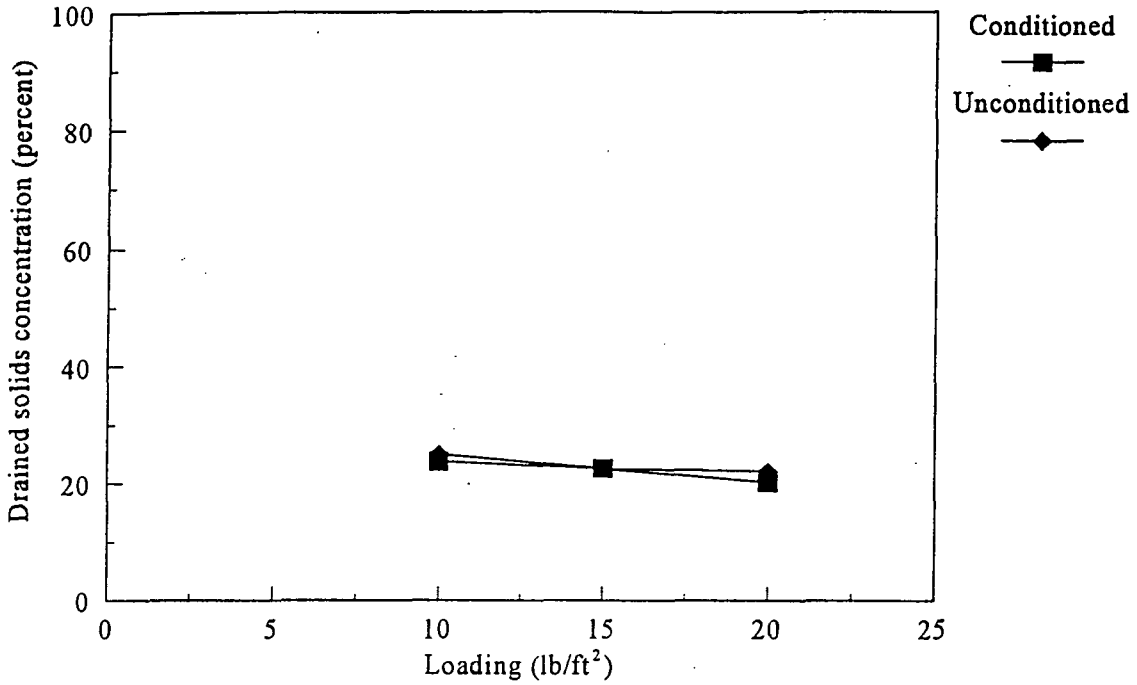

Figure 4.11 Pilot drainage tests for Findlay, Ohio

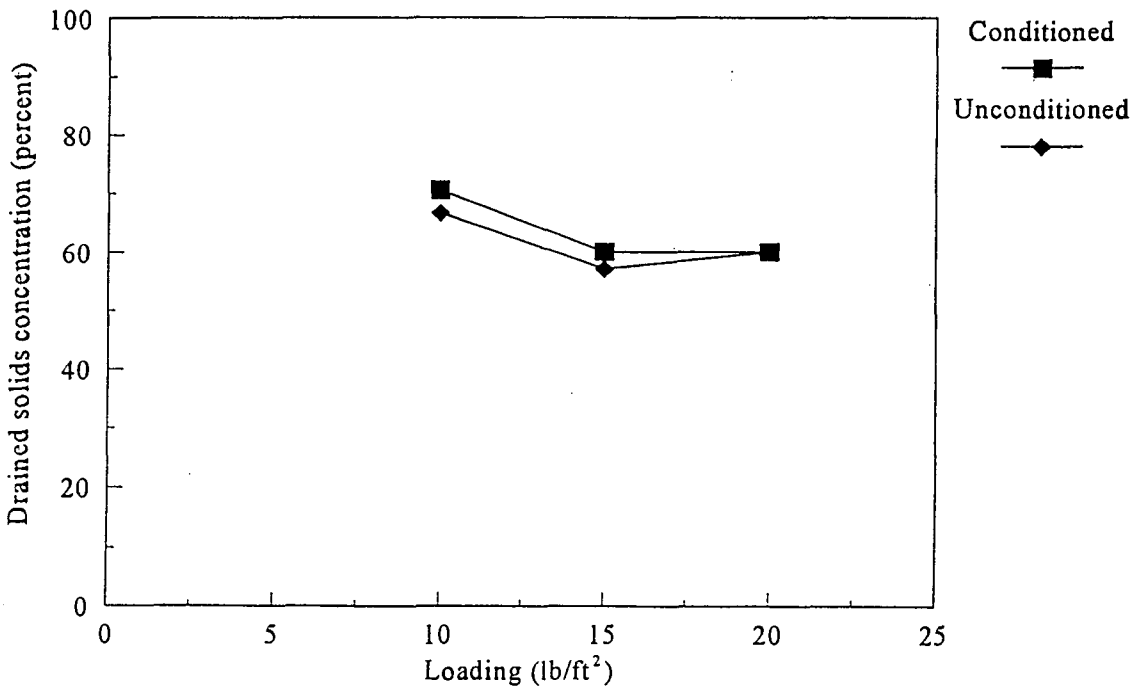

Figure 4.12 Pilot drainage tests for Taylorville, Ill.

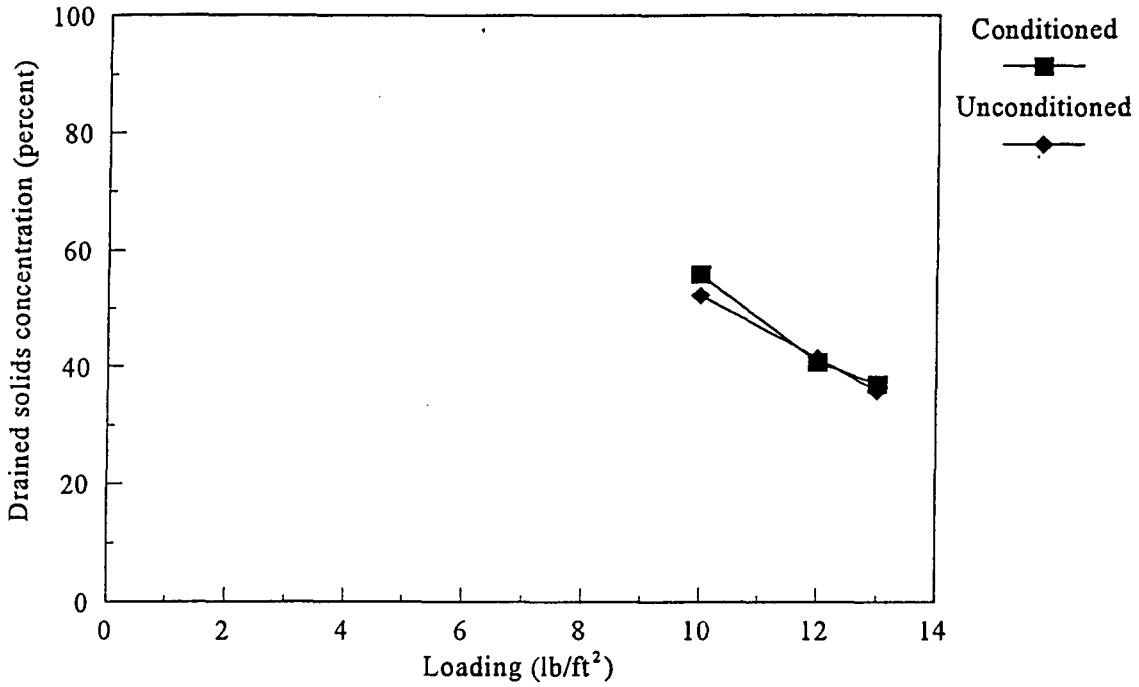

Figure 4.13 Pilot drainage tests for Midland, Mich.

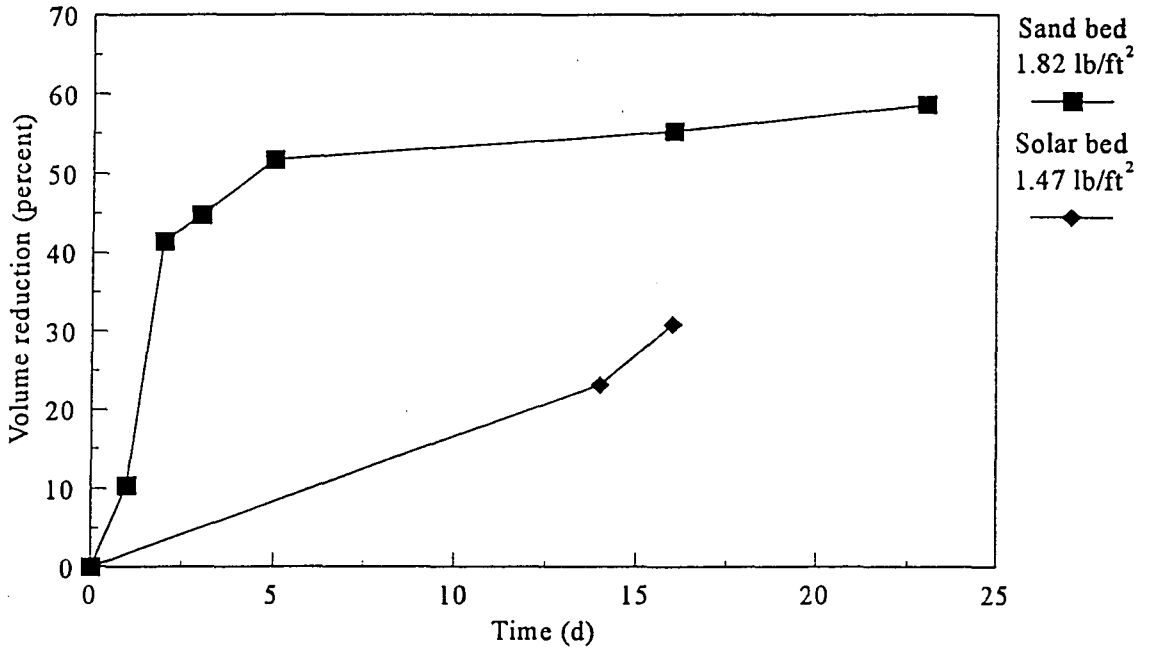

Figure 4.14 Unconditioned residuals drainage rate comparing sand beds and solar beds

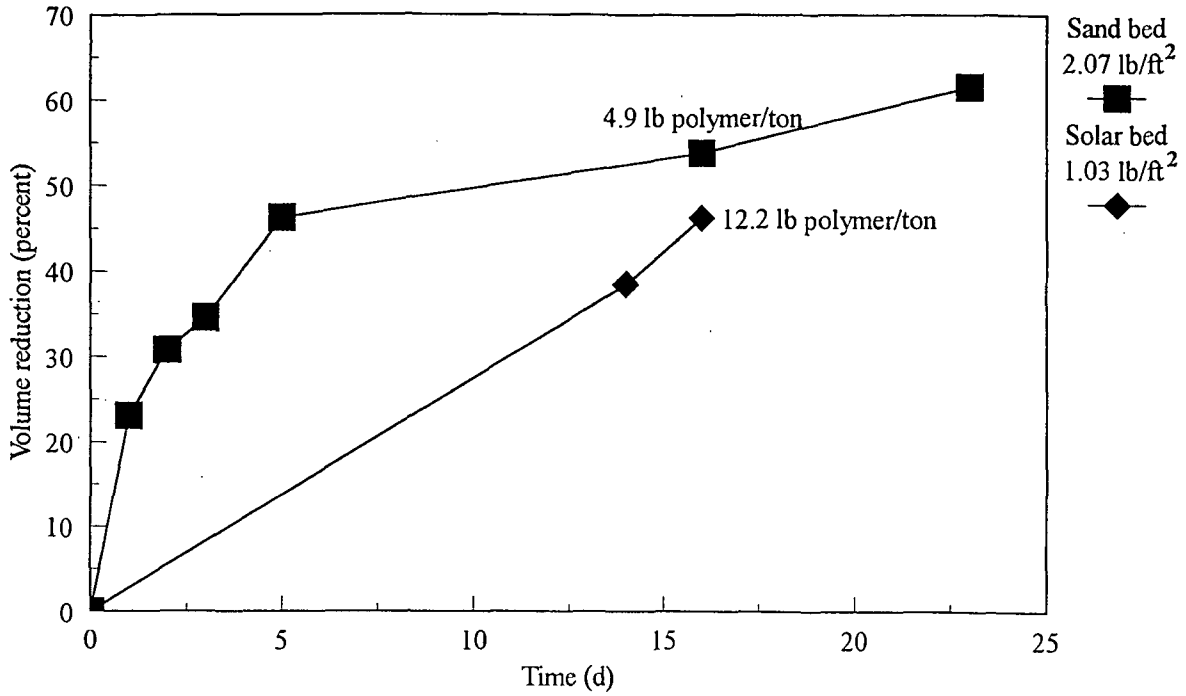

Figure 4.15 Conditioned residuals drainage rate comparing sand beds and solar beds

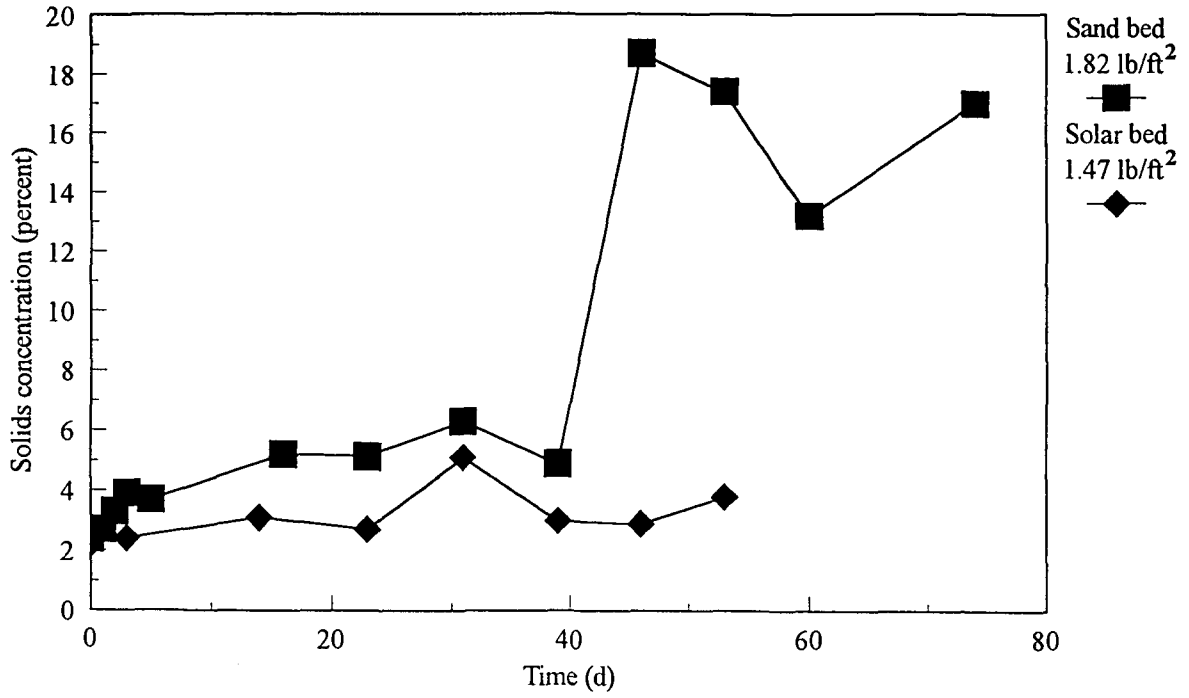

Figure 4.16 Unconditioned residuals drying rates comparing sand beds and solar beds

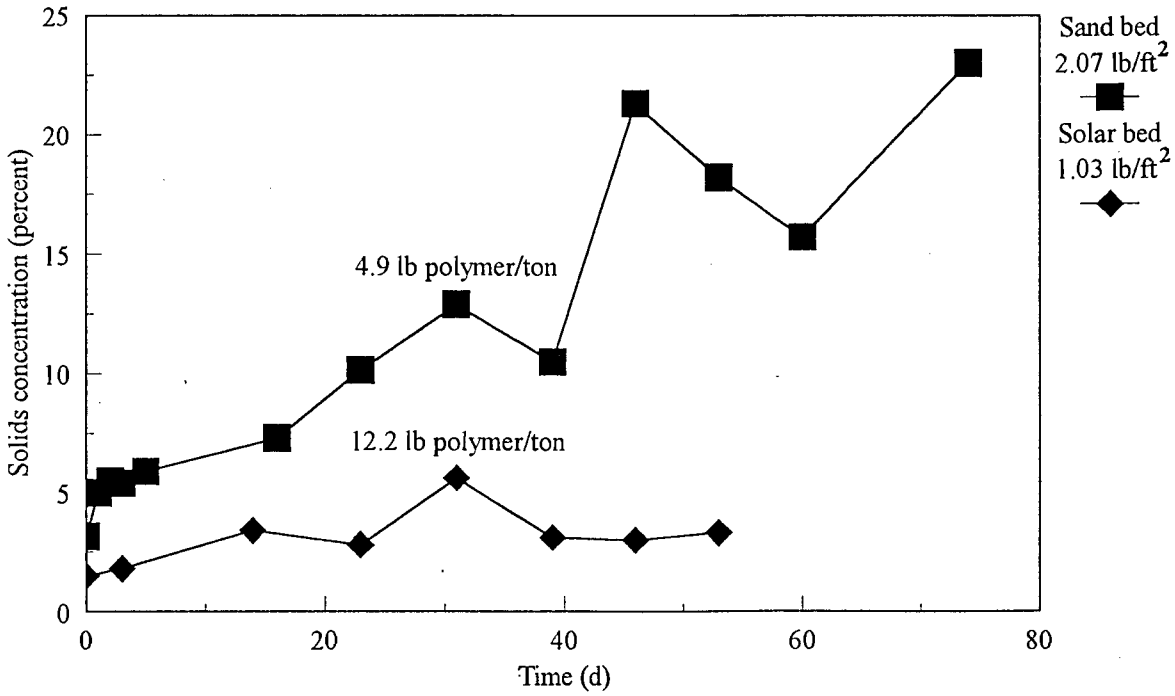

Figure 4.17 Conditioned residuals drying rates comparing sand beds and solar beds

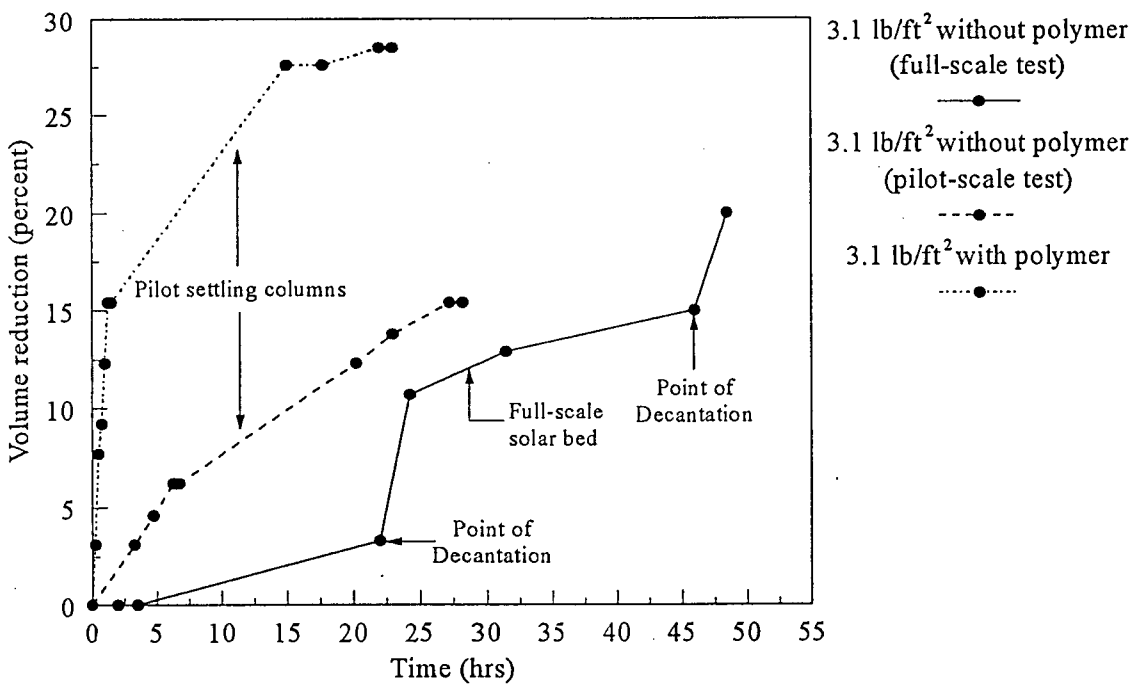

Figure 4.18 Boulder City, Nev., full- and pilot-scale test results

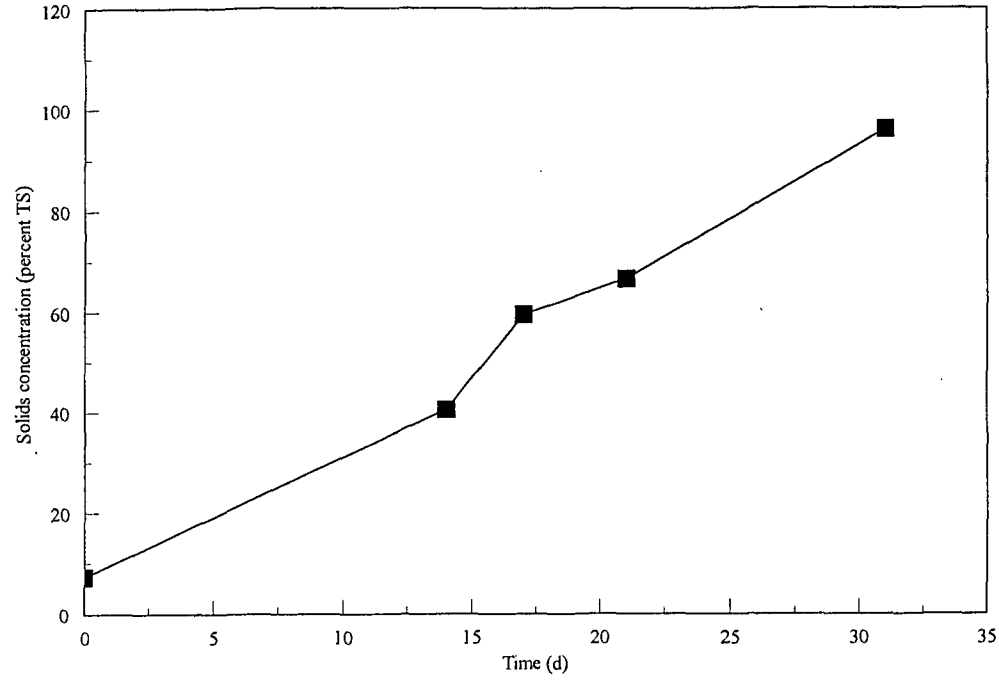

Figure 4.19 Boulder City, Nev., bed solids concentration versus time

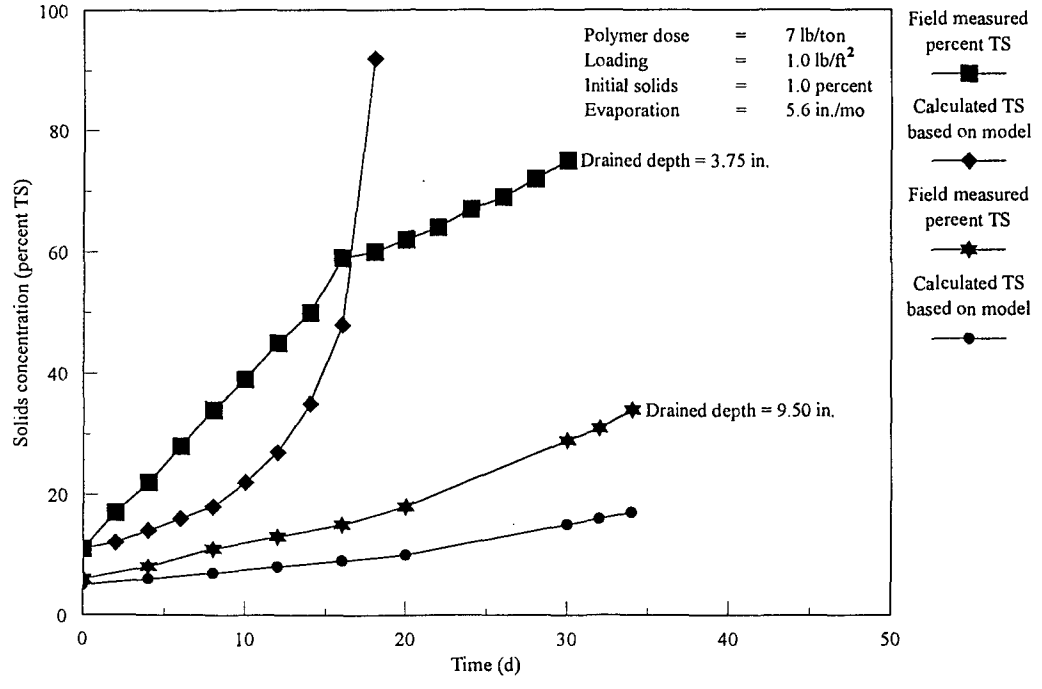

Figure 4.20 Residuals evaporation characteristics for Durham, N.C.

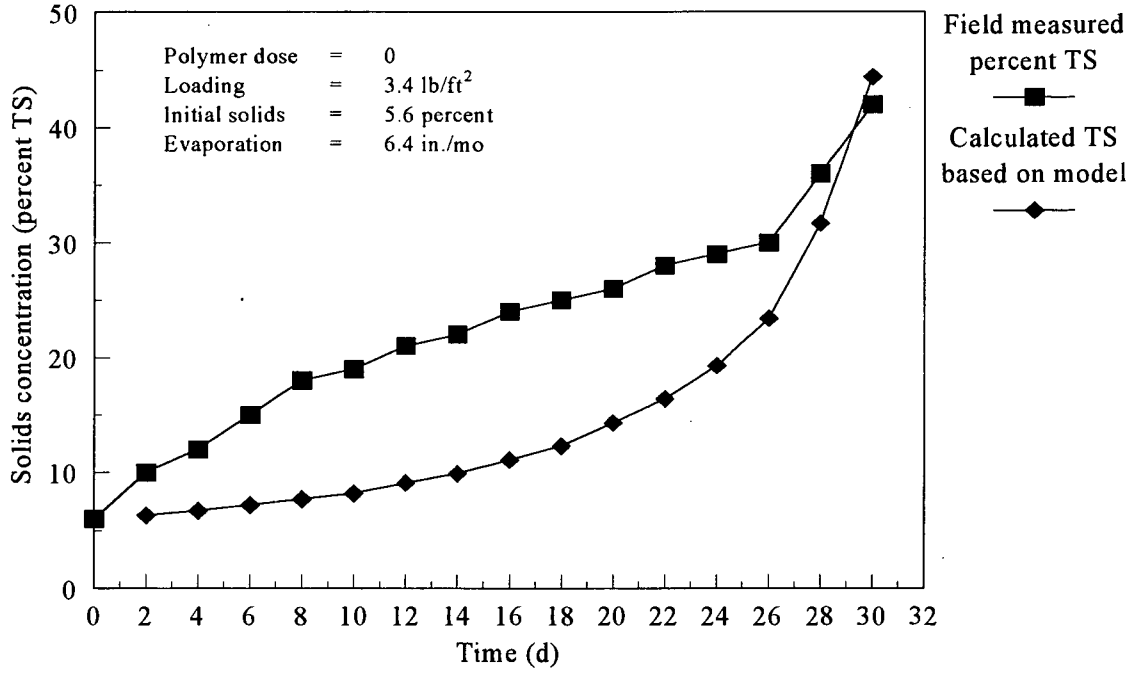

Figure 4.21 Residuals evaporation characteristics for Huntsville, Ala.

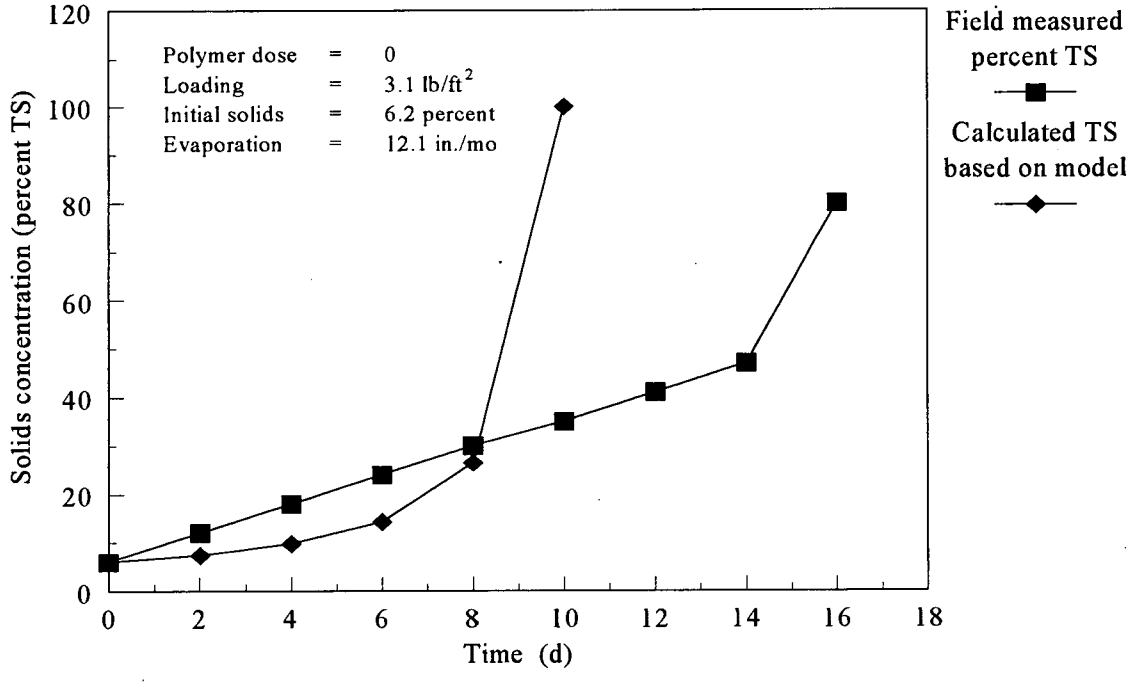

Figure 4.22 Residuals evaporation characteristics for Boulder City, Nev.

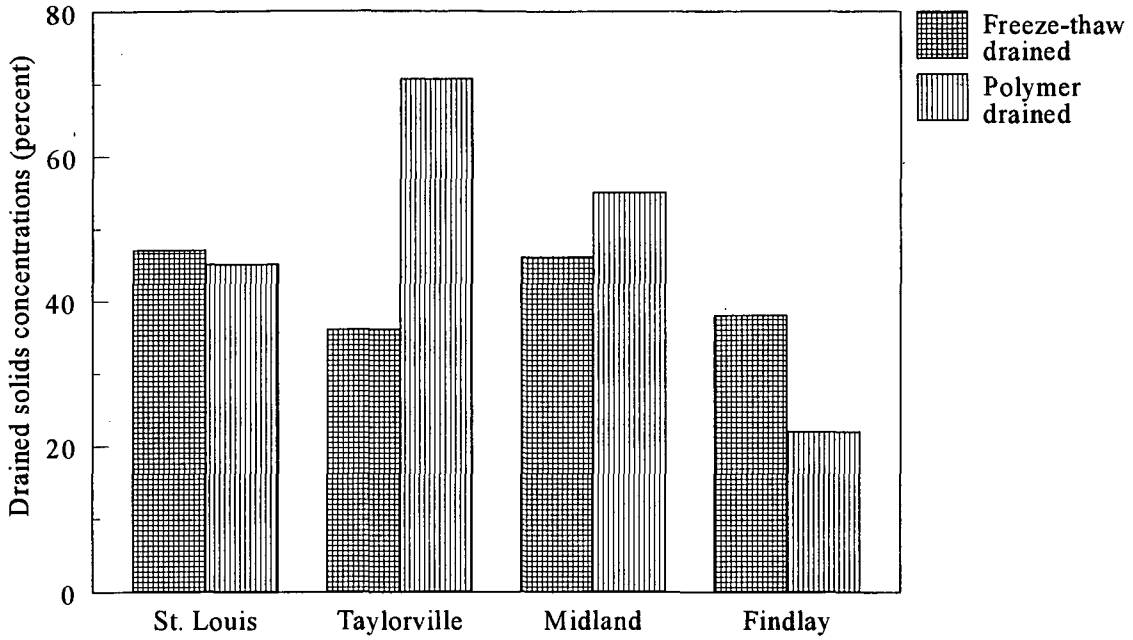

Figure 4.23 Comparison of drainage conditioned by freeze-thaw and polymer for lime residuals

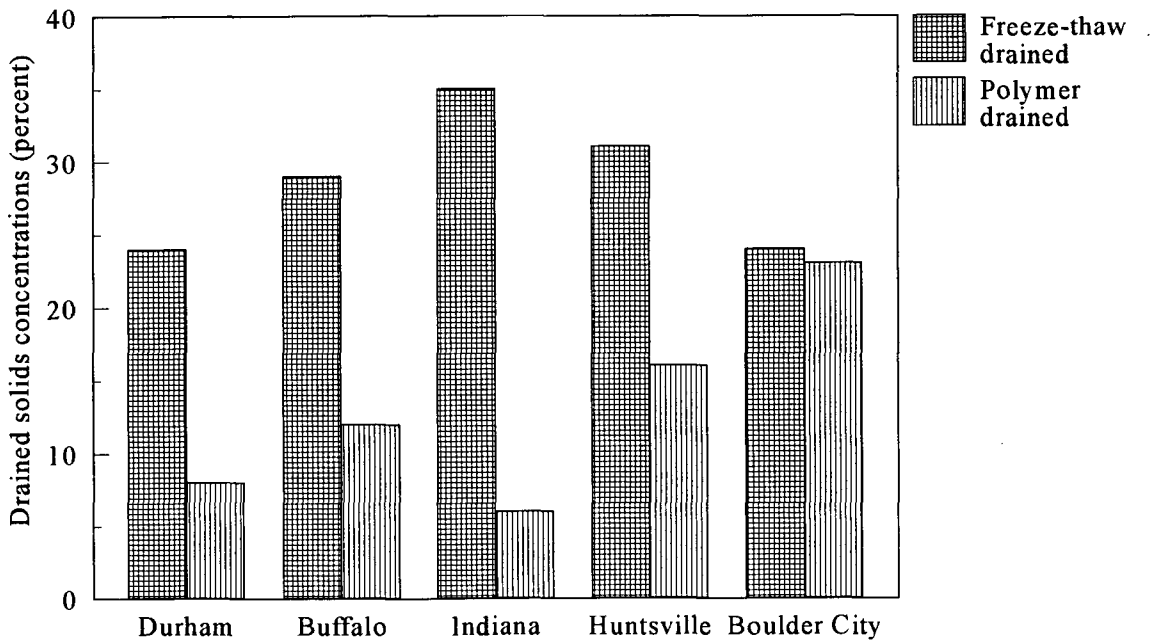

Figure 4.24 Comparison of drainage conditioned by freeze-thaw and polymer for coagulant residuals

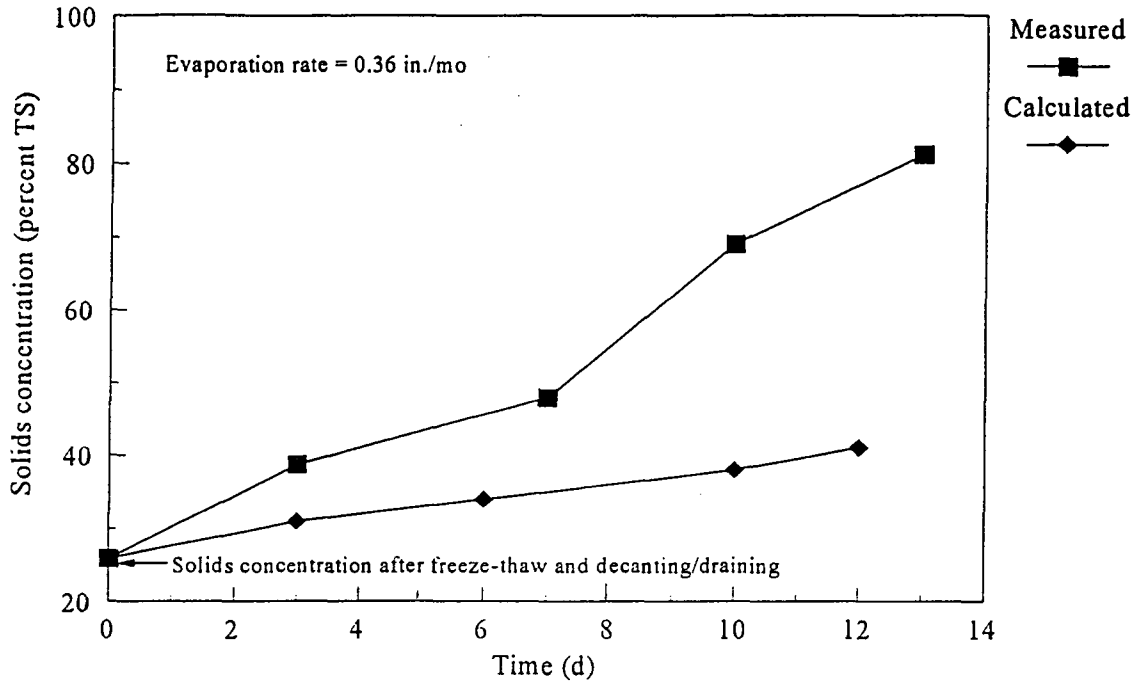

Figure 4.25 Drying rate for post freeze-thaw material (PACI residuals)

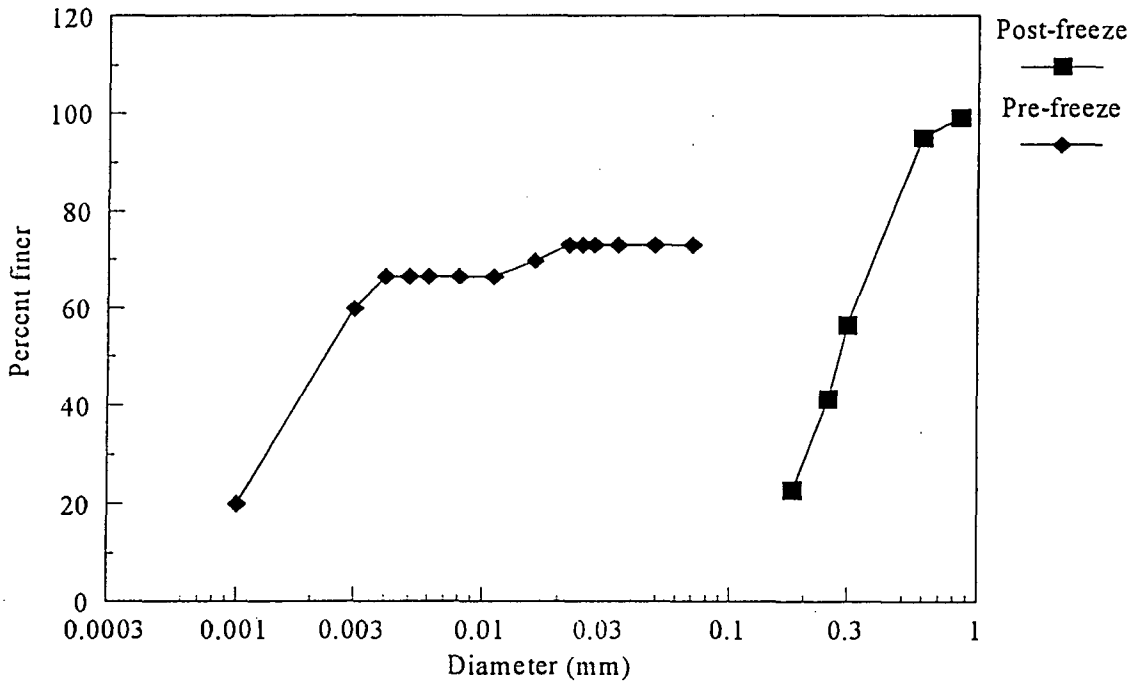

Figure 4.26 Particle size distribution for raw and freeze-thawed residuals

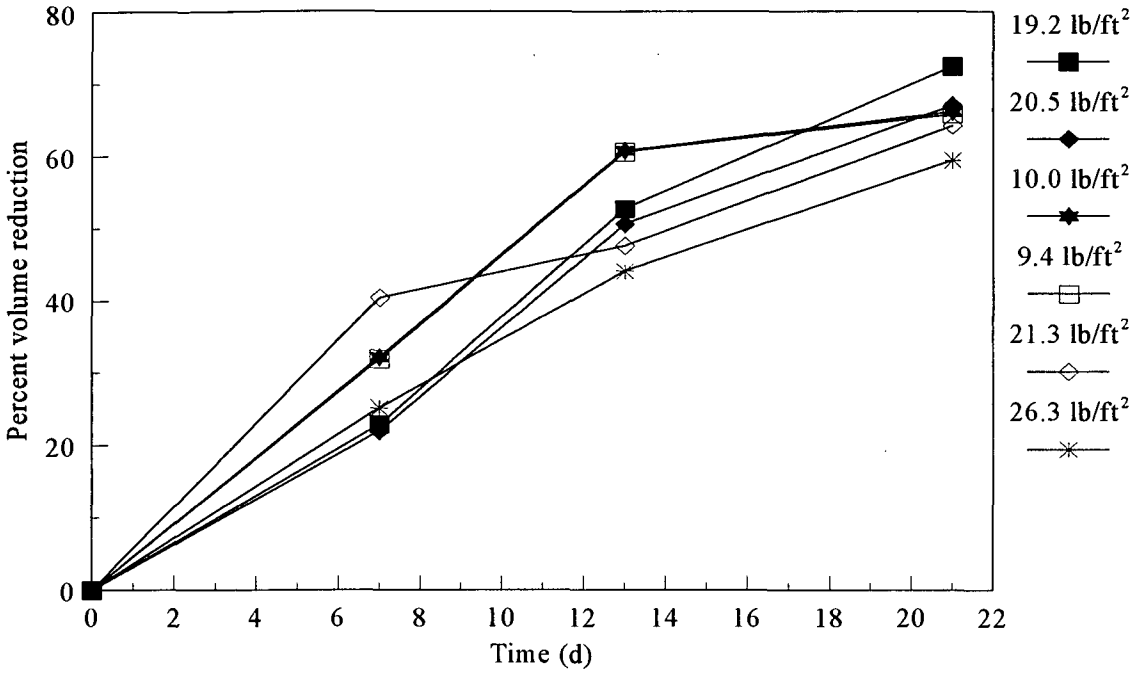

Figure 4.27 Erie County pilot freeze-thaw bed initial volume reduction

CHAPTER 5
MODELING OF NONMECHANICAL DEWATERING

INTRODUCTION

The pilot and field test data presented previously in Chapter 4 indicated that drainage and evaporation are the two most important elements of nonmechanical dewatering. By maximizing the removal of water from the residuals through polymer conditioning, draining, and decanting, the amount of residuals drying required through evaporation is minimized. This concept should be valid for all types of nonmechanical dewatering including sand drying beds, drying lagoons, solar drying beds, and freeze-thaw beds or lagoons. For freeze-thaw, maximizing the drainage and decanting would be advantageous in reducing the volume of residuals to be frozen.

The purpose of this chapter is to show the utilization of the pilot and field test data presented previously in Chapter 4 in order to size nonmechanical dewatering facilities.

SAND DRYING BED PERFORMANCE MODELING

Existing Theory and Empirical Modeling

Several models have been developed previously to estimate a required sand drying bed area for a particular water utility. In a book published by AWWA and ASCE (1990) the drying bed size is based on the effective number of residuals applications on each bed and the depth of residuals applied onto the bed, which is based on the following equation:

$$A = \frac{V}{AA \times D(i) \times 7.5} \tag{5.1}$$

where

A	=	drying bed area (ft^2)
AA	=	number of bed applications per year
D(i)	=	depth of residuals applied (ft)
V	=	annual volume of residuals (gal)

In this particular model, the number of uses for each bed per year must be estimated. This would be a function of the drainage time, drying of the residuals through evaporation, and cleaning of the bed after the desired final solids concentration has been achieved.

A better criterion for sizing drying beds would be the use of a specific drying bed yield in terms of $lb/ft^2/yr$. An appropriate yield, however, should take into account seasonal conditions such as temperature, wind velocity, precipitation, residuals characteristics, and initial residuals solids concentration. Ignoring such factors and using only average annual conditions could result in under sizing of the sand drying beds.

The operation of a sand drying bed is primarily a function of the following parameters:

1. The initial solids concentration of the applied residuals
2. The depth of the residuals applied on the beds
3. The loss of free water through the underdrain or decant system
4. The net evaporation rate
5. The desired final solids concentration

All of these factors need to be considered in order to determine the optimum loading rate and yield for a given location. Since most of these factors are very site specific, any mathematical modeling for determining the drying bed design should take these local factors into consideration.

Rolan (1980) developed a series of equations which can be used to determine the sand drying bed yield based on a certain loading rate. The mathematical model also takes into account the operational parameters listed above and is a comprehensive mathematical approach to assess the sand drying bed performance and size for a particular location. The model calculates the initial

loading (L) in lb/ft^2 for a given application based on the residuals depth applied, D(i), and the initial residuals solids concentration, SS(i), by using the following equation:

$$L = \frac{D(i)}{12} \times \frac{SS(i)}{100} \times 62.4 \tag{5.2}$$

where

L = the initial loading (lb/ft^2)
D(i) = the initial depth (in.)
SS(i) = the initial solids concentration (percent)

The final residuals depth, D(f), which is a function of the initial residuals depth, the solids concentration, and the final dry solids concentration desired, SS(f), can be calculated as follows:

$$D(f) = D(i) \times \frac{SS(i)}{SS(f)} \tag{5.3}$$

where

D(f) = the final residuals depth (in.)
D(i) = the initial depth (in.)
SS(i) = the initial solids concentration (percent)
SS(f) = the final dewatered solids concentration (percent)

The change in residuals depth, ΔD, necessary to achieve the final desired solids concentration is determined by subtracting the final residuals depth, D(f), from the initial depth, D(i), as shown below:

$$\Delta D = D(i) - D(f) \tag{5.4}$$

where

ΔD = the total change in depth (in.)

D(i) = the initial depth (in.)

D(f) = the final depth (in.)

The ΔD term is a function of the total loss of moisture due to decanting, underdrainage, and evaporation. The loss of moisture to the underdrain system and decanting is reflected in the rapid change in depth of the residuals, $\Delta D(u)$, shortly after the application of the residuals to the bed. Any water decanted from the bed would also be included in the term $\Delta D(u)$. The change in depth, $\Delta D(u)$, due to the loss of free water to the underdrains can be calculated as follows:

$$\Delta D(u) = D(i) \times P(u) \tag{5.5}$$

where

$\Delta D(u)$ = the change in depth due to drainage (in.)

D(i) = the initial depth (in.)

P(u) = the percent of the initial depth lost to drainage

A value for the percentage loss, P, to the underdrains and decanting must be determined based on pilot test results or from comparable full-scale facilities. The change in depth due to evaporation accounts for the remaining loss in depth and can be calculated with the following equation:

$$\Delta D(e) = \Delta D - \Delta D(u) \tag{5.6}$$

where

$\Delta D(e)$ = the change in depth due to evaporation (in.)

ΔD = the total change in depth (in.)

$\Delta D(u)$ = the change in depth due to drainage (in.)

The time, t, required to achieve the evaporation of the remaining water content in the residuals until the desired final residuals solids concentration is dependent on the evaporation rate,

E, expressed in in./mo. Evaporation and the resulting change in residuals depth may not be linear because of changes in the residuals characteristics prior to and following the formation of surface cracks in the residuals. For the purpose of this model, evaporation and depth change were assumed to be unaffected by these factors, and thus a linear relationship is assumed. Because evaporation rates exhibit seasonal variations, the annual average evaporation rate should be used with careful consideration. Since winter evaporation rates can be significantly lower than summer rates, consideration should be given to providing residuals storage capacity when designing residuals facilities to be used in conjunction with drying beds. An alternative to providing residuals storage would be to use the average evaporation rate for the winter months, rather than the annual average rate.

The drying time, t, can be calculated as follows:

$$t = \frac{\Delta D(e)}{E} \tag{5.7}$$

where

t = the required residuals drying time (month)

$\Delta D(e)$ = the change in depth due to evaporation that is necessary to meet the final desired solids concentration (in.)

E = the evaporation rate (in./month)

The number of applications, AA, which can be accomplished in a year to the sand drying beds is, therefore, dependent on the evaporation time, t, and can be calculated with the following equation:

$$AA = \frac{12\ \text{months/year}}{t} \tag{5.8}$$

where

AA = the number of bed applications per year

t = the required residuals drying time (month)

Finally, the drying bed yield, Y, in lb/ft^2/yr is a function of the residuals loading applied to the bed (L) and the number of applications per year (AA). The drying bed yield can be calculated as follows:

$$Y = L \times AA \tag{5.9}$$

where

Y	=	the drying bed yield (lb/ft^2/yr)
L	=	the initial loading (lb/ft^2)
AA	=	the annual number of applications

The model equations can be used as a tool to size sand drying beds as well as to determine, at least theoretically, the optimum performance. The major assumption that must be made in the model is the percent drainage of free water to the underdrain system. This value, however, is influenced by numerous factors, including (1) the initial solids concentration, (2) the residuals depth or loading rate, (3) the residuals' physical characteristics, and (4) the addition of polymers to the residuals. In general, a drainage value of 40 to 70 percent is considered reasonable, but there is not a more rational approach to determine the drainage value other than performing pilot scale tests, as demonstrated in Chapter 4. Further characterization of the drainage values under various scenarios will be necessary to truly develop an optimization model.

Existing Model Example

An example of the model developed by Rolan is presented to illustrate the data input requirements and the resulting data generated by the model. For the purpose of this example, the impact of initial residuals loading (L) was evaluated at 1, 2, 3, and 4 lb/ft^2. Assumptions for this example include the following:

- Initial solids concentration = 2.0 percent
- Final solids concentration = 20 percent

- Percent drainage to underdrains = 60 percent
- Evaporation rate = 3.0 in./month
- Annual residuals production = 365 dry tons/yr

By utilizing the model equations, the sand drying bed yield was determined for each loading as shown in Table 5.1. The increase in initial loading rate from 1 lb/ft^2 to 4 lb/ft^2 did not influence the resulting drying bed yield. As shown in Table 5.1, the final drying bed yield is 12.5 lb/ft^2/yr for all four loadings. This is a result of utilizing the same percent drainage for all four conditions. The example illustrates, furthermore, that as loading increases, the number of applications per year decreases proportionally. If this were a situation wherein the percent drainage did not change between 1 and 4 lb/ft^2 loading, then the design decision would be based on the desired number of applications per year. Since the cost of cleaning a bed is often quite high, it may be advantageous in this example to use a high loading and minimize the bed cleanings. One of the limitations of this approach is that the monthly variations in evaporation are not accounted for.

Table 5.1

Sand drying bed model example

	Loading (lb/ft^2)			
Parameter	1	2	3	4
Initial residuals depth (in.)	9.6	19.2	28.8	38.5
Final residuals depth (in.)	0.96	1.92	2.88	3.85
Change in depth (in.)	8.6	17.3	25.9	34.7
Loss to underdrains (in.)	5.8	11.5	17.3	23.1
Loss to evaporation (in.)	2.9	5.8	8.6	11.6
Evaporation time required (month)	0.96	1.92	2.87	3.87
Annual applications	12.5	6.25	4.18	3.10
Drying bed yield (lb/ft^2/yr)	12.5	12.5	12.5	12.5

Assumptions:

Initial solids concentration	=	2 percent
Final solids concentration	=	20 percent
Drainage volume	=	60 percent
Evaporation rate	=	3 in./month
Annual solids production	=	365 tons/yr

Utilization of Field and Laboratory Test Data

Chapter 4 presented examples of test data from five different utilities to determine the volume reduction achieved through drainage on the sand drying bed. The volume reduction was influenced by the initial solids concentration, solids loading and polymer conditioning. For any utility interested in the use of sand drying beds, the first task would be to determine the optimum combination of solids loading and initial solids concentration that would yield the largest drained solids concentration. The fact that maximizing the drained solids concentration also maximizes the yield, and therefore minimizes the sand bed area required, can be shown by rearranging the drying equations to result in:

$$Y = (0.624)\frac{SS(f)\,SS(d)\,(E)}{SS(f) - SS(d)} \qquad (5.10)$$

where

Y	=	drying bed yield, lb/ft^2/yr
SS(f)	=	desired final dewatered solids concentration, percent
SS(d)	=	drained solids concentration, percent
E	=	evaporation rate, in./mo

Since E is fixed and SS(f) is set as desired, the only variable is the drained solids concentration. Clearly maximizing SS(d) will maximize Y. Therefore, a utility would run a series of pilot drainage tests in order to find SS(d). The first variable would be the initial suspended (or total) solids concentration. Two suspended solids values may be sufficient to run. One would be the suspended solids concentration as directly obtained from the sedimentation basins. A second condition to test would be after a thickener. This comparison would essentially allow a cost trade-off to be made between thickener cost and sand drying bed cost. The next variable to evaluate would be the solids loading. In this research, good results for coagulant sludges were found for loadings between about 2 to 6 lb/ft^2; for lime sludge the loadings could be more in the range of 10 to 15 lb/ft^2. The final variable would be polymer conditioning. Therefore, to test two solids concentrations with three

loading rates, with and without polymer, 12 pilot drainage tests would be needed. For each condition the drained solids concentration should be calculated. Those conditions that maximize the drained solids concentrations would be logical to carry over for sizing analysis. For example, it may be desirable to carry over the best condition with polymer and the best without polymer to see the impact on bed sizing. The best results with and without a thickener could also be compared.

An initial rough estimate of the sand bed area required could be made based on annual average conditions using equation (5.10). Using Durham, N.C., from Table 4.3 as an example of the effect of polymer on bed sizing at 1.1 percent SS and loading 2 lb/ft^2, the drained solids concentration was found from the pilot studies to be 4.0 percent without polymer and 7.3 percent with polymer. Using an average annual net evaporation of 4.1 in. and a sludge production of 1,000 tons/yr, then for a 20 percent final solids concentration:

$$Y\left(\text{without polymer}\right)=\left(0.624\right)\frac{\left(20\right)\,4\left(4.1\right)}{20-4}=12.8\ \text{lb/ft}^2/\text{yr}$$

and the required area would be:

$$\text{Area}=\frac{1{,}000\left(2{,}000\right)}{12.8}=156{,}000\ \text{ft}^2$$

Finding the required area with polymer would be:

$$Y\left(\text{with polymer}\right)=\left(0.624\right)\frac{\left(20\right)\left(7.3\right)\left(4.1\right)}{20-7.3}=29.4\ \text{lb}/\text{ft}^2/\text{yr}$$

$$\text{Area}=\frac{1{,}000\left(2{,}000\right)}{29.4}=68{,}000\ \text{ft}^2$$

In this case the use of polymer would reduce the required drying area by about 55 percent. This type of comparative analysis, perhaps coupled with general cost assumptions, would result in the selection of the desired design conditions.

The next step in the analyses would be to actually size the bed accounting for monthly solids production variability. This calculation needs to be done based on a mass balance approach by determining the bed area required each month to accommodate the sludge production and determining how long the bed is used to provide the necessary drying. There are several approaches to this calculation, but the most straightforward is to convert the evaporative drying required into inches of evaporation required This can be found as:

$$\Delta D(e) = D(d) - \left(D(d) \frac{SS(d)}{SS(f)} \right) \tag{5.11}$$

where

$\Delta D(e)$ = required depth change due to evaporation (in.)

$D(d)$ = drained depth (in.)

$$D(d) = D(i) \frac{SS(i)}{SS(d)} \tag{5.12}$$

Again, using the example from above in Table 4.3, D(i) was 35 in. and SS(d) with polymer was 7.3 percent, therefore:

$$D(d) = 35 \frac{1.1}{7.3} = 5.27 \text{ in.}$$

$$\Delta D(e) = 5.27 - \left(5.27 \frac{7.3}{20} \right) = 3.4 \text{ in.}$$

In order to dry the solids to 20 percent, 3.4 in. of net pan evaporation is required. On the average, this would take less than one month for each loading, but there can be large variability in the monthly evaporation.

The first step in the month tabulations is done in Table 5.2. Table 5.2 shows the average daily solids production and the net evaporation for each month. The drying bed area that must be loaded that month is calculated as the daily production times 30 days/month divided by the chosen solids loading, in this case 2 lb/ft^2. The area indicates the amount of drying bed that must be available for loading during the month. Next the solids drying time is calculated as the sum of the monthly evaporations until the desired evaporation ($\Delta D(e)$) is reached, in this case 3.4 in. So for January,

$$\Delta D(e) = 3.4 = 1.0\ (\text{Jan}) + 1.9\ (\text{Feb}) + 0.1(3.5)\ (\text{Mar})$$

or 2.1 months are needed—January, February, and a tenth of March. This calculation is completed for each month and shown in Table 5.2.

Table 5.2

Tabulation of monthly sand drying bed area requirements

Month	Solids production (lb/d)	Net evaporation rate (in./month)	Solids drying time (month)	Drying bed area loaded* (ft^2)
January	7,820	1.0	2.1	117,000
February	8,275	1.9	1.4	124,000
March	9,145	3.5	1.0	137,000
April	9,350	4.7	0.7	140,000
May	5,265	5.8	0.6	79,000
June	3,395	6.9	0.5	51,000
July	3,240	7.0	0.5	49,000
August	4,880	6.5	0.5	73,000
September	3,145	4.5	0.8	47,000
October	4,125	3.5	1.0	62,000
November	3,650	2.6	1.4	55,000
December	4,470	1.8	2.3	67,000

*Design solids loading is 2.0 lb/ft^2

A mass balance can now be constructed. In this example, it has been assumed that all the solids for the month are produced on day one of the month and that they are on the bed all of that month. This will result in oversizing the beds. A bed that has solids on it from a previous month is not available at all during the month with the assumption that the solids are all loaded on day one. The mass balance can be broken down to a weekly basis for more accurate analysis.

The mass balance can begin in any convenient month. In this case October is convenient since a review of the drying time data would clearly show that there would be no carry-over beds for this month. Table 5.3 shows the mass balance approach.

Table 5.3

Monthly mass balance example for sand drying bed

Month	Bed loading area (ft^2)	Carry-over bed area (ft^2)	Net bed area required (ft^2)
October	62,000	0	62,000
November	55,000	0	55,000
December	67,000	55,000 (Nov)	122,000
January	117,000	67,000 (Dec)	184,000
February	124,000	67,000 (Dec) 117,000 (Jan)	308,000
March	137,000	117,000 (Jan) 124,000 (Feb)	378,000
April	140,000	0	140,000
May	79,000	0	79,000
June	51,000	0	51,000
July	49,000	0	49,000
August	73,000	0	73,000
September	47,000	0	47,000

The second column of Table 5.3 shows the bed area that must be loaded that month (from Table 5.2), and the third column shows the bed area that is still in use from previous months. Using this approach, the required bed area is 378,000 ft^2. This required area is about five times the area required based on the average annual sludge production and loading rate shown previously

(68,000 ft^2). This high required area compared to the annual average is due to this utility having a high winter sludge production when the net evaporation is quite low.

As indicated, the bed area can be reduced if a bed is cleaned and made available as soon as the theoretical drying time is reached. For example, the sludge production in January takes 2.1 months to dry, but based on the monthly mass balance above, three months of time are occupied since this bed is not available on day 1 of the third month. By breaking the months into weeks, and again assuming the sludge is cleaned off the bed right away and available for use by the new month's production, this area can be reduced. Such a calculation for the carry-over months is shown in Table 5.4. In this approach sludge production is uniformly spread into weeks, evaporation is uniformly spread into weeks, and a bed is available any week in which the drying cycle is ended, that is, 0.4 months drying would be available the third week of the month. In this case the drying bed area is reduced to 291,950 ft^2 as controlled by the first week of March. This analysis would ultimately need to be checked once individual beds are actually sized.

In this example, designing ten beds each about 30,000 ft^2 and allowing for two weeks of sludge storage or sizing 20 beds of about 15,000 ft^2 each and one week of storage would seem to be a good starting point for the actual sizing.

SOLAR DRYING BED

The solar bed sizing process would be similar to the sand drying bed. This process consists of loading the solar bed to a certain depth and, after a settling period, decanting the supernatant. The remaining residuals depth and solids concentration would be exposed to the evaporative cycle until the desired final cake solids concentration is achieved. In this case there is generally no drainage and the first step would be to maximize the amount of decant that can be achieved in order to minimize the amount of evaporation. Again, polymers may aid in increasing the water that can be removed. As discussed in Chapter 4, pilot settling tests under varying conditions could be conducted in order to determine the volume of decant and hence the drained solids concentration. A mass balance approach would then be conducted similarly to the sand drying bed example.

Table 5.4

Weekly mass balance example for sand drying bed

Week	Bed loading area (ft^2)	Carry-over bed area (ft^2)	Net bed required (ft^2)
Nov 1	13,750	0	13,750
2	13,750	13,750	27,500
3	13,750	27,500	41,250
4	13,750	41,250	55,000
Dec 1	16,750	55,000	71,750
2	16,750	71,750	88,500
3	16,750	88,500 – 13,750 (Nov 1)	91,500
4	16,750	91,500 – 13,750 (Nov 2)	94,500
Jan 1	29,250	94,500 – 13,750 (Nov 3)	110,000
2	29,250	110,000 – 13,750 (Nov 4)	125,500
3	29,250	125,500	154,750
4	29,250	154,750	184,000
Feb 1	31,000	184,000	215,000
2	31,000	215,000	246,000
3	31,000	246,000 – 16,750 (Dec 1)	260,250
4	31,000	260,250 – 16,750 (Dec 2)	274,500
Mar 1	34,200	274,500 – 16,750 (Dec 3)	291,950
2	34,200	291,950 – 16,750 (Dec 4) –29,250 (Jan 1)	280,150
3	34,200	280,150 – 29,250 (Jan 2) –31,000 (Feb 1)	254,100
4	34,200	254,100 – 29,250 (Jan 3) –31,000 (Feb 2)	228,050
Apr 1	35,000	228,050-29,250 (Jan 4) – 31,000 (Feb 3)-34,200 (Mar 1)	168,600
2	35,000	168,600 – 31,000 (Feb 3) –34,200 (Mar 2)	138,400
3	35,000	138,400 – 34,200 (Mar 3)	139,200
4	35,000	139,200 – 34,200 (Mar 4) –35,000 (Apr 1)	105,000

Using the data from the sand drying bed example, but at a loading of 1 lb/ft^2, assume that a 4 percent decanted solids concentration could be achieved, which would be typical for a polymer conditioned alum sludge. Then the amount of water that must be evaporated is found with equations (5.12) and (5.11) as:

$$D(d) = 17\frac{1.1}{4} = 4.68\,\text{in.}$$

$$\Delta D(e) = 4.68 - \left(4.68\frac{4}{20}\right) = 3.75\,\text{in.}$$

Using only the beginning of the month bed availability criteria results in the mass balance Tables 5.5 and 5.6. In the example, 757,000 ft^2 of solar bed area would be required, as compared to 378,000 ft^2 for the sand drying bed using the first of the month availability criteria. In general, a sand bed will result in a lower area requirement except for a residual that can be settled and decanted to reach the same drained solids concentration as that to which it can be drained and decanted. However, in areas with a high evaporation rate, solar drying beds may still be preferred over sand beds due to their ease of construction, low maintenance, and ease of cleaning.

Table 5.5

Tabulation of monthly solar bed area requirements

Month	Solids production (lb/d)	Net evaporation rate (in./month)	Solids drying time (month)	Solar drying area loaded (ft^2)
January	7,820	1.0	2.2	235,000
February	8,275	1.9	1.5	248,000
March	9,145	3.5	1.1	274,000
April	9,350	4.7	0.8	280,000
May	5,265	5.8	0.7	158,000
June	3,395	6.9	0.5	102,000
July	3,240	7.0	0.5	97,000
August	4,880	6.5	0.6	146,000
September	3,145	4.5	0.8	94,000
October	4,125	3.5	1.1	124,000
November	3,650	2.6	1.6	109,000
December	4,470	1.8	2.5	134,000

Table 5.6

Monthly mass balance example for solar drying bed

Month	Bed loading area (ft^2)	Carry-over bed area (ft^2)	Net bed area required (ft^2)
October	124,000	0	124,000
November	109,000	124,000 (Oct)	233,000
December	134,000	109,000 (Nov)	243,000
January	235,000	134,000 (Dec)	369,000
February	248,000	134,000 (Dec) 235,000 (Jan)	617,000
March	274,000	235,000 (Jan) 248,000 (Feb)	757,000
April	280,000	274,000 (Mar)	554,000
May	158,000	0	158,000
June	102,000	0	102,000
July	97,000	0	97,000
August	146,000	0	146,000
September	94,000	0	94,000

DEWATERING LAGOON SIZING

Dewatering lagoons are vary similar to sand drying beds except that they operate at much higher loadings. The dewatering lagoon should be equipped with a decant structure and underdrains. For a dewatering lagoon, the lagoon is filled over a long time period and then allowed to dry for a long period while another lagoon is filled. Dewatering lagoons can have an advantage over sand drying beds in reducing peaks, since the loading is often spread over several months. Because dewatering lagoons use a much higher loading rate, the drainage volume would generally be lower than a sand drying bed. The main difficulty in sizing a dewatering lagoon is in predicting the drained solids concentration after the loading is complete. Plugging of the sand media on the bottom of the

dewatering lagoon with multiple loadings is difficult to predict and would require a carefully planned pilot test with 2-in. or 6-in. dewatering columns, or pilot-scale dewatering lagoons may even be necessary to accurately size and design the system. The bottom of the lagoon would have a higher solids concentration than the top of the lagoon, and a net average solids concentration must be estimated. During the evaporation phase the bottom layers often do not dry out. Some utilities have found that tilling the sludge during the evaporative cycle helps to expose all of the residuals to drying.

Again, considering the same example as before, a lagoon can be sized by selecting a desired fill cycle and estimating the drained solids concentration. In this example a 6-month fill cycle was chosen to help reduce the winter sludge production peaks. January to June is the highest production period, wherein about 650 tons of sludge are produced.

If a 5-ft depth of sludge in the lagoon is selected, then the lagoon area can be calculated for varying drained solids concentrations as:

$$\text{Dewatering lagoon area} = \frac{(\text{lb sludge})}{(\text{depth})(\text{percent SS(d)})(0.624)} \tag{5.13}$$

Table 5.7 shows the required area for drained solids concentrations of 4, 6, and 8 percent.

Table 5.7

Sizing example for a dewatering lagoon

Drained solids concentration (percent)	Area required/lagoon (ft^2)	Drying time required (yr)	Number of lagoons	Total area required (ft^2)
4	104,000	1.0	3	312,000
6	69,000	0.9	3	207,000
8	52,000	0.7	3	156,000

The required drying time is found by ΔD(e), so that at 6 percent SS(d) the required change in depth is:

$$\Delta D(e) = 60 - \left(60\frac{6}{20}\right) = 42 \text{ in.}$$

Since the average evaporation is 4.1 in./mo it takes about one year to dry the lagoon if evaporation can reach the complete depth through tilling. Therefore, a total lagoon cycle time would be 18 months, and three lagoons would be needed. The total lagoon area required would be 207,000 ft^2 if a 6 percent drained solids concentration could be achieved as an average in the 5-ft sludge depth. In the example all scenarios required three lagoons. A slightly higher solids concentration than 8 percent, such that the drying time is reduced to six months, may be able to reduce the number of lagoons to two. Two lagoons may also be feasible in this case because the high sludge production is in the winter, which is the fill cycle, and the high evaporation is in the summer, which is the drying cycle of the "fullest" lagoon. Several treatment scenarios could be done using different fill cycle times, etc., to minimize the area. However, the largest impact on the required area is still the estimated drained solids concentration, which is difficult to determine, and oversizing would be appropriate.

FREEZE-THAW SIZING

The area required for a freeze-thaw bed is generally determined by the depth of residual that can be frozen. For some climates with long freezing periods, the depth that can be thawed can be the controlling depth. Martel (1989) developed equations to allow the calculation of these two depths. (Note: In some very cold climates the time for thawing could be limited, and the Martel reference should be consulted to determine the thaw time.) The freezing depth can be found by:

$$D(z) = \frac{t(f)(T_f - T)}{\rho_f F\left(\frac{1}{h} - \frac{d(z)}{2K}\right)} \qquad (5.14)$$

where

$D(z)$	=	total depth of sludge that can be frozen (m)
T_f	=	freezing point temperature = 0°C
T	=	average ambient temperature (°C)
$t(f)$	=	the freezing time (hours)
ρ_f	=	density of frozen sludge = 917 kg/m^3
F	=	latent heat of fusion = 93 W·hr/kg
h	=	convection coefficient = 7.5 W/m^2°C
$d(z)$	=	the thickness of the sludge layer (m)
K	=	conductivity coefficient = 2.21 W/m°C

Since many of these parameters are known or assumed constants, the equation can be reduced to :

$$D(z) = \frac{-t(f)T}{11{,}371 + 19{,}294\left(d(z)\right)} \tag{5.15}$$

The above equation would be used when the design calls for multiple layers of sludge to be frozen, with each layer of thickness being d(z). In this case the utility personnel would apply the layer to the bed, and as soon as one layer had frozen then another would be applied. According to Martel, this application method will increase the total depth of sludge that can be frozen as compared to a onetime bed loading. He reports that the minimum practical depth for d(z) is 0.08 m, or about 3 in. In equation (5.15) t(f) and T can be attained (for U.S. locations) from the NOAA through records that are generally on file at the National Climatic Data Center in Asheville, N.C.

For the case of a onetime bed loading D(z) would be set equal to d(z). Solving this equation requires use of the quadratic rule, which results in the following expression:

$$D(z) = \frac{-11{,}371 - \sqrt{1.3\times10^8 - 7.7\times10^4\, Tt(f)}}{3.9\times10^4} \tag{5.16}$$

In Chapter 4 data were presented in freeze-thaw results for Erie County Water Authority near Buffalo, N.Y. In that particular example, the number of freeze hours that were available for the study period was 1,512 hours. The average temperature during the period was –2.1°C. Therefore, the freeze depth using the layered method with a 0.08-m depth for each freeze layer would be found by using equation (5.15).

$$D(z)=\frac{-(-2.1)(1{,}512)}{11{,}371+19{,}294(0.08)}=0.25\,\text{m or } 9.7\,\text{in.}$$

Therefore, about three layers of sludge, each 0.08 m (3 in.) thick could be frozen.

If a onetime loading was used, then the freeze depth would be found by using equation (5.16).

$$D(z)=\frac{-11{,}371+\sqrt{1.3\times10^{8}-7.7\times10^{4}\,(1{,}512)(-2.1)}}{3.9\times10^{4}}$$

$$D(z) = 0.2 \text{ m or } 8 \text{ in.}$$

Therefore, under these climatic conditions the onetime freeze depth is nearly the same (8 in.) as the layer method (9 in.), and there would be no particular advantage in using the more operator intensive layered method. Since there was not a difference in freeze depths by the two procedures, the onetime loading method was used for the Erie County studies.

CHAPTER 6
DESIGN AND OPERATION OF NONMECHANICAL DEWATERING SYSTEMS

SAND DRYING BEDS*

Sand drying beds are designed to take advantage of percolation and evaporation. The basic operating principle of sand drying beds is to apply the residuals to the bed at a certain depth and loading rate, remove free water through draining and decanting, and allow sufficient evaporation time to reach a desired final cake solids concentration. To operate properly year round, sand drying beds should be sized for winter evaporation rates, which ensure sufficient bed area is available for residuals drying. If designed and operated properly, sand drying beds can produce cake solids similar to or even higher than most mechanical dewatering devices. Other advantages of sand drying beds include low power consumption, low operator attention and skill, and low capital cost for small to medium size water treatment plants. Disadvantages of sand drying beds include large land requirements, impact of climatic effects, and potentially significant costs for bed cleaning systems.

Elements of Design

Sidewalls

Sand drying beds should be divided into one or more sections, each sized to accept a full loading from a residuals thickener or batch holding tank. Divider walls are typically constructed of poured reinforced concrete, concrete masonry blocks, or earthen berms. The divider walls should sufficiently extend above the sand medium to accept the design loading depth plus 12 in. of freeboard. Typically, walls are 24 to 36 in. high and are a function of the residuals loading depth plus freeboard. The design should consider the method of residuals application and removal from the bed. The walls should not become an obstacle to residuals application nor should they interfere with cleaning equipment.

*Much of this section was prepared by A.T. Rolan of the City of Durham, N.C.

Careful consideration should be given to the bed dimensions. Bed widths of the sites visited during this project ranged from 20 to 62 ft and were primarily a function of the residuals removal method. Bed lengths should be less than 75 ft if polymer is applied to the residuals in order to avoid uneven residuals distribution. Length to width ratios of 1.7 to 2.5 appeared to be most successful for the sites visited during this project. For longer beds, multiple residuals application points could be considered to maintain reasonable length to width ratios.

Underdrains

Underdrains should be provided in all sand drying beds to collect water percolated down through the sand and gravel and transport this water to a point of collection or discharge. Perforated plastic piping would be acceptable for use as underdrains. Underdrains should be no less than 4 in. diameter, spaced 8 to 20 ft apart, and have a minimum slope of 1 percent. The spacing should consider the type of residuals removal equipment to avoid damage to the underdrains.

The underdrains should be laid in well-graded properly placed gravel to a depth of 10 to 12 in. below the underdrains and to approximately 6 in. above the crown of the pipes.

Underdrains should be designed and placed to provide adequate drainage for an entire bed. The underdrains from several beds would be connected to a main collection header that also receives water from the decant mechanisms. The main collector header should be sized adequately to allow multiple bed loading at one time.

A typical section through a sand drying bed is shown in Figure 6.1 and shows the underdrain arrangement.

Media

The sand media should consist of a 12- to 18-in. layer of good quality sand. The effective size should be from 0.3 to 0.75 mm with a uniformity coefficient not over 4.0 and preferably under 3.5. Media used in the pilot studies consisted of 0.45 to 0.55 mm effective size and yielded

acceptable performance. The sand should be well washed and free from clay, loam, dust, or other foreign matter. The gravel layer under the sand should be graded from 0.1 to 1.0 in. in effective diameter from the relatively coarse material at the bottom to a layer of torpedo sand at the top. The overall gravel depth should be 8 to 18 in. and sufficient to include the underdrain as previously discussed.

Liners

An impermeable liner system may be required by local regulators. Clay liners should have a permeability of at least $1x10^{-7}$ cm/s. Synthetic liners of 40 to 60 mils would be suitable as well. If synthetic liners are used, care should be taken when placing the gravel to prevent puncturing the liner system. Liner manufacturers should be consulted for guidance. Another option would be to use poured concrete slabs as a barrier below the media.

Inlet Structures

Liquid residuals may be applied to drying beds through either a distribution box or application nozzle. Piping conveying residuals to the point of application is typically ductile iron and should be designed for a velocity of at least 2.5 ft/s to avoid residuals settling. Once residuals discharge onto the bed, this velocity must be dissipated to prevent scour of sand in the drying bed. Distribution boxes and application nozzles provide a means of dissipating the incoming velocity and applying the residuals in an even layer on the bed. The distribution box accomplishes this by channeling the residuals into the box where they pool and pour out onto the bed (see Figure 6.2). The application nozzle directs the residuals stream onto a splash block. This splash block prevents the residuals stream from scouring out the underlying sand on the bed and also allows the residuals flow to radiate out from the block to cover the bed (see Figure 6.3). Multiple inlets may be considered for residuals distribution, although the inlets should not interfere with the residuals cleaning equipment.

Plug valves should be used to isolate each drying bed from the main residuals supply header. All piping and valves should be protected from freezing, and flushing with clean water should be

considered after the bed has been loaded. This would avoid potential plugging problems between bed loadings.

Decant Systems

Methods for decanting the supernatant from the drying bed should be provided. Dilute and polymer treated residuals should develop significant volumes of supernatant, which should be removed as quickly as possible to accelerate the start of the evaporative dewatering cycle. An example of a typical decant system is shown in Figure 6.4. This system consists of a swivel pipe that can be set at any elevation. This flexibility is beneficial and allows variable residuals loading depths.

Runners and Ramps

Runners are essential for sand drying beds. Constructed of reinforced concrete, these runners serve several valuable functions. Runners protect the underdrain system and prevent excess sand removal during cleaning. Spacing of runners should be sufficient to allow mechanical cleaning equipment to drive on the bed and remove dried residuals. Orientation of the runners should be parallel to the longitudinal axis of the bed to allow efficient cleaning of the bed.

Runners prevent both removal of excessive amounts of sand from the bed and sand compaction during cleaning operations. Also, runners provide a convenient point of depth reference during sand replacement. The underdrain system can become damaged when heavy equipment rolls over it. The concrete runners protect the underdrains by providing a place for the equipment to operate. Runner area should be minimized, however, because any area taken up by concrete runners diminishes the area available for drainage. The proper sizing and spacing of the runners is a function of the equipment used, wheel spacing, wheel size, and bucket width.

Access to the sand drying bed should be provided by ramps or sealed stop gates. Ideally, there should be access located on both ends of the sand drying beds. This allows easy access to the entire bed. Open areas on either side of the bed also allow residuals to be removed and stored for supplemental drying and for preparation of the bed for the next application. If the beds are cleaned

mechanically, the access points should not be an obstruction in cleaning the beds. Access to the bed corners should be provided.

Possible considerations in selecting access ramps or stop gates include the type of equipment used to clean the bed, slope of the ramp, and amount of excavation required. While ramps would provide the most access, they generally result in more excavation because the entire bed elevation is being lowered. A typical ramp arrangement is shown in Figure 6.5.

Sizing Considerations

Appropriate sizing of sand drying beds should consider optimization of the solids loading rate, initial solids concentration, and polymer treatment. As was previously discussed in Chapter 5, various models could be used for evaluating different loading rate scenarios and their effect on the volume reduction and drying bed yield. To adequately size a drying bed for proper operation on a year round basis requires development of monthly residuals production rates. These production rates should be evaluated in conjunction with monthly evaporation data. Only this type of analysis would accurately size the drying bed for the worst case condition. Sizing drying beds based on average annual residuals production and evaporation data could result in undersizing the beds.

Chapters 3 and 5 provide an overview of how the initial solids loading rate and solids concentration affect the volume reduction and subsequent drying bed sizing. The models provided in Chapter 5 should be used to size sand drying beds. Supplemental site specific pilot tests would be useful as well to establish final design criteria.

Operational Considerations

Residuals Application

Sand drying bed operation should be a batch process where one complete drying bed is loaded at a time, rather than multiple small loadings. Multiple loadings would have the potential of partially dried residuals clogging the sand and thereby reducing the volume reduction of

subsequent loadings. To operate effectively in a batch process, a residuals storage tank or thickener should be provided that could hold at least several bed volumes.

The residuals storage tank or thickener would collect the residuals directly from the sedimentation basins. After several days or weeks (depending on the size of the sand drying bed), a sufficient quantity of residuals would become stored for one bed loading. Measurements of the residuals blanket depth and solids concentration would be essential. Electronic sensing devices or "sludge judge" sampling tubes would assist the operator in measuring the residuals volume.

After sufficient residuals have been stored to load one complete bed at a specific loading rate, the operator would prepare the required polymer batch.

Depending on the geographical location, a sand drying bed could act like a freeze-thaw bed in the winter months. The residuals holding tank or thickener would be well suited for allowing periodic placement of residuals onto the bed in shallow layers. This would provide for efficient freeze-thaw treatment of the residuals. When considering such a strategy, it is warranted to size the holding tank or thickener to store more residuals than for one bed. The proper freezing temperature could become sporadic and, therefore, more storage would be needed.

Sand Replacement

Some amount of sand is removed each time the beds are cleaned. The amount of sand lost depends on the cleaning method. Periodic inspection of the sand media should be performed from a known reference point such as the top of the walls or the concrete runners to measure the rate of sand loss. In addition, the sand should be periodically raked to maintain an even level and to break up the top surface layer. Sand addition should be part of the annual maintenance procedures.

Polymer Feed Systems

The data provided in Chapters 3 and 5 showed that polymer addition enhances the release of free water from the residuals and allows higher loading rates with enhanced volume reduction. As a result, polymer feed systems should be an integral part of the residuals dewatering system

similar to that required by a mechanical dewatering system. To prevent excessive use of polymer, it would be advantageous to conduct a CST or TTF test on each residuals batch for establishing the optimum polymer dose. Anionic and nonionic polymers tend to be most effective with inorganic residuals produced by coagulant water treatment processes. The polymer feed rate to the residuals should be matched with the residuals pumping rate to provide a consistent dose during the loading of the bed. Multiple polymer feed points including a point at the feed pump suction and discharge side as well as at the drying bed influent point provide for a flexible system that maximizes polymer detention time and effectiveness. In-line static mixers could be useful as well.

Residuals Cleaning

Considerations that dictate when the residuals should be cleaned from the bed include the desired final cake solids concentration that meets the disposal or final use program and the cake solids concentration that is handleable by the removing equipment. For residuals to be handled by heavy equipment, at least a 20 percent solids concentration should be attained. Local regulations would dictate the solids concentration for landfill disposal or other beneficial use.

Increased labor costs have made manual residuals removal uneconomical except for the smallest plants. Mechanical removal equipment such as front-end loaders or truck mounted vacuum removal systems would be the preferred method but require the installation of concrete runners in the bed to protect the underdrain system.

Normal Operating Procedure Checklist

Normal sand drying bed procedures should be established to allow for consistent practices each time the beds are loaded. General operating guidelines include the following:

Initial Inspection

1. All lines should be clear of debris and valves checked for free operation.
2. The sand surface should be level and all irregularities raked smooth.
3. Clear all debris from the surface of the bed.
4. Install stoplogs or other blocking device at vehicle entrance to drying bed (if provided).
5. Make sure a splash plate or other diffusion device is in place where the residuals enter the bed.
6. Check drainage return system and piping.

Startup

1. Prepare a polymer solution of adequate volume to dose the residuals. Verify the polymer dose with a CST or TTF test.
2. Start flow of liquid residuals and polymer into bed. Stop flow when a uniform loading design loading rate throughout the bed is achieved.
3. Do not apply new residuals on top of a layer of dry residuals.

Routine Operations

1. Inspect the bed every few days and decant as needed.
2. Remove any weed growth.
3. When the residuals are dry (normally three weeks or longer depending on weather and depth of residuals) remove the residuals taking care not to damage the sand and gravel layers. Remove as little sand with the residuals as possible.
4. Vehicles and equipment should not be operated directly on the sand but should be operated on planks or plywood laid on top of the bed if permanent vehicle treadways (runners) are not provided.

5. After the residuals are removed, inspect the bed, rake the surface of the sand to level it and to remove any debris, and add makeup sand if necessary.
6. The bed is ready for the next residuals application.

SOLAR DRYING BEDS

Solar drying beds rely exclusively on decanting and evaporation to dry the residuals. As a result, high evaporation rates in conjunction with low application rates would be preferred to maintain the drying times within reasonable levels. Solar drying beds would be appropriate mainly in the southwest where net evaporation rates are greater than 60 in./yr. For proper year round operation the solar drying beds should be sized for winter evaporation and corresponding residuals production rates to ensure sufficient bed area is available for residuals drying.

The advantages of solar drying beds include simple operation, minimal operator skill and attention, ease of cleaning with front-end loaders, and minimal bed maintenance. Disadvantages include large area requirements for drying beds.

Elements of Design

Sidewalls and Bottoms

Solar drying beds should be divided into multiple smaller sections similar to sand drying beds. The solids loading depth of solar drying beds is usually only 1 to 2 ft. Each section should be sized to accept a full batch at one time. The divider walls between sections should have at least 12 in. of freeboard.

Solar drying beds are typically square or rectangular with length to width ratios of up to 2:1. Even residuals distribution over the entire drying bed is important for proper operation. When polymer is applied to the residuals the use of square beds or length to width ratios of less than 2:1 would be preferred to ensure the residuals are equally distributed over the bed.

Solar bed bottoms would be sealed and consist of concrete, asphalt, or soil cement. The bottom area should be sloped a minimum of 1.0 to 1.5 percent to allow for drainage away from the bed.

Inlet and Decant Systems

Liquid residuals would be applied to the bed through a closed conduit or pipeline system with a valve at each bed. The inlets could be similar to those shown in Figures 6.2 and 6.3 for sand drying beds. Again, the inlet design should minimize splashing of the residuals while the bed is being loaded.

Decant systems should be provided to remove supernatant from the bed after the residuals have settled. The height of the decant system should be variable over a large enough range to accommodate both dilute and thickened residuals. Decant systems would include drop tubes as shown in Figure 6.4 or rotating pipe assemblies as shown in Figure 6.6. Decant systems should be located such that they would not interfere with the cleaning equipment.

Ramps and Access

Each solar drying bed should be provided with a ramp or removable wall sections such as stoplogs to accommodate front-end loaders entering the bed for cleaning. Considerations for the access points include the size of the equipment used to clean the bed and allowable slope of the ramp.

Sizing Considerations

Solar drying bed sizing should be based on minimizing the decanting of supernatant and subsequent drying of a shallow layer of settled residuals. The settled layer of residuals should be around 6 in. or less at the start of the evaporation cycle, although higher depths could be used in areas with high evaporation rates.

In order to maximize the decant and settled solids concentration, the use of polymer may be advantageous as demonstrated in Chapters 3 and 5.

Effective sizing of solar drying beds would involve consideration of monthly residuals production, evaporation rates, volume reduction through decanting, and optimization of solids loading rates. Chapter 5 outlined a modeling procedure that should assist in evaluating the required solar drying bed size for a particular utility.

Operational Considerations

Solar drying bed operations are fairly simple. Loading of the solar bed should be standardized such that the loading depth and solids concentration are generally uniform each time a bed is loaded. Polymer addition could be beneficial, and operational issues related to the polymer feed system and feed points should be similar to those previously discussed for sand drying beds. After the beds are loaded with residuals, decanting should proceed as soon as possible to allow direct sun exposure to the actual residuals layer. After decanting, the drying process should be monitored on a regular basis. Rain water should be removed as soon as possible. Representative dried samples should be collected at various times to determine the solids concentration on the bed. After the beds are cleaned with front-end loaders, any residuals remaining in corners should be manually removed.

DEWATERING LAGOONS

The basis for design of dewatering lagoons is very similar to that for sand drying beds. The difference is that the residuals depth applied to the dewatering lagoon is higher, and at times multiple loadings on top of each other are applied. As a result, the residuals drying time would be longer than with sand drying beds and the number of cleanings per year would be less. Dewatering lagoons are often simple structures with earth or concrete side covered slopes. Their advantages include simple operation, minimal operator attention, and little power consumption. Disadvantages include space requirements and cost.

Elements of Design

Sidewalls and Bottoms

Dewatering lagoons are typically between 5 and 10 ft deep. The sides are usually sloped at 2:1 horizontal to vertical ratios and may be covered with concrete, stone, asphalt, or grass. The dewatering lagoon bottom would be similar to the sand drying bed with 18 to 24 in. of sand, 8 to 12 in. of gravel and an underdrain network. The lagoons may be square or rectangular, but the latter generally provides an easier shape for cleaning the residuals. With rectangular lagoons, the design should consider the potential of residuals unevenly distributing throughout the lagoon. This can be mitigated by properly locating one or more residuals inlet points to the lagoon.

Inlet and Decant Systems

Residuals inlets to a dewatering lagoon can be a simple piped system, but energy dissipation should be provided to prevent scouring of previously settled solids. This can be accomplished by constructing a target baffle several feet in front of the inlet pipe or by discharging the residuals into an inlet chamber. The inlet pipe should be located near the top of the anticipated maximum residuals levels in the lagoon.

The decant system should be located on the opposite end of the lagoon inlet to prevent solids mounting in front of the decant pipes. Because dewatering lagoons could encompass a fairly large depth, multiple decant points should be provided. Typically a decant structure with multiple valved pipes located at different depths is provided. Telescoping sluice gates are also used.

Media and Underdrains

General guidelines for sand, gravel, and underdrains previously discussed for sand drying beds should be considered for dewatering lagoons as well. The bottoms of sand drying beds and dewatering lagoons are constructed in a similar manner.

Runners and Ramps

Access must be provided into the dewatering lagoon for front-end loaders to remove the dewatered residuals. For a front-end loader to effectively operate inside a dewatering lagoon, one side of the lagoon should be an access ramp. Concrete runways to support front-end loaders should be provided on the lagoon bottom to prevent damage to the underdrain system. The spacing of the underdrains and runways should be coordinated.

Sizing Considerations

Chapter 5 presented an example for calculating the required dewatering lagoon area based on a given solids production and evaporation rate in conjunction with various pilot data for volume reduction. Additional sizing considerations include the area of one lagoon and the time frame one lagoon requires to dewater residuals. For example, at a given solids loading rate, one lagoon would be provided for 1 month, 1 season, or 1 yr of residuals. Because of side slopes and working areas between lagoons, multiple smaller lagoons take up more space than a few large lagoons. Smaller lagoons, however, could provide more even distribution of the residuals than large lagoons, unless multiple inlets are provided.

It is not uncommon, however, that a water treatment plant has only two lagoons, each sized to store 1 yr of residuals. While one lagoon is receiving residuals, the second lagoon is in a drying mode for up to one year. High residuals depths under this scenario should be avoided. Dried material on top of the residuals layer could effectively seal the underlying residuals from being exposed to the evaporative cycle. Solids mixing equipment could become necessary to physically blend and turn over the residuals to ensure that the entire solids mass obtains a certain final cake solids concentration.

FREEZING BEDS

The design elements and operational considerations for freezing beds are extensively covered by Martel (1989) and by Cornwell and Koppers (1990). The basis of design for a freezing bed allows shallow layers of residuals to be applied to a bed. Each layer should be allowed to freeze prior to application of a subsequent layer on top. Martel (1989) demonstrated that this procedure maximizes the total cumulative freezing depth of the residuals and thereby minimizes the required freezing bed area and cost. Some operator attention would be necessary every day to ensure the layer has completely frozen and to apply the next residuals layer.

Another consideration in the design of layered freezing beds is the basis of design with respect to the residuals quantity. The two approaches that could be considered are as follows:

- Design the layered freezing beds only for the residuals generated during the winter season.
- Design the layered freezing beds to process the residuals generated during the entire year. This would require storage of the residuals generated during the spring, summer, and fall.

If the residuals have to be stored from the spring through the fall prior to being applied to the freezing beds, the design should carefully size the residuals storage facilities and evaluate how to pump these residuals to the beds after 9 months of storage.

The beds could be designed to operate as layered freezing beds during the winter months and as sand drying beds during the spring, summer, and fall. A sizing analysis of both the freeze-thaw and sand drying bed would have to be done to determine which scenario is limiting and requires the most area. This type of design would eliminate the need for extensive residuals storage that is necessary for processing all the residuals through a layered freeze-thaw method.

Another viable approach for sizing freezing beds would be to calculate the freezing and thawing depth of only a single bulk loading. This type of design would be similar to a sand drying bed or a dewatering lagoon, but in the winter months the residuals on the bed are subjected to a

freeze-thaw treatment cycle. While freezing a onetime bulk loading is not as efficient as multiple shallow layers, it would provide for a less operator intensive operation, and the combined sand drying bed and freeze-thaw bed would eliminate storage facilities.

Regardless of which freeze-thaw design approach is selected, each design should incorporate a sand bottom, underdrains, an inlet with energy dissipation devices, and an effective decant system. Examples previously shown for sand drying beds could be considered for freeze-thaw beds as well. Polymer addition should be considered to maximize the removal of water from the residuals prior to freezing. This would reduce the residuals depth to be frozen and would allow a higher solids loading rate and depth. After the freeze-thaw cycle, the freezate should be decanted as soon as possible. The remaining residuals must be allowed to air dry in order to achieve their typical coffee ground texture. With freeze-thaw treatment, the air drying process is usually much faster than for residuals that have not experienced freeze-thaw treatment.

Cleaning of the freeze-thaw beds could be done with front-end loaders provided runways and ramps are installed similar to those in sand drying beds.

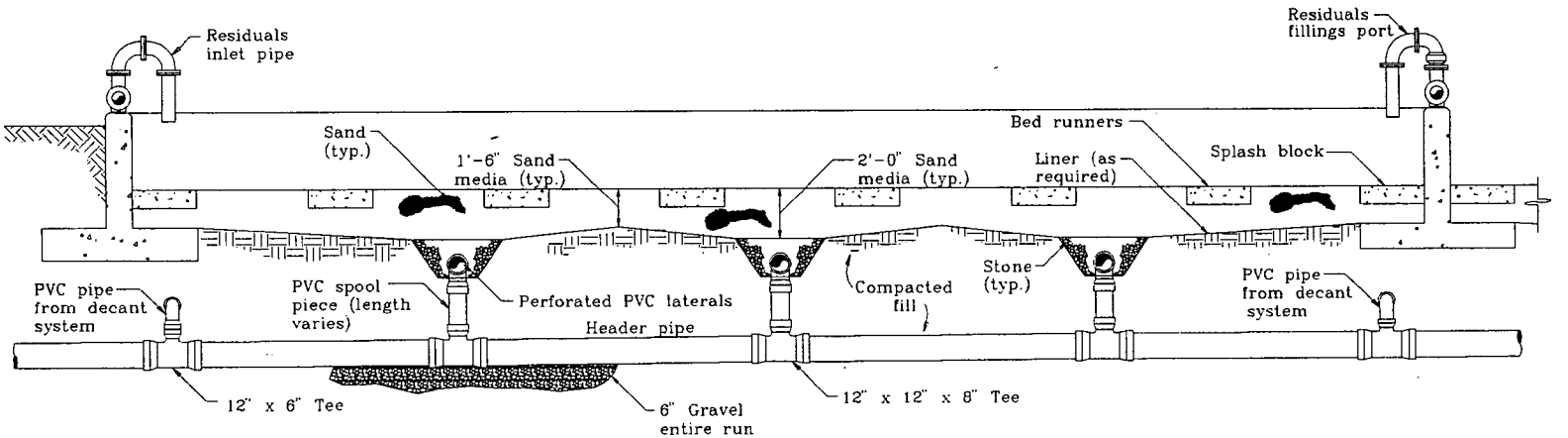

Figure 6.1 Typical sand drying bed section

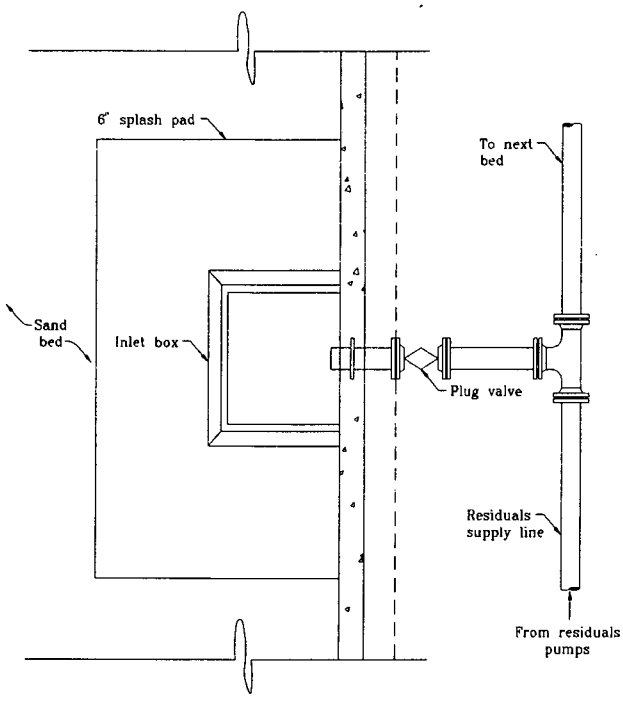

Figure 6.2 Typical residuals inlet box plan

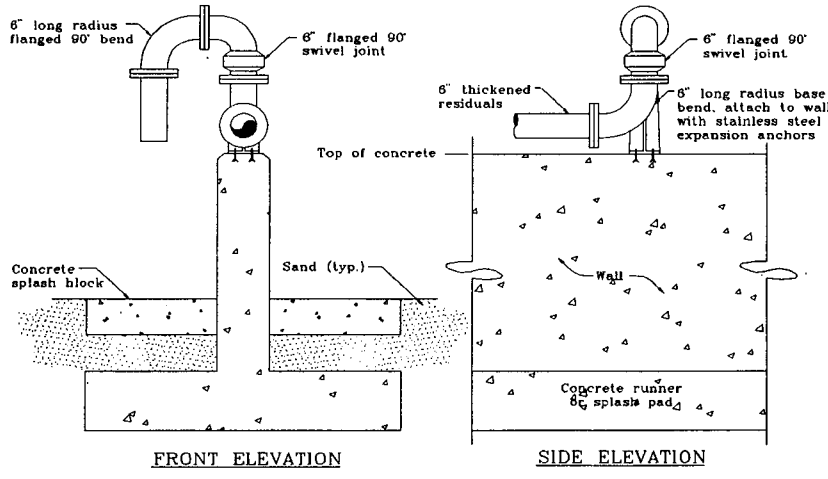

Figure 6.3 Typical residuals inlet pipe plan

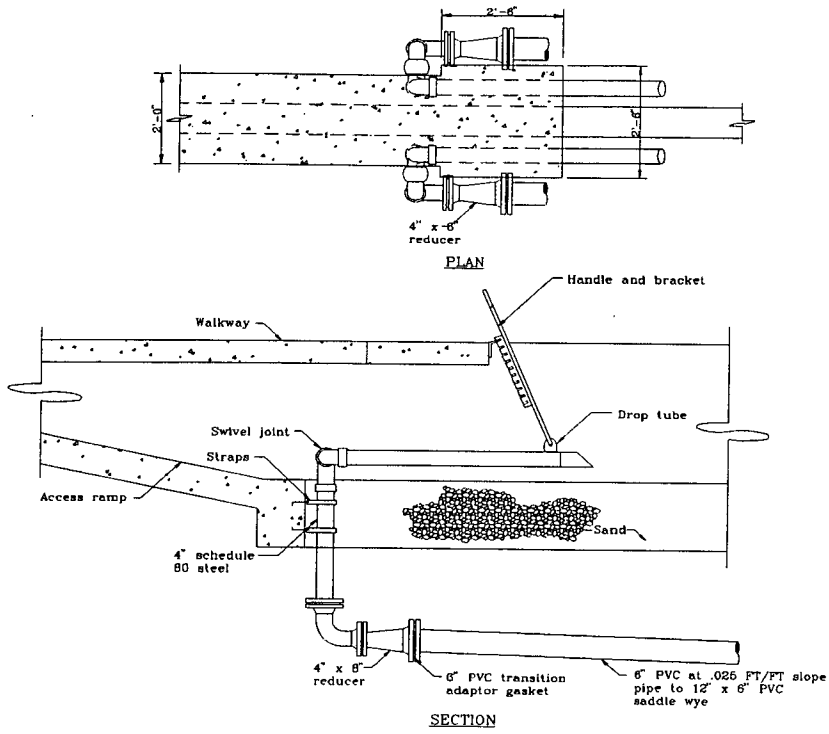

Figure 6.4 Typical decant piping system

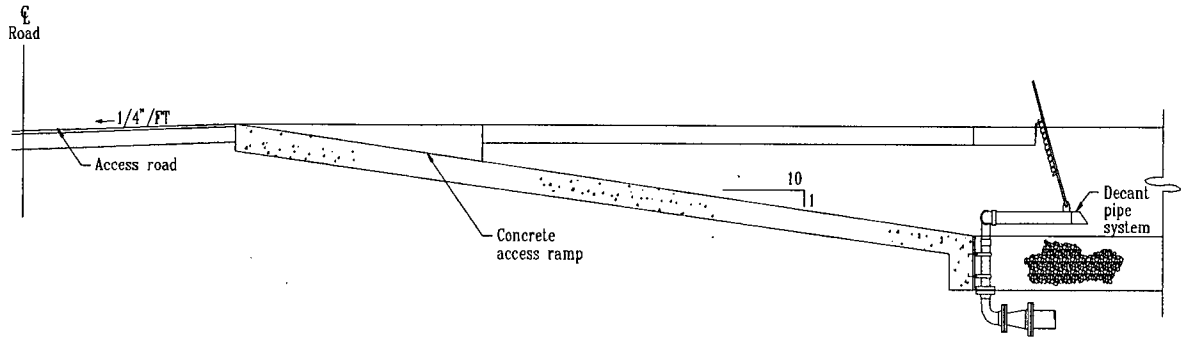

Figure 6.5 Typical sand drying bed ramp

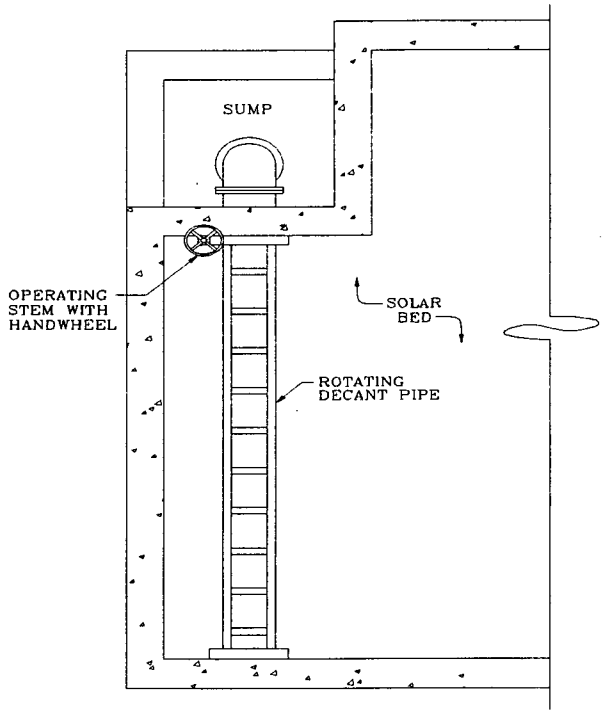

Figure 6.6 Typical rotating decant pipe assembly

APPENDIX A
LABORATORY TEST PROCEDURES

CAPILLARY SUCTION TIME (CST) TEST

Required Apparatus

1. CST apparatus—The CST apparatus consists of a digital timer and a testing block. The testing block is comprised of two plexiglass plates containing electrical contact points and two steel cylinders or reservoirs, referred to as "wide" and "narrow." This application requires the use of the narrow sludge reservoir.
2. CST paper—Use Whatman number 17 chromatography paper cut into 7 x 9 cm sections with the grain parallel to the long side.
3. Large bore glass pipette.
4. CST data sheet (Figure A.1).

Procedure

1. Turn on and reset CST meter.
2. Dry CST test block and sludge reservoir.
3. Place new CST paper on test block. It is important that the rough side of the CST paper is face up. It is equally important that the grain of the paper be parallel with the 9-cm side of the test block.
4. Add upper half of the test block. Insert the sludge reservoir. This test requires the use of the narrow, tall reservoir or cylinder. Pressing firmly, turn the reservoir one quarter turn to prevent surface leaks.
5. Using the large bore pipette, pipette 5-7 mL out of sludge sample container.
6. Pipette the 5-7 mL aliquot into the narrow sludge reservoir.

Sample origin: _____

_____

Sample number: _____

Date of sample: _____

Date analyzed: _____

Analyst: _____

Percent solids: _____

Coagulant type: _____

Coagulant dose (mg/L)	Number 1	Number 2	Number 3	Average CST

Remarks

Figure A.1 CST data sheet

7. The CST device will automatically start the timer and stop it once the sample has traveled the specified distance to the second contact.
8. Record time displayed on the digital timer.
9. Clean and dry the test block.
10. Repeat a minimum of three times.

PARTICLE SIZE DISTRIBUTION USING HYDROMETER ANALYSIS

Required Apparatus

1. ASTM 152-H hydrometer.
2. Two 1,000 mL graduated cylinders—one is the settling cylinder and the other one is the standard cylinder.
3. Thermometer.
4. Analytical balance.
5. 4 percent solution of $NaPO_3$ (sodium hexa-metaphosphate) deflocculating agent. (This solution is prepared by dissolving 40 g of $NaPO_3$ in 1 L of deionized water and mixing thoroughly.)
6. 250 mL graduated cylinder.
7. Large beaker able to contain 1,125 mL of liquid.
8. Large pan suitable for drying 1,000 mL of liquid.
9. Oven capable of reaching 103 to 105°C.
10. 100 mL volumetric flask.
11. Stopwatch.
12. Vacuum pump.
13. Grain size analysis data sheet (Figure A.2).
14. Tables A.1 to A.3

Project: AWWARF Nonmechanical

Sample origin _____ (utility)
_____ (location)
_____

Sample number _____

Date analyzed _____

Analyst _____

Hydrometer Analysis

Hydrometer no. _____ G_s of solids = _____ a = _____

Dispersing agent _____ Amount _____ Wt. of soil, W_s _____

Zero correction _____ Meniscus correction _____

Date	Time of reading	Elapsed time (min)	Temp. (°C)	Actual hyd. reading (R_a)	Corr. hyd. reading (R_c)	Percent finer	Hyd. corr. only for meniscus (R)	L from Table A.3	$\frac{L}{t}$	K from Table A.2	D (mm)

$R_c = R_{actual}$ - zero correction + C_r Percent finer = $R_c(a)/W_s$ $D=K\sqrt{L/t}$

Figure A.2 Grain size analysis: Hydrometer method

Table A.1

Temperature correction factors (C_r)

Temperature (°C)	C_r
15	-1.10
16	-0.90
17	-0.70
18	-0.50
19	-0.30
20	0.00
21	-0.20
22	-0.40
23	-0.70
24	-1.00
25	-1.30
26	-1.65
27	-2.00
28	-2.50
29	-3.05
30	-3.80

Source: Adapted from ASTM D421-85

Table A.2

Values of K for use in equation (A.5) for several unit weights of soil solids and temperature combinations

Temperature	Unit weight of soil solids (g/cm^3)							
(°C)	2.50	2.55	2.60	2.65	2.70	2.75	2.80	2.85
16	0.0151	0.0148	0.0146	0.0144	0.0141	0.0139	0.0137	0.0136
17	0.0149	0.0146	0.0144	0.0142	0.0140	0.0138	0.0136	0.0134
18	0.0148	0.0144	0.0142	0.0140	0.0138	0.0136	0.0134	0.0132
19	0.0145	0.0144	0.0140	0.0138	0.0136	0.0134	0.0132	0.0131
20	0.0143	0.0143	0.0139	0.0137	0.0134	0.0133	0.0131	0.0129
21	0.0141	0.0139	0.0137	0.0135	0.0133	0.0131	0.0129	0.0127
22	0.0140	0.0137	0.0135	0.0133	0.0131	0.0129	0.0128	0.0126
23	0.0138	0.0136	0.0134	0.0132	0.0130	0.0128	0.0126	0.0124
24	0.0137	0.0134	0.0132	0.0130	0.0128	0.0126	0.0125	0.0123
25	0.0135	0.0133	0.0131	0.0129	0.0127	0.0125	0.0123	0.0122
26	0.0133	0.0131	0.0129	0.0127	0.0125	0.0124	0.0122	0.0120
27	0.0132	0.0130	0.0128	0.0126	0.0124	0.0122	0.0120	0.0119
28	0.0130	0.0128	0.0126	0.0124	0.0123	0.0121	0.0119	0.0117
29	0.0129	0.0127	0.0125	0.0123	0.0121	0.0120	0.0118	0.0116
30	0.0128	0.0126	0.0124	0.0122	0.0120	0.0118	0.0117	0.0115

Source: Adapted from ASTM D421-85

Table A.3

Values of L (effective depth) for use in Stokes' formula for diameters of particles for ASTM soil hydrometer 152-H

Original hydrometer reading (corrected for meniscus only)	Effective depth L (cm)	Original hydrometer reading (corrected for meniscus only)	Effective depth L (cm)	Original hydrometer reading (corrected for meniscus only)	Effective depth L (cm)
0	16.3	21	12.9	42	9.4
1	16.1	22	12.7	43	9.2
2	16.0	23	12.5	44	9.1
3	15.8	24	12.4	45	8.9
4	15.6	25	12.2	46	8.8
5	15.5	26	12.0	47	8.6
6	15.3	27	11.9	48	8.4
7	15.2	28	11.7	49	8.3
8	15.0	29	11.5	50	8.1
9	14.8	30	11.4	51	7.9
10	14.7	31	11.2	52	7.8
11	14.5	32	11.1	53	7.6
12	14.3	33	10.9	54	7.4
13	14.2	34	10.7	55	7.3
14	14.0	35	10.5	56	7.1
15	13.8	36	10.4	57	7.0
16	13.7	37	10.2	58	6.8
17	13.5	38	10.1	59	6.6
18	13.3	39	9.9	60	6.5
19	13.2	40	9.7		
20	13.0	41	9.6		

Source: Adapted from ASTM D421-85

Procedure

1. Prepare sludge sample. This should be done ahead of time because some soaking of the sample is required. Pour 1 L of sludge sample as received into a graduated cylinder. To this add 125 mL of the $NaPO_3$ solution and mix by agitation for approximately 1 min. Allow this solution to stand for 1 hr (or longer).
2. After the sample-deflocculating agent mixture has been allowed to stand transfer 1 L of this mixture to the settling cylinder.
3. Prepare the standard cylinder. The standard cylinder will serve as a control. This is done by combining 125 mL of the $NaPO_3$ solution and 1 L of water in the large beaker so that the final volume is 1,125 mL. Pour 1 L of this solution into the standard cylinder.
4. Place the hydrometer into the standard cylinder. The zero correction value is obtained by recording the hydrometer reading in the sodium hexametaphosphate solution. The meniscus correction is obtained by measuring the height of the meniscus on the hydrometer. Measure the temperature of the standard cylinder with a thermometer. Temperature correction values are obtained by using the recorded temperature and recording the corresponding temperature correction value from Table A.1.
5. Use the palm of your hand to cover the settling cylinder. Agitate by inverting the cylinder for approximately 1 min.
6. Once agitation is complete, set the cylinder down and insert the hydrometer. Take readings at 1, 2, 3, and 4 min of elapsed time.
7. Reagitate the settling cylinder and take another series of 1, 2, 3, and 4-min readings. These should agree within 1 unit of the previous readings. Repeat this procedure until agreement between two sets of readings is obtained.
8. Take additional readings of 8, 15, 30, 60, and 120 min. Continue taking readings after this time. It is not necessary to have exact spacing of points, just ones that give a good spread of points. Continue taking readings until the diameter of particles still in suspension is on the order of $1x10^{-3}$ mm. Using Equation A.5 (p. 132), the diameter can be estimated using the effective depth value (L) obtained in Table A.3 of the ASTM method included in this appendix and the test duration in minutes. K can

be estimated as 0.01 to calculate the diameter or obtained from Table A.2 of the method. As the elapsed time increases it is important to take temperature readings so that correction for temperature can be accomplished.

9. Once the diameter of particles still in suspension reaches the order of $1x10^{-3}$ mm, the contents of the settling cylinder should be poured into the large pan and dried at 103-105°C. After drying is complete, the weight of the material left in the pan should be recorded as sample weight (W_s).
10. Determine the specific gravity (G_s) of the sludge sample solid phase. This is done by filling the 100-mL volumetric flask with deaired water. Deaired water can be obtained by subjecting the water to a vacuum. Determine the weight of 100 mL of deaired water (W_1). Pour dried sludge solid phase into the volumetric flask and fill to the mark. Subject this to a vacuum to deair this water as well. Determine the weight of the solid phase and water (W_2). Specific gravity can be determined by the following equation:

$$G_S = \frac{W_3}{(W_1 + W_3) - W_2} \tag{A.1}$$

11. If the G_s is not equal to 2.65, a correction factor must be employed. This correction factor (a) can be calculated by the following equation:

$$a = \frac{G_S(1.65)}{(G_S - 1)2.65} \tag{A.2}$$

12. The hydrometer reading (R) must be corrected for the percent finer calculation. The equation to calculate the corrected hydrometer reading is as follows:

$$R_c = R_{actual} - \text{zero correction} + C_r \tag{A.3}$$

where C_r can be found using Table A.1 of the ASTM method.

13. Percent finer can be calculated using the following equation:

$$\text{Percent Finer} = \frac{R_c a}{W_s} 100 \tag{A.4}$$

14. Particle size diameter can be determined using the following equation:

$$D = K\sqrt{L/t} \text{ mm} \tag{A.5}$$

where

K = constant from Table A.2 of ASTM

L = effective depth from Table A.3 of ASTM

t = elapsed time

SPECIFIC RESISTANCE (SR) TO FILTRATION TEST

Required Apparatus

1. Vacuum pump or other vacuum source.
2. 9-cm diameter Buchner funnel with 24/40 neck connection with fritted glass side arm.
3. Standard 100 mL graduated cylinder.
4. 250 mL graduated cylinder with a 24/40 fritted glass neck.
5. Filter paper (Whatman number 1 or 2 or equivalent).
6. Assorted vacuum tubing.
7. Stopwatch.
8. SR data sheet (Figure A.3).

Procedure

1. Place Buchner funnel into graduated cylinder and attach to vacuum.
2. Place filter paper in Buchner funnel. Using a small amount of deionized water (5-10 mL) wet the filter paper to seal it. Discard water in graduated cylinder.
3. Pour 100 mL of sludge sample into the 250 mL graduated cylinder.
4. Start vacuum pump (adjusting to proper vacuum level).
5. Pour measured sludge sample into Buchner funnel and start stopwatch.
6. Record vacuum applied.
7. Record volume (v) of filtrate generated at specific times (t), usually 1, 2, 3, 4, 5, 6, 7, 8, 9, and 10 minutes.
8. Continue test until cake cracks and vacuum pressure is lost.
9. Once data has been recorded a plot of t/v versus v should be plotted. The slope of this line is b. SR of the sludge cake can be calculated using the following equation:

$$SR = \frac{2PA^2b}{mW} \tag{A.6}$$

where

P = vacuum pressure applied

A = area of Buchner funnel

b = slope as defined above

μ = viscosity

w = weight of cake deposited per volume of filtrate

Sample origin: _____

_____

Sample number: _____

Date of sample: _____

Date analyzed: _____

Analyst: _____

Percent solids: _____

Coagulant type: _____

Time (min)	Volume of filtrate (mL)

Figure A.3 SR data sheet

TIME TO FILTER (TTF) TEST

Required Apparatus (Large Volume TTF)

1. Vacuum pump or other vacuum source.
2. 9 cm diameter Buchner funnel with 24/40 fritted glass neck connection with fritted glass side arm.
3. Standard 100 mL graduated cylinder.
4. 250 mL graduated cylinder with a 24/40 fritted glass neck.
5. Filter paper (Whatman number 1 or 2 or equivalent).
6. Assorted vacuum tubing.
7. Stopwatch.
8. TTF data sheet (Figure A.4).

Procedure (Large Volume TTF)

1. Assemble apparatus.
2. Place filter paper in Buchner funnel. Using a small amount of deionized water (5-10 mL) wet the filter paper to seal it. Discard water in graduated cylinder.
3. Pour 100 mL of sludge sample into the 250 mL graduated cylinder.
4. Start vacuum pump.
5. Pour measured sludge sample into Buchner funnel and start stopwatch.
6. Record time required for 50 percent of the sample volume to collect in the graduated cylinder.
7. Repeat test a minimum of three times.

Sample origin: _____

_____

Sample number: _____

Date of sample: _____

Date analyzed: _____

Analyst: _____

Percent solids: _____

Coagulant type: _____

Sample volume: _____

Filtrate volume: _____

Coagulant dose (mg/L)	Number 1	Number 2	Number 3	Average TTF

Remarks:

Figure A.4 TTF data sheet

APPENDIX B
UTILITY DESCRIPTIONS

COAGULANT RESIDUALS UTILITIES

Sturgeon Point Water Treatment Plant

Plant name:	Sturgeon Point Water Treatment Plant
Location:	Erie County Water Authority, Buffalo, N.Y.
Capacity:	90 mgd
Residuals type:	PACl
Dewatering method:	Lagoons with supplemental air drying

Current residuals management practices at the Sturgeon Point Water Treatment Plant (see summary in Table B.1) consist of sedimentation basin solids and filter backwash wastewater being discharged to three thickener-clarifier tanks. Supernatant from the thickener-clarifier tanks are recycled to the plant headworks and blended with the raw water from Lake Erie. Thickened residuals are currently sent to one of three residuals storage lagoons where solids are stored for up to five years. Supernatant from the lagoons is also recycled to the plant headworks. The lagoons are cleaned out every five years, and the residuals are placed in the retention area located on-site for supplemental air drying and freeze-thaw dewatering. The dried residuals are currently being stored on-site in the retention area for eventual disposal in a landfill. The plant also has the capability to dewater thickened residuals with a conventional plate and frame filter press; however, for the past five years the plant has employed nonmechanical dewatering practices.

The work described in this report at this plant concentrated on tests using six pilot scale freeze-thaw/sand drying beds. The design of the six freeze-thaw beds consisted of a 10-ft by 10-ft bottom with 1:1 side slopes. The depth of each bed was 5 ft. Side slopes and the bed bottom were overlain with a 10 mil polyethylene liner to prevent seepage of filtrate or decant water. To facilitate filtrate water removal, an underdrain system consisting of 3 in. perforated pipe, 6 in. of sand, and

6-in. of gravel was also installed. A gravity drain-type decant assembly was also installed to allow decant water to be removed from the bed during filling. The pilot scale beds were loaded at various depths and loading rates to quantify the effects of the solids concentration and polymer dose on the drainage rate. Sand utilized on the sand drying bed had an effective size (D_{10}) = 0.55 mm, a d_{60} of 2.6 mm, and a corresponding uniformity coefficient (C_μ) of 4.

Table B.1

Sand drying lagoon description: Buffalo, N.Y.

Dewatering system	Sand drying beds; freeze-thaw beds (winter)
Number of beds	6
Bed dimensions	10 ft x 10 ft bottom
Total surface area	600 ft^2
Sand effective size	0.55 mm
Number of laterals per bed	4
Filtrate/decant handling	N/A
Cleaning method	Shovel

Southwest Water Treatment Plant

Plant name:	Southwest Water Treatment Plant
Location:	Huntsville, Ala.
Capacity:	36 mgd
Residuals type:	Alum
Dewatering method:	Sand drying beds

The Southwest Water Treatment Plant obtains its raw water from the Tennessee River. Alum is used as a primary coagulant and lime is added for pH control. Residuals are produced in two, 1 MG sedimentation basins. Residuals are collected daily via a floating bridge siphon system. Once collected, clarifier solids are transferred to a 160,000-gal gravity residuals thickener where the solids thicken to approximately 6 percent solids concentration. From the thickener, residuals are transferred through two 350-gpm constant speed pumps to one of 40 100 ft^2 sand drying beds. Each bed is 20 ft wide and 50 ft long.

Solids are applied to the sand drying beds via a filling nozzle at a rate of 240 gpm. Each sand drying bed is equipped with a splash block underneath the filling nozzle to prevent scour of bed sand during residuals application. Filling nozzle design allows one nozzle to fill two adjacent beds. Flow for each nozzle can be controlled using a valve supplied to each filling nozzle. Residuals are typically applied at a depth of 11.5 to 12.5 in. at an average applied solids concentration of 5.6 percent; this yields a typical loading rate of 3.4 lb/ft^2.

The Southwest Water Treatment Plant sand drying bed underdrain collection system consists of two 6-in. perforated laterals per bed connected to an 8-in. perforated collection pipe. This collection pipe is common to all beds on a particular row (four rows of ten beds). Drying bed media consists of 9-in. sand with a 0.4 mm effective size, underlain by gravel. Additional gravel and a clay liner constitute the base of the bed. Filtrate water is collected in a common sump where it is pumped in turn to the washwater recovery basin. Four concrete runners have been installed in each bed to facilitate cleaning. Each bed is equipped with ramps at either end to allow front-end loaders access to the bed for cleaning.

Since the Southwest Water Treatment Plant is a "zero discharge" plant, supernatant from both the washwater recovery basin as well as overflow from the residuals thickener and sand drying bed filtrate are all recycled to the plant headworks.

A summary of the details for the sand drying beds is shown in Table B.2.

Table B.2

Sand drying bed description: Huntsville, Ala.

Dewatering system	Sand drying bed
Number of beds	40
Bed dimensions	20 ft x 50 ft (width x length)
Total bed area	40,000 ft^2
Sand:	
Effective size	0.4 mm
Uniformity coefficient	1.75
Number of laterals per bed	2, 6-in. perforated
Filtrate/decant handling	Recycled
Cleaning method	Front-end loader
Number of concrete runners	4 per bed

Williams Water Treatment Plant

Plant name:	Williams Water Treatment Plant
Location:	Durham, N.C.
Capacity:	22 mgd
Residuals type:	Alum
Dewatering method:	Sand drying beds

Residuals are removed from the plant's sedimentation basins through a drain valve system (six basins) and a continuous sludge collection system (two basins). Upon removal from the sedimentation basins the residuals are pumped to decant tanks where the solids are thickened to approximately 3 to 4 percent solids concentration.

Residuals are subsequently blended with polymer and pumped to the sand drying beds. Conditioned residuals are applied to the bed through a distribution box. Pumping lasts for up to 90

minutes at approximately 600 gpm. Typical loading rates are 2 to 3 lb/ft^2 or 20 to 30 in. depths at 2 percent solids concentration. When optimum polymer dosing is achieved, residuals volumes can be reduced up to 70 percent through decant and drainage.

The sand drying beds have both underdrains and decant mechanisms. The sand drying bed medium consists of 24 in. of sand over a clay liner. Sieve analysis of the sand medium indicates that the sand effective size (D_{10}) is 0.4 mm and the corresponding uniformity coefficient is 2.75. Six equally spaced 6-in. diameter perforated laterals connected to a common 12-in. diameter header pipe constitute the underdrain system. The decant system consists of two 4-in. diameter pipes mounted on rotating bases. These pipes can be raised or lowered to the appropriate depth required to effectively remove decant water. Filtrate from the underdrains and clean out water are collected in a sump and subsequently discharged to the sanitary sewer. Other details for the sand drying beds are shown in Table B.3.

Table B.3

Sand drying bed description: Durham, N.C.

Dewatering system	Sand drying bed
Number of beds	4
Bed dimensions	36 ft x 145 ft
Total bed area	20,880 ft^2
Sand:	
Effective size	0.4 mm
Uniformity coefficient	2.75
Number of laterals per bed	Six, 6-in. perforated
Filtrate/decant handling	Discharge to sewer
Cleaning method	Vac-haul truck

Midland, Michigan, Purification Plant

Plant name:	Midland Water Purification Plant
Location:	Midland, Mich.
Capacity:	36 mgd
Residuals type:	Ferric chloride and lime
Dewatering method:	Sand drying beds

The Midland Water Purification Plant produces both domestic and industrial grade water. The plant employs ferric chloride as the primary coagulant (4.1 ppm). Lime is also added for softening (7.0 ppm for domestic and 40.0 ppm for industrial grade water). Water from Lake Huron is pumped 65 miles through a pipeline and is treated using conventional methods. Residuals are generated in solids contact clarifiers. After transfer to the 106,000 gal gravity thickener building, the residuals are pumped unconditioned onto one of four 310 ft long x 55 ft wide x 4 ft deep sand drying beds. Residuals are applied through one of three application nozzles per bed (see summary in Table B.4).

Residuals application is accomplished in layers. Beginning with a clean bed, residuals are pumped onto the bed through the first nozzle. Application depths vary, but an average of 8 in. is representative. At an application solids concentration of 24 percent, this translates to approximately 11 lb/ft^2 loading rate. Several applications are made on top of this initial application before switching to the next nozzle. This process is repeated until the depth on the entire bed is approximately 3.5 feet.

Beds are cleaned once every two years. Three beds are cleaned at once with one bed in reserve. An average of 1,500 yd^3 of residuals are removed from each bed at the time of cleaning. The City of Midland is currently in the third year of a three year contract with a contractor that both removes the residuals and markets them to local farmers who land apply them.

The drying beds have underdrains that consist of four 6 in. perforated laterals running the length of the bed. These laterals slope from the ends to an 8 in. perforated header pipe located approximately halfway along the bed. This 8 in. collector pipe is common to all four beds and carries and discharges collected filtrate to the local storm sewer.

As originally designed, the beds contained access gates to allow front-end loaders onto the bed. Through operational experience it was determined that front-end loaders would sink into the sand if driven onto the beds, and therefore these gates have not been used in quite some time. The solution to this problem has been driving a backhoe out onto the dried residuals and loading dump trucks that drive onto the two access roads. The sand is a single media sand which is quite course. It varies in depth from 10 to 18 in. at the header location. The beds are underlain with a clay base.

Field estimates indicated that on a clean bed approximately 8.4 in. application depth yields a 34 percent volume reduction. The drained solids concentration is approximately 30 percent after 3 days. Solids concentrations as removed from the bed are typically greater than 70 percent.

Table B.4

Sand drying bed description: Midland, Mich.

Dewatering system	Sand drying bed
Number of beds	4
Bed dimensions	55 ft x 310 ft
Total bed area	68,200 ft^2
Sand:	
Effective size	0.3 mm
Uniformity coefficient	3.3
Filtrate/decant handling	Discharge to storm sewer
Cleaning method	Backhoe (contracted)

Alfred Merritt Smith Water Treatment Plant

Plant name:	Alfred Merritt Smith Water Treatment Plant
Location:	Boulder City, Nev.
Capacity:	400 mgd
Residuals type:	Ferric chloride
Dewatering method:	Solar beds

The Alfred Merritt Smith Water Treatment Plant receives its low turbidity water from Lake Mead, created by the construction of Hoover Dam. Residuals are produced through conventional treatment. The primary coagulant utilized is ferric chloride. See the summary in Table B.5.

Because of southern Nevada's arid climate, the plant utilizes solar beds for residuals dewatering. The solar beds consist of concrete basins 60 feet wide by 100 feet long. On one end there is an access ramp and residuals application structure, and on the opposite end a decant mechanism is installed. Solar beds seem to work well in arid regions such as southern Nevada where annual net evaporation is very high. All drainage is accomplished through decantation. Field observations noted that typical values for percent volume reduction through decantation were approximately 21 percent.

Typically residuals are applied in 9 to 11 in. depths to the bed with a corresponding loading rate of 3.1 lbs/ft^2. Once initial decantation and drying is complete, additional residuals are pumped onto the bed. This process is repeated until the final residuals application depth of 18 in. is achieved. Once drying is complete, the solids are removed from the bed using a front-end loader and are subsequently hauled to a landfill site.

Decant water is piped to a central sump common to all beds. From this sump, the decant water is pumped back to the spent backwash water thickener. Decant from the spent backwash water thickener is recycled to the plant headworks.

The decant mechanism consists of a 12 in. pipe section with several rectangular openings cut along the pipe length. The section is oriented horizontally, and located on one end of the section is a gear assembly. When turned it rotates the section about its longitudinal axis. This in turn rotates the openings on the section closer to the residuals level. Continued rotation brings the openings to the water level and beyond. Decant water then pours into the section and is collected and piped to the sump.

Table B.5

Solar drying bed description: Boulder City, Nev.

Dewatering system	Solar beds
Number of beds	20
Bed dimensions	60 ft x 100 ft
Total bed area	120,000 ft^2
Filtrate/decant handling	Recycle
Cleaning method	Front-end loader

Two Lick Water Treatment Plant

Plant name:	Two Lick Water Treatment Plant
Location:	Indiana, Pa.
Capacity:	6 mgd
Residuals type:	Ferric chloride
Dewatering method:	Lagoons with sand drying beds

Residual management practices at the Two Lick Water Treatment Plant consist of combining residuals from the sedimentation basins with backwash water in one of two holding lagoons. These lagoons are used to store residuals until they are applied to the sand drying beds. Decant water from the lagoons is discharged into the adjoining Two Lick River. Residuals continue to build up in the lagoon until such time as they are to be cleaned.

Cleaning of residuals from these storage lagoons is accomplished by pumping solids onto each of the two sand drying beds. The Pennsylvania-American Water Company contracts the cleaning of the lagoons to an outside company. Representatives of the company were on site during the site visit and 50 procedures used to transfer residuals to the sand drying beds were observed.

The contractor supplied the necessary equipment to conduct the residuals transfer operations. The equipment was set up and the contractor began by decanting all free water from the lagoons. Once that task was completed, a front-end loader was used to move all residuals in the lagoon toward a submersible hydraulic pump. The submersible hydraulic pump was used in series with a trailer mounted diesel centrifugal pump. From the lagoon, the residuals were pumped to the sand drying beds.

Beds were filled near to overflowing. Measurements from the first pumping indicated that the average solids concentration applied to the bed was close to 2 percent. Typical depth measurements indicated the solids loading rate to be 2.4 lbs/ft^2.

The contractors allowed the residuals to settle and drain overnight. The following morning additional residuals were pumped onto the bed. This process was repeated again after 2 days.

Measurements conducted on sand samples collected in the field indicate that the sand drying bed media had an effective size of 0.2 mm and a uniformity coefficient of 7.5, indicating a well graded soil. Other details for the sand drying beds are shown in Table B.6.

Table B.6

Sand drying bed description: Indiana, Pa.

Dewatering system	Sand drying bed
Number of beds	2
Bed dimensions	62 ft x 113 ft
Total bed area	14,000 ft^2
Sand:	
Effective size	0.2 mm
Uniformity coefficient	7.5
Filtrate/decant handling	Discharge to stream
Cleaning method	Front-end loader

LIME RESIDUALS UTILITIES

Findlay Water Treatment Plant

Plant name:	Findlay Water Treatment Plant
Location:	Findlay, Ohio
Capacity:	16 mgd
Residuals type:	Lime
Dewatering method:	Freeze thaw/sand drying beds

The Findlay WTP utilizes lime for water softening with the addition of ferric chloride as a settling aid (see summary in Table B.7). The WTP has two circular solids contact units (SCUs) for water clarification. Solids settle and thicken in the SCUs and are drained to a residuals holding tank for three minutes every three hours. The plant has the capability of recycling solids from the holding tank back into the SCU to maintain an adequate solids blanket for water clarification. Solids from the residuals holding tank are pumped into tanker trucks and hauled either to farmland or to off-site sand drying beds for dewatering and storage. When favorable conditions exist, the solids are sprayed from the tanker truck onto nearby wheat fields. When the wheat fields are too soft for the truck or are under cultivation, the solids are applied to the sand drying beds. The WTP operates 13 sand drying beds, which are 20 ft x 120 ft x 5 ft deep. The beds have perforated plastic underdrains embedded in gravel with concrete runners alongside the pipe for protection during mechanical

residuals removal. There is a fine rock layer above the gravel and 12 in. of sand on top of the rock. Residuals are pumped from the truck directly to the sand drying beds. When the residuals on the sand drying beds have sufficiently dewatered, the beds are cleared by bulldozer and backhoe. The residuals are stockpiled at the same site prior to land application. Currently a private contractor collects the dewatered residuals and sells them to local farmers. The WTP carefully monitors the land application process and is obligated to report all operations to the state EPA, including a listing of disposal sites and loading rates for residual applications.

Table B.7

Residuals handling data: Findlay, Ohio

Dewatering system	Sand drying bed/freeze-thaw beds
Number of beds	13
Bed dimensions	20 ft x 120 ft x 5 ft deep
Total surface area	31,200 ft^2
Filtrate/decant handling	Discharge to wastewater plant
Cleaning method	Bulldozer/front-end loader

Three Rivers Water Filtration Plant

Plant name:	Three Rivers Water Filtration Plant
Location:	Ft. Wayne, Indiana
Capacity:	75 mgd
Residuals type:	Lime
Dewatering method:	Freeze thaw/drying lagoons

The Three Rivers plant treats water from the St. Joes River in Ft. Wayne, Ind. Lime is added for water softening and ferric sulfate is used as a settling aid. The treatment plant utilizes a system of both primary and secondary clarification. The primary clarifier typically releases 12 percent of its solids blanket to off-site lagoons every ten minutes. The secondary clarifier releases 8 percent of its blanket every ten minutes. Currently backwash water is recycled to the raw water line prior to any treatment.

The treatment plant is under the process of modifying its method of residual disposal. The plant is being retrofitted in order to discontinue its current practice of recycling backwash

wastewater. The new plan will instead add the backwash water to the thickener clarifier "blowdown" to dilute the residuals prior to pumping to the off-site lagoons.

The lagoons for residuals storage and dewatering are located approximately seven miles from the treatment plant. The lagoon operations are under the control of the city's water pollution control plant. There are currently 19 lagoons, each having a surface area of seven acres and a depth of five feet. Once the lagoons are completely full, they are allowed to dry for four to five years before mechanical residuals removal by bulldozers and front-end loaders. The residuals are then stockpiled and later land applied on local farmland. Table B.8 summarizes this data.

Table B.8

Residuals handling data: Ft. Wayne, Ind.

Dewatering system	Lagoons
Number of lagoons	19
Total surface area	304,921 ft^2 (7 acres)
Filtrate/decant handling	Discharge to wastewater plant
Cleaning method	Bulldozer/front-end loader

St. Louis County South Water Treatment Plant

Plant name:	South Water Treatment Plant
Location:	St. Louis, Missouri
Capacity:	56 mgd
Residuals type:	Lime
Dewatering method:	Drying and freeze-thaw lagoons

The South WTP treats water from the Merrimac River on the southeast side of St. Louis, Mo. The plant uses ferric sulfate as a settling aid and lime for water softening. The WTP has four horizontal settling basins, each with two mechanical rakes for residuals thickening. Residuals are continuously piped from the settling basins to two on-site lagoons for residuals storage and dewatering. Decant water is allowed to overflow into a nearby creek. The residuals are allowed to

dry to about 40 percent solids concentration and are then removed by bulldozer and backhoe. Dump trucks haul the residuals to a nearby city-owned monofill. Here the residuals are allowed further dewatering by air drying prior to landfilling. Each lagoon is operated for two years prior to cleaning. Other details about the lagoons are presented in Table B.9.

Table B.9

Residuals handling data: St. Louis, Mo.

Dewatering system	Lagoons
Number of lagoons	2
Lagoon dimensions	1 - 500 ft x 300 ft x 15 ft 1 - 400 ft x 300 ft x 15 ft
Total surface area	5.5 acres
Filtrate/decant handling	Discharge to creek
Cleaning method	Bulldozer/backhoe

Taylorville Water Treatment Plant

Plant name:	Taylorville Water Treatment Plant
Location:	Taylorville, Ill.
Capacity:	4 mgd
Residuals type:	Lime
Dewatering method:	Lagoons/freeze-thaw

The Taylorville WTP employs alum as a settling aid while lime is added for water softening. The WTP uses two cone shaped solids contact clarifiers. The solids contact clarifiers allow the residuals to thicken prior to application to on-site lagoons. Filter backwash water is also piped to the dewatering lagoons. The solids contact clarifiers typically "blow down" residuals to the lagoons for three minutes per hour.

The WTP currently has five lagoons, which are 120 ft long x 15 ft wide x 5 ft deep. The lagoons have a perforated pipe underdrain system and an overflow pipe. The lagoon underdrain effluent and supernatant are released to a nearby creek.

In order to maintain an effluent release permit, samples are periodically sent to the Illinois State EPA for analysis. The Taylorville Sanitary District also performs suspended solids testing on the lagoon effluent.

Residuals are sent to each lagoon for a period of one week up to two or three months depending on the raw water quality. Once full, the lagoons are allowed to dewater for a period of time before cleaning. The lagoon residuals are cleaned out by a backhoe and stockpiled prior to land application. See Table B.10 for more details.

Table B.10

Residuals handling data: Taylorville, Ill.

Dewatering system	Lagoons
Number of lagoons	5
Lagoon dimensions	120 ft x 15 ft x 2 ft
Total surface area	9,000 ft^2
Filtrate/decant handling	Discharge to stream
Cleaning method	Backhoe

Easton WTP, Easton, Conn.

Plant name:	Easton Water Treatment Plant
Location:	Bridgeport, Conn.
Capacity:	20 mgd
Residuals type:	Alum
Dewatering method:	Lagoons/freeze-thaw

The 20 mgd Easton WTP generates solids in each of three basins equipped with plate settlers. Solids settle and are collected with rakes that move the solids in the direction of the residuals pumps. These residuals pumps are activated when solids reach a specified thickness in the bottom of the basin. When operating, the pumps transfer residuals material up to one of four residuals holding/drying lagoons (see summary in Table B.11).

The four residuals holding/drying lagoons are each approximately 16,000 ft^2 in area. They are designed to hold solids until the winter months when they are used in a freeze-thaw mode. These lagoons do not have underdrains and it appears that the lack of underdrains is a problem in terms of

drainage. There is no ability to remove either water that is liberated from the residuals as it settles or to remove ponded rainwater or snowmelt.

Lagoons are typically filled in shallow layers to a depth of 6 to 12 in. After this level is reached, the next available lagoon is used and the process continued. Placing solids in the lagoon in shallow layers should allow the applied solids to dry or freeze. Easton O&M manuals state that the lagoons should continually be filled until a depth of 2 ft is achieved at which time they would be taken out of service and cleaned. Operators expect a residuals concentration of 40 to 50 percent solids under optimum conditions, but this is rarely achieved. Typically, operators have to remove solids when they just become handleable and dry them supplementally by stockpiling.

The operators indicated that they are trying to turn their residuals by tractor in an effort to increase the rate at which the solids dry.

Table B.11

Residuals operation details: Easton WTP

Dewatering system	Lagoon/freeze-thaw
Number of lagoons	4
Lagoon dimensions	16,000 ft^2
Total lagoon area	64,000 ft^2
Filtrate/decant handling	None
Cleaning method	Front-end loader

APPENDIX C
SI EQUIVALENTS

CONVERSION CHART

Water Distribution Parameters	To Convert From Customary Units		To SI Units	Multiply By
Area	mi^2		km^2	2.590
		or	m^2	2.590×10^{6}
Area	acre		ha	4.047×10^{-1}
Head loss	ft		kPa	2.989
		or	m	3.048×10^{-1}
Hydrant spacing	ft		m	3.048×10^{-1}
Hydraulic gradient	ft/1,000 ft		mm/m	—
		or	m/km	—
Level gauging	ft		m	3.048×10^{-1}
Metering	gph		m^3/h	3.785×10^{-3}
Metering	ft^3/h		m^3/h	2.832×10^{-2}
Pipe cross-section	$in.^2$		mm^2	6.452×10^{2}
Pipe diameter	in.		mm	2.540×10
Pipe flow velocity	ft/s		m/s	3.048×10^{-1}
Pipe length	ft		m	3.048×10^{-1}
Pressure	psi		kPa	6.895
Pump capacity	gpm		m^3/s	6.309×10^{-5}
		or	L/s	6.309×10^{-2}

(chart continues)

Water Distribution Parameters (cont.)	To Convert From Customary Units		To SI Units	Multiply By
Pump capacity	ft^3/min		m^3/s	4.720×10^{-4}
		or	L/s	4.720×10^{-1}
Residual chlorine	ppm		mg/L	—
Storage elevation	ft		m	3.048×10^{-1}
Storage volume	gal		m^3	3.785×10^{-3}
		or	ML	3.785×10^{-6}
Storage volume	ft^3		m^3	2.832×10^{-2}
		or	ML	2.832×10^{-5}
Water consumption	gal		m^3	3.785×10^{-3}
		or	L	3.785
		or	ML	3.785×10^{-6}
Water consumption	ft^3		m^3	2.832×10^{-2}
		or	ML	2.832×10^{-5}

Water Treatment Parameters	To Convert From Customary Units		To SI Units	Multiply By
Chemical dosage	ppm		mg/L	—
Chemical feed rate	lb/d		kg/d	4.536×10^{-1}
Chemical feed rate	gph		L/h	3.785
		or	mL/s	1.052
Displacement velocity	ft/s		m/s	3.048×10^{-1}
Filter backwash rate	gpm/ft^2		$L/m^2/s$	6.790×10^{-1}

(chart continues)

Water Treatment Parameters (cont.)	To Convert			
	From Customary Units		To SI Units	Multiply By
Filter head loss	ft		kPa	2.989
		or	m	3.048×10^{-1}
Filtration rate	gpm/ft^2		m/h	2.444
		or	$m^3/m^2/h$	2.444
Gas feeder differential pressure	in. H_2O (4°C)		kPa	2.491×10^{-1}
Gas feeder supply pressure	psi		kPa	6.895
Gas feeder vacuum pressure	in. Hg		kPa	3.377
Plant capacity	mgd		m^3/d	3.785×10^{3}
		or	ML/d	3.785
Power	hp		watt	7.46×10^{2}
Raw water flow	gpm		m^3/s	6.309×10^{-5}
		or	L/s	6.309×10^{-2}
Raw water flow	ft^3/min		m^3/s	4.720×10^{-4}
		or	L/s	4.720×10^{-1}
Raw water temperature	°F		°C	(°F−32) × 5/9
Retention time	h		h	—
Settling rate	fph		m/h	3.048×10^{-1}
Weir overflow rate	gal/ft/d		L/m/s	1.437×10^{-4}

REFERENCES

ASTM. (American Society for Testing and Materials). 1985. ASTM D421-85. *Standard Practice for Dry Preparation of Soil Samples.* Philadelphia, Pa: ASTM.

ASTM. 1963. ASTM D422-63. *Standard Test Method for Particle Size Analysis of Soils.* Philadelphia, Pa: ASTM.

AWWA (American Water Works Association). 1993. Water Industry Database. Denver, Colo.: AWWA.

AWWA and ASCE (American Water Works Association and American Society of Civil Engineers). 1990. *Water Treatment Plant Design.* New York, N.Y.: McGraw-Hill.

Cornwell, David A., M.M. Bishop, R.G. Gould, and C. Vandermeyden. 1987. *Handbook of Practice: Water Treatment Plant Waste Management.* Denver, Colo.: AWWA Research Foundation.

Cornwell, David A., and Hay Koppers, eds. 1990. *Slib, Schlamm, Sludge.* Denver, Colo.: AWWA Research Foundation and KIWA.

Cornwell, David A., and R.G. Lee. 1993. *Recycle Stream Effects on Water Treatment.* Denver, Colo.: AWWA Research Foundation.

Dempsey, Brian A., James DeWolfe, and Leslie McGeorge. 1993. Evaluation of Chemical and Physical Characteristics of Water Treatment Residuals Before and After a Freeze-Thaw Cycle. New Jersey DEPE Report. Pennsylvania State University, University Park.

Martel, C. James. 1989. Development and Design of Sludge Freezing Beds. *JEED*, 115(4):799-808.

Martel, C. James, and Carel J. Diener. 1991. A Pilot-Scale Study of Alum Sludge Dewatering in a Freezing Bed. *Jour. AWWA*, 83(12):51-55.

Rolan, A.T. 1980. Determination of Design Loading for Sand Drying Beds. *Journal North Carolina Section*, AWWA and North Carolina WPCA, L5:1:25.

Vesilind, P. Arne. 1988. Capillary Suction Time as Fundamental Measure of Sludge Dewaterability. *JWPCF*, 60(2):215-219.

ABBREVIATIONS

ΔD	total change in depth (in.)
$\Delta D(e)$	change in depth due to evaporation (in.)
$\Delta D(u)$	change in depth due to drainage (in.)
μ	viscosity (centipoise)
μm	micrometer
ρ_f	density of frozen sludge = 917 kg/m^3
Φ	dimensionless instrument constant for CST test
χ	filterability constant (kg^2/s^2m^4)
A	drying bed area (ft^2)
AA	number of bed applications per year
ASCE	American Society of Civil Engineers
ASTM	American Society for Testing and Materials
atm, ATM	atmospheric pressure
AWWA	American Water Works Association
AWWARF	American Water Works Association Research Foundation
°C	degrees Celsius (centigrade)
cm	centimeter
cm^3	cubic centimeter
corr.	corrected
CST	capillary suction time
cu	color unit
d	day
d_{20}	diameter that 20 percent is finer

d_{50}	median diameter (50 percent finer)
DCB	dithionite-citrate-bicarbonate
D(d)	drained residuals depth after the free water has been removed
D(f)	final residuals depth (in.)
D(i)	initial residuals depth (in.)
D(t)	residuals depth at time t
d(z)	thickness of the sludge layer to be frozen (m)
D(z)	total depth of sludge that can be frozen (m)
E	evaporation rate (in./month)
ECWA	Erie County Water Authority
EE&T	Environmental Engineering & Technology, Inc.
EPA	Environmental Protection Agency
F	latent heat of fusion = 93 W·hr/kg
ft	foot (feet)
ft^2	square foot (feet)
g	gram
G	gallon
gal	gallon
gpm	gallons per minute
h	convection coefficient = 7.5 W/m^2 °C
hr	hr
hrs	hours
hyd.	hydrometer
in.	inch
$in.^2$	square inch

K	conductivity coefficient = 2.21 W/m°C
kg	kilogram
L	initial loading (lb/ft^2)
lb	pound
m	meter
m^2	square meter
m^3	cubic meter
mean	mean value
MG	million gallon
mgd	million gallons per day
mg/L	milligrams per liter
min	minute
mL	milliliter
mm	millimeter
mo	month
MWD 1	Mission Water District number 1
n	number of samples
NA	not applicable
no.	number
NOAA	National Oceanic and Atmospheric Administration
NPDES	National Pollutant Discharge Elimination System
ntu	nephelometric turbidity units
O&M	operation and maintenance
P	phosphorus
PACl	polyaluminum chloride
P(u)	percent of the initial depth lost to drainage

P.E.	professional engineer
pH	negative logarithm of the effective hydrogen-ion concentration
PVC	polyvinyl chloride
R^2	correlation coefficient
s	second
s^2	standard deviation
SCU	solids contact unit
SR	specific resistance
SS	solids concentration
SS(d)	drained solids concentration
SS(f)	final dewatered solids concentration (percent)
SS(i)	initial solids concentration (percent)
SS(t)	solids concentration at time t
t	CST (s)
t	residuals drying time
T	average ambient temperature (°C)
T_f	freezing point temperature = 0°C
t(f)	freezing time
temp.	temperature
THM	trihalomethane
THMFP	trihalomethane formation potential
TKN	total Kjeldahl nitrogen
TOC	total organic carbon
TS	total solids concentration
TTF	time to filter
TTHM	total trihalomethane
typ., TYP.	typical

U.S.	United States
V	annual volume of residuals (gal)
W	watt
WFP	water filtration plant
WIDB	Water Industry Database
wt	weight
WTP	water treatment plant
Y	drying bed yield ($lb/ft^2/yr$)
yd^3	cubic yard
yr	year

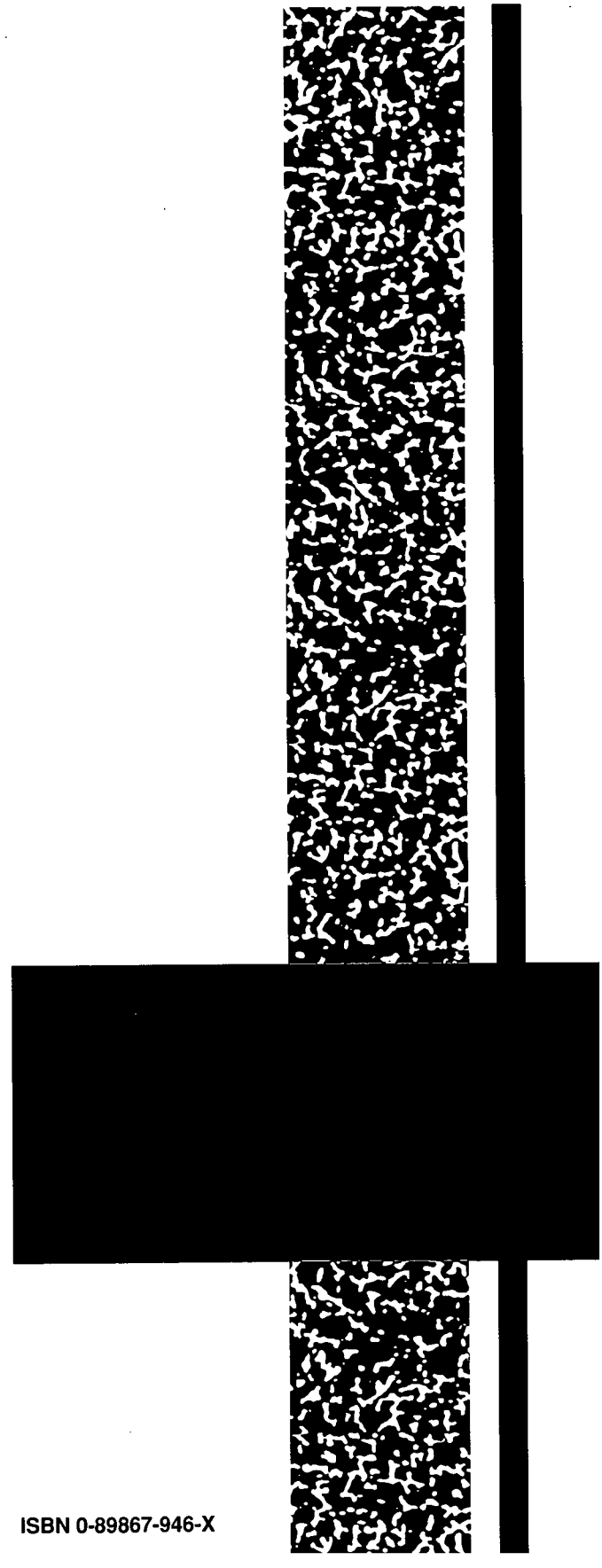

American Water Works Association
RESEARCH FOUNDATION
®

6666 W. Quincy Avenue, Denver, CO 80235
(303) 347-6100

1P-2.5C-90749-6/98-CG

ISBN 0-89867-946-X